

**Towards Highly-Reactive Pyri(mi)dinol-Based  
Fluorescent Antioxidant Indicators  
And  
Cyclopropane Lipids: Autoxidizability and Potential as  
Inhibitors of Lipoxygenases**

by

Jianxing Yang

A thesis submitted to the Department of Chemistry

In conformity with the requirements for

the degree of Master of Science

Queen's University

Kingston, Ontario, Canada

(November, 2011)

Copyright ©Jianxing Yang, 2011

## Abstract

### Chapter 2

In solution, py(mi)ridinols **1.33**, **1.34** and **1.35** are 2-, 5- and 28-fold more reactive antioxidants, respectively, than  $\alpha$ -TOH (the most potent lipid-soluble antioxidant in nature). In order to develop a highly-reactive fluorescent indicator of lipid peroxidation in cells, we sought to couple these antioxidants with boron-dipyrromethene (BODIPY) dyes, such that the resulting conjugates will display a significant fluorescence enhancement upon oxidation. This chapter details efforts towards the synthesis of these compounds.

### Chapter 3

Lipoxygenases are a family of important enzymes that catalyze the dioxygenation of arachidonic acid to yield a variety of potent lipid mediators that have been implicated in the pathogenesis of numerous degenerative conditions. We have undertaken a preliminary study of the effect of replacing the unsaturation in the related polyunsaturated lipid linoleic acid with cyclopropane rings on both the oxidizability of the lipid, as well as lipoxygenase's ability to utilize it as a substrate. We anticipate that these analogs will be useful in co-crystallization studies with the enzyme that will provide unique insight into substrate acquisition, binding and the necessary conformation for catalysis.

## **Acknowledgements**

First and foremost, I would like to thank my supervisor, Dr. Derek Pratt, for giving me this wonderful opportunity to study and work in this lab; for all the helpful knowledge, useful skills and valuable lessons he have taught me; for all the efforts he made to assist me with my projects, and most of all, for his enthusiastic and optimistic attitude towards both science and life, which has impacted me a great deal over the two years.

I also want to thank Jason Hanthorn for all the useful suggestions on my projects and for the patience on my countless questions; Philip Lynett, for helping me with HPLC and for going through the two years of master's program together; Graham Garrett, for all the brilliant ideas and fun he brought in at group meetings; Alaina McGrath, for giving me her course notes and for putting up with my pink chemistry for a whole year; Nathalie Presseau, for organizing one of the best camping trips I've ever been to, and all the old and present members of Pratt's lab for making the lab such a friendly and fun place to work in.

In addition I want to thank all my Chinese friends here for keeping me from getting homesick. Thanks Di Hu, Yingdong Lu for always cheering me up, thanks Feng Zheng for letting me know when I made mistakes in doing chemistry. Thanks Weiwen Zhao and Xinyun Wu for making great Chinese food.

Lastly, I want to thank my parents for always been there for me; their support when I decided to attend graduate school in Canada, and letting me choose what I want to do in life.

## **Statement of Originality**

Except the calculations relating to the methyl cyclopropanated linoleate, which were carried out by my supervisor, Professor Derek Pratt, I hereby certify that the rest of the work described within this thesis is my original work. Any published (or unpublished) ideas and/or techniques from the work of others are fully acknowledged in accordance with the standard referencing practices.

Jianxing Yang

November, 2011

## Table of Contents

Abstract.....	ii
Acknowledgements .....	iii
Statement of Originality.....	iv
List of Schemes.....	vii
List of Figures.....	xi
List of Tables.....	xiii
List of Abbreviations.....	xiii
Chapter 1 Introduction.....	1
1.1 Autoxidation.....	2
1.2 Lipid Peroxidation.....	4
1.3 Antioxidants.....	7
1.4 Phenolic Antioxidants.....	9
1.5 Improving Antioxidant Activity.....	11
1.6 BODIPY.....	13
1.7 Lipoxygenases.....	16
1.8 Lipoxygenase Inhibitors.....	19
1.9 Research Objectives .....	23
1.9.1 Synthesis and Study of Pyri(mi)dinol-Based Fluorescent Antioxidant Indicators.....	23
1.9.2 Preliminary Studies of Cyclopropanated Lipids as Substrates of Autoxidation and Enzyme-Catalyzed Oxygenation. ....	25
1.10 References.....	26
Chapter 2 Towards Highly-Reactive Pyri(mi)dinol-Based Fluorescent Antioxidant Indicators .....	30
2.1 Introduction.....	31
2.1.1 Potential Approaches to Pyri(mi)dinol BODIPY Conjugates.....	32
2.1.2 Aryl-Linked Pyri(mi)dinol-BODIPY-Conjugates.....	33
2.1.3 Amine or Ether Linked Pyri(mi)dinol-BODIPY-Conjugates.....	35
2.1.4 Carboxyl- or Carbamoyl-Linked Pyr(imi)dinol-BODIPY Conjugates.....	41
2.1.5 Alkene-Linked Pyri(mi)dinol-BODIPY Conjugates.....	45
2.2 Results and Discussion.....	46
2.2.1 Formation of Aryl-Linked Pyrimidinol-BODIPY-Conjugates.....	46
2.2.1.1 Para-Substitution.....	46
2.2.1.2 Radical-Trapping Activity of para-Pyrimidyl-BODIPY.....	49
2.2.1.3 Synthesis,Fluorescent and Kinetic study of Meta,and Ortho-Pyrimidyl-BODIPY.....	54
2.2.2 Formation of Amine or Ether Linked Pyri(mi)dinol-BODIPY-Conjugates.....	59
2.2.3 Formation of Carboxyl- or Carbamoyl-Linked Pyri(mi)dinol-BODIPY Conjugates.....	67
2.2.4 Formation of Alkene-Linked Pyri(mi)dinol-BODIPY Conjugates.....	76
2.3 General Experimental Procedures.....	78
2.4 References.....	98
Chapter 3 Cyclopropane Lipids: Autoxidizability and Potential as Inhibitors-	

of Lipoxygenases.....	101
3.1 Introduction.....	102
3.1.1 Potential Selective Lipoxygenase Inhibitors Design Based on Linoleic Acid.....	103
3.1.2 Synthetic Approaches to Cyclopropanated Lipids.....	107
3.2 Results and Discussion.....	110
3.2.1 Synthesis of Cyclopropanated Linoleate Derivatives.....	110
3.2.2 Autoxidizability of Methyl Mono-CP Linoleate.....	111
3.2.3 Inhibition of Soybean Lipoxygenase by Cyclopropanated Linoleic Acids.....	114
3.2.3.1 Synthesis of Cyclopropanated Linoleic Acids.....	114
3.2.3.2 Soybean Lipoxygenase Assays.....	114
3.3 Experimental Procedures.....	118
3.4 References.....	122

## List of Schemes

Scheme 1.1 Radical Chain Mechanism of Hydrocarbon Autoxidation.....	3
Scheme 1.2 The pentadienyl radical intermediate arising in polyunsaturated lipid peroxidation.....	4
Scheme 1.3 Mechanism of peroxidation of methyl linoleate, where $k_{\beta I} = 2.4 \times 10^6 \text{ s}^{-1}$ , $k_{\beta II} = 27 \text{ s}^{-1}$ , $k_{\beta III} = 430 \text{ s}^{-1}$ .....	6
Scheme 1.4 The dipyrromethene core structure of BODIPY fluorophores.....	14
Scheme 1.5 Different hydroperoxides derived from arachidonic acid catalyzed by different LOXs.....	16
Scheme 1.6 General mechanism of polyunsaturated fatty acid dioxygenation catalyzed by lipoxygenases.....	18
Scheme 2.1 Potential approaches to pyri(mi)dinol BODIPY conjugates.....	33
Scheme 2.2 Synthesis of BODIPY using aromatic aldehyde as starting material.....	34
Scheme 2.3 Synthesis of BODIPY using acid chloride as starting material.....	34
Scheme 2.4 Synthesis of BODIPY using anhydride as starting material.....	34
Scheme 2.5 Retrosynthesis of aryl-linked pyri(mi)dinol-BODIPY-conjugates.....	35
Scheme 2.6 Reductive amination of <i>meso</i> -formyl-BODIPY.....	36
Scheme 2.7 Retrosynthesis of pyri(mi)dinol-BODIPY-conjugates through reductive amination.....	36
Scheme 2.8 Synthesis of BODIPY bearing an alkyl halide at the meso position.....	37
Scheme 2.9 Retrosynthesis of amine linked pyri(mi)dinol-BODIPY-conjugates.....	38

Scheme 2.10 Alkylating benzylamine with oxirane.....	39
Scheme 2.11 Nonaqueous chloro-de-diazonation of pyri(mi)dyl amines.....	39
Scheme 2.12 Reductive amination of pyrimidinol amine with formaldehyde.....	39
Scheme 2.13 Retrosynthesis of ether linked pyri(mi)dinol-BODIPY-conjugates.....	40
Scheme 2.14 Hydrolysis of PM650.....	40
Scheme 2.15 Transformation of alkyl alcohol to alkyl triflate.....	40
Scheme 2.16 Retrosynthesis of pyri(mi)dinol-BODIPY-conjugates through triflate activated BODIPY.....	41
Scheme 2.17 Alkylating aniline with methyl bromoacetate.....	42
Scheme 2.18 Esterification of PMOH with EDC activated trolox.....	42
Scheme 2.19 Retrosynthesis of carboxyl-linked pyri(mi)dinol-BODIPY-conjugates using pyri(mi)dinol acid species.....	43
Scheme 2.20 Synthesis of BODIPY acid using anhydride as starting material.....	44
Scheme 2.21 Retrosynthesis of carboxyl-linked pyri(mi)dinol-BODIPY-conjugates using BODIPY acid species.....	44
Scheme 2.22 Synthesis of carbamoyl-linked BODIPY conjugates using CDI activated BODIPY species.....	45
Scheme 2.23 Synthesis of alkene linked BODIPY conjugate through olefin metathesis .....	45
Scheme 2.24 Retrosynthesis of alkene-linked pyri(mi)dinol-BODIPY conjugates.....	46
Scheme 2.25 Synthesis of para-Pyrimidyl-BODIPY.....	47
Scheme 2.26 Mechanism of formation of mono-lithium amide in the reaction of	



pyridylamine with n-BuLi.....	48
Scheme 2.27 A. Thermolysis of AIBN in the presence of Oxygen. B. Scavenging of AIBN derived peroxy radicals by para-Pyrimidyl-BODIPY.....	50
Scheme 2.28 General mechanism for perester peroxy radical clock.....	52
Scheme 2.29 Synthesis of meta-Pyrimidyl-BODIPY 2.36.....	56
Scheme 2.30 Attempted synthesis of ortho-Pyrimidyl-BODIPY.....	59
Scheme 2.31 Attempted synthesis of pyri(mi)dinol-BODIPY-conjugates through reductive amination using 2,6 diethyl-substituted BODIPY aldehyde...60	
Scheme 2.32 Attempted synthesis of pyri(mi)dinol-BODIPY-conjugates through reductive amination using 2,6 dichloro-substituted BODIPY aldehyde .....	61
Scheme 2.33 A. Formation of BODIPY-I. B. Attempted synthesis of pyridinol-BODIPY-conjugate through alkylation with BODIPY-I.....	62
Scheme 2.34 Attempted synthesis of triflate-activated BODIPY.....	63
Scheme 2.35 Installation of butylamine group onto pyrimidyl compound 2.7.....	64
Scheme 2.36 Synthesis of amine-linked pyrimidyl-BODIPY-conjugate.....	65
Scheme 2.37 Attempted synthesis of amine linked pyrimidinol-BODIPY-conjugate.	65
Scheme 2.38 Installation of pentanol group onto aminopyrimidine 2.5.....	66
Scheme 2.39 Attempted synthesis of ether linked pyrimidyl-BODIPY-conjugate.....	67
Scheme 2.40 Installation of butyric acid group onto amino pyrimidinol.....	68
Scheme 2.41 Attempted EDC coupling using BODIPY-OH and pyrimidinol-butyric acid.....	69

Scheme 2.42 EDC coupling using BODIPY-OH and pyrimidyl-butyric acid.....	69
Scheme 2.43 CDI coupling using PMOH and pyrimidyl-butyric acid.....	70
Scheme 2.44 Attempted synthesis of carbamoyl-linked pyrimidyl-BODIPY conjugate using CDI activated BODIPY species.....	71
Scheme 2.45 Synthesis of BODIPY acid.....	71
Scheme 2.46 DCC coupling using BODIPY acid with hydroxyethyl pyrimidinol 2.68 .....	72
Scheme 2.47 Attempted synthesis of pyrimidyl-acetic acid.....	73
Scheme 2.48 Synthesis of pyridinol-acetic acid.....	74
Scheme 2.49 Synthesis of compound 2.6.....	74
Scheme 2.50 Mechanism of formation of pyridine imines from direct alkylation of pyridyl compound 2.6 with methyl bromoacetate.....	75
Scheme 2.51 Attempted CDI coupling using BODIPY-OH and pyridinol acetic acid .....	75
Scheme 2.52 Formation of putative acyl pyridinium ion intermediate.....	76
Scheme 2.53 Synthesis of BODIPY-butene.....	77
Scheme 2.54 Synthesis of allylated pyrimidinol 2.83.....	77
Scheme 2.55 Attempted metathesis of an allylated pyrimidinol and homoallylated BODIPY. ....	78
Scheme 2.56 Coordination of Grubs II catalyst with allylated pyrimidinol. ....	78
Scheme 3.1 Mechanism of formation of possible peroxide products.....	107
Scheme 3.2 Cyclopropanation of cyclohexene .....	107

Scheme 3.3 Selective cyclopropanation reaction through complexation.....	108
Scheme 3.4 Selective cyclopropanation using steric effects.....	109
Scheme 3.5 Synthesis of methyl monocyclopropanated and dicyclopropanated linoleate. ....	111
Scheme 3.6 Mechanism of slow peroxy radical clock approach, where $k_{\beta\text{II}} = 27 \text{ s}^{-1}$ , $k_{\beta\text{III}} = 430 \text{ s}^{-1}$ .....	111
Scheme 3.7 Synthesis of cyclopropanated linoleic acids.....	114

## List of Figures

Figure 1.1 Illustration of the H-atom transfer (HAT) and proton-coupled electron transfer (PCET) mechanisms for the reaction of a phenol and a peroxy radical.....	10
Figure 1.2 General mechanism of reductive PeT and oxidative PeT.....	15
Figure 1.3 B-TOH and its reaction with peroxy radicals.....	16
Figure 1.4 The structure of Stable-5LOX. The N-terminal C2-like domain is in dark gray, and the catalytic domain in light gray. The distinctive arched helix is in blue, and helix $\alpha 2$ in red. The internal cavity, generated with CastP (32), is in pink, and the Fe is an orange sphere. The positions of the mutated amino acids are indicated in mesh rendering: green, putative membrane insertion residues; yellow, proximal cysteines; and blue, the KKK to ENL	

substitution.....	17
Figure 2.1 Emission intensity time profiles for para-Pyrimidyl-BODIPY (A) incubated at 55°C with (■) or without (◆) AIBN and B-TOH (B) incubated at 55°C without (■) or with (◆) AIBN in toluene.....	51
Figure 2.2 Ratio of conjugated to non-conjugated products <i>versus</i> 1/[PPB] (A) and 1/[B-TOH] (B) obtained from peroxy radical clock experiments(incubated at 37°C in benzonitrile by perester 2.28 radical clock) .....	53
Figure 2.3 Predicted three-dimensional structures of para-Pyrimidyl BODIPY 2.23 (A) and B-TOH (B) .....	54
Figure 2.4 A. Emission intensity time profiles for Meta-Pyrimidyl-BODIPY incubated at 55°C with (■) and without(◆) AIBN in toluene. B. Clocking experiments, ratio of conjugated:nonconjugated products <i>versus</i> 1/[MPB] (incubated at 37°C in benzonitrile by perester 2.28 radical clock) .....	57
Figure 2.5 Predicted three-dimensional structure of ortho-Pyrimidyl-BODIPY.....	58
Figure 2.6 Emission intensity time profiles for Dye 2.67 incubated at 55°C with(■) and without(◆) AIBN in toluene.....	72
Figure 3.1 Ratio of <i>cis,trans</i> to <i>trans,trans</i> methyl hydroperoxyoctadecadienoate oxidation products as a function of mono-(●) and di-(■) cyclopropanated methyl linoleate concentration in MeOAMVN-initiated autoxidations of methyl linoleate at 37°C in chlorobenzene.....	113
Figure 3.2 Michealis-Menten plots for the utilization of mono-Cp linoleic acid(■) and linoleic acid(●) by sLOX-1 in borate buffer pH 9.2.....	115

Figure 3.3 Soybean lipoxygenase activity plotted as a function of added inhibitor concentration determined relative to the initial rates measured under identical experimental conditions, but without added inhibitor. Inhibitors: dicyclopropanated linoleic acid 3.30 (●) and monocyclopropanated linoleic acid 3.31 and 3.32 (■) .....116

### List of Tables

Table 3.1 Calculated BDE and experimental  $k_p$  for 3.4-3.7.<sup>a</sup>Calculated at the CBS-QB3 level of theory. <sup>b</sup>Data from reference 3.....105

### List of Abbreviations

ArOH	phenolic antioxidant
$\alpha$ -TOH	$\alpha$ -tocopherol
BDE	bond dissociation enthalpy
BODIPY	boron-dipyrromethene
B-TOH	BODIPY- $\alpha$ -tocopherol

CAT	catalase
CFAs	cyclopropane fatty acids
CP	cyclopropanated
CDI	1,1'-Carbonyldiimidazole
DDQ	2,3-Dichloro-5,6-dicyano-1,4-benzoquinone
DCC	N,N'-Dicyclohexylcarbodiimide
EDC	1-Ethyl-3-(3-dimethylaminopropyl)carbodiimide
ED	electron donating
EW	electron withdrawing
FLAP	5-lipoxygenase-activating protein
GPx	glutathione peroxidase
HAT	H-atom transfer
13-HPODE	13-hydroperoxyoctadecadienoic acid
HOMO	highest occupied molecular orbital
IC <sub>50</sub>	the half maximal inhibitory concentration
LDL	low density lipoprotein
LOX	lipoxygenase
LUMO	lowest unoccupied molecular orbital
ML	methyl linoleate
PCET	proton-coupled electron transfer
PeT	photoinduced electron transfer
PLA2	phospholipase A2

PCC	pyridinium chlorochromate
PDC	pyridinium dichromate
ROS	reactive oxygen species
rt	room temperature
SOD	superoxide dismutase
sLOX-1	soybean lipoxygenase-1
TFA	trifluoroacetic acid

**Chapter 1**  
**Introduction**



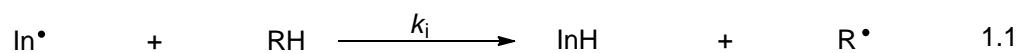
## 1.1 Autoxidation

For centuries it has been known that fats and oils turn rancid and deteriorate when they are exposed to air. This phenomenon, known as autoxidation, is due to the formal reaction between lipids and molecular oxygen, and is the reason that all petroleum-derived products degrade over time, including polymers, lubricating oils and fuels. Documented scientific study about rancidification was not carried out until the early 19th century, when Nicolas Théodore de Saussure, a Swiss chemist, published his work: "Recherches Chimiques sur la Vegetation",<sup>[1]</sup> in which he used a mercury manometer to follow the absorption of oxygen during the storage of plant oil and reported an associated increase in viscosity and bad smell. Later, Berzelius, who discovered selenium, suggested that the phenomenon de Saussure had observed might be involved in the spontaneous ignition of wool lubricated with linseed oil in textile mills. Parmentier, a pharmacist known for advocating the growing and consumption of potatoes in France, hypothesized also that oxygen, in combining with fats, was the agent of rancidity.<sup>[2]</sup>

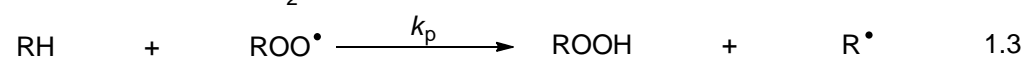
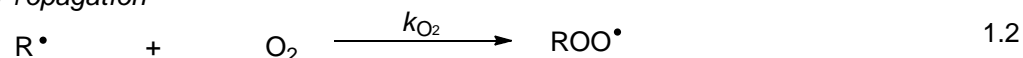
The development of methods to measure peroxides, which was demonstrated by Carl Engler and co-workers to be the primary products in the oxidation of various hydrocarbon substrates in the absence of water, enabled the investigation of the fundamental mechanism of hydrocarbon autoxidation. The first step of understanding the mechanism was taken by Stephens,<sup>[3]</sup> who was able to isolate a cyclohexene-derived peroxide which was later identified by Criegee<sup>[4]</sup> to be cyclohexene 3-hydroperoxide. Farmer and co-workers greatly extended the number of

hydroperoxides known to be products of olefin oxidation, which further proved the hydroperoxide hypothesis of lipid autoxidation. Subsequent work by Bolland, Bateman and colleagues at the British Rubber Producers Research Association clearly defined the role of free radicals in the autoxidation process, which led to the radical chain mechanism shown in Scheme 1.1<sup>[5]-[8]</sup> that is generally accepted nowadays.

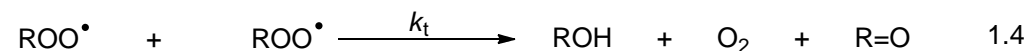
*Initiation*



*Propagation*



*Termination*



**Scheme 1.1** Radical chain mechanism of hydrocarbon autoxidation.<sup>[5]-[8]</sup>

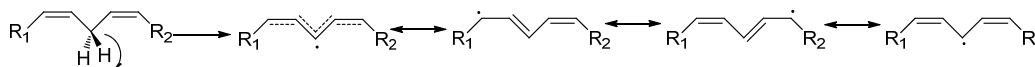
As with any radical chain reaction, hydrocarbon autoxidation can be divided into three steps: chain initiation, propagation and termination. In the initiation step, an initiating radical (In<sup>•</sup>) abstracts a hydrogen atom from the hydrocarbon molecule and generates an alkyl radical (R<sup>•</sup>). The initiating radical can be any radical that can abstract a hydrogen atom from the hydrocarbon, and is usually generated thermally or photochemically, from azo compounds or organic peroxides and their derivatives (e.g. peroxyesters, diacylperoxides). In the propagation step, the alkyl radical generated from the hydrocarbon reacts with oxygen at or near a diffusion-controlled rate to form the peroxy radical (ROO<sup>•</sup>), which readily reacts with another hydrocarbon molecule

to give a hydroperoxide (ROOH) and a new alkyl radical (R'). The chain reaction terminates when two chain-carrying radicals react to yield non-radical products (Eq 1.4).<sup>[9],[10]</sup>

## 1.2 Lipid Peroxidation

Lipid peroxidation refers to the autoxidation of biological lipids, including fatty acids (e.g. arachidonic acid and linoleic acid) and sterols (e.g. cholesterol).

Polyunsaturated fatty acids are particularly susceptible to autoxidation because they contain multiple double bonds in between which lie methylene (-CH<sub>2</sub>-) groups that possess especially weak C-H bonds (bond dissociation enthalpy, BDE ~ 76 kcal/mol) owing to the high stability of the resultant radical species. As Scheme 1.2 shows, the so-called pentadienyl radical is stabilized through resonance with the  $\pi$  electrons of the two adjacent double bonds.



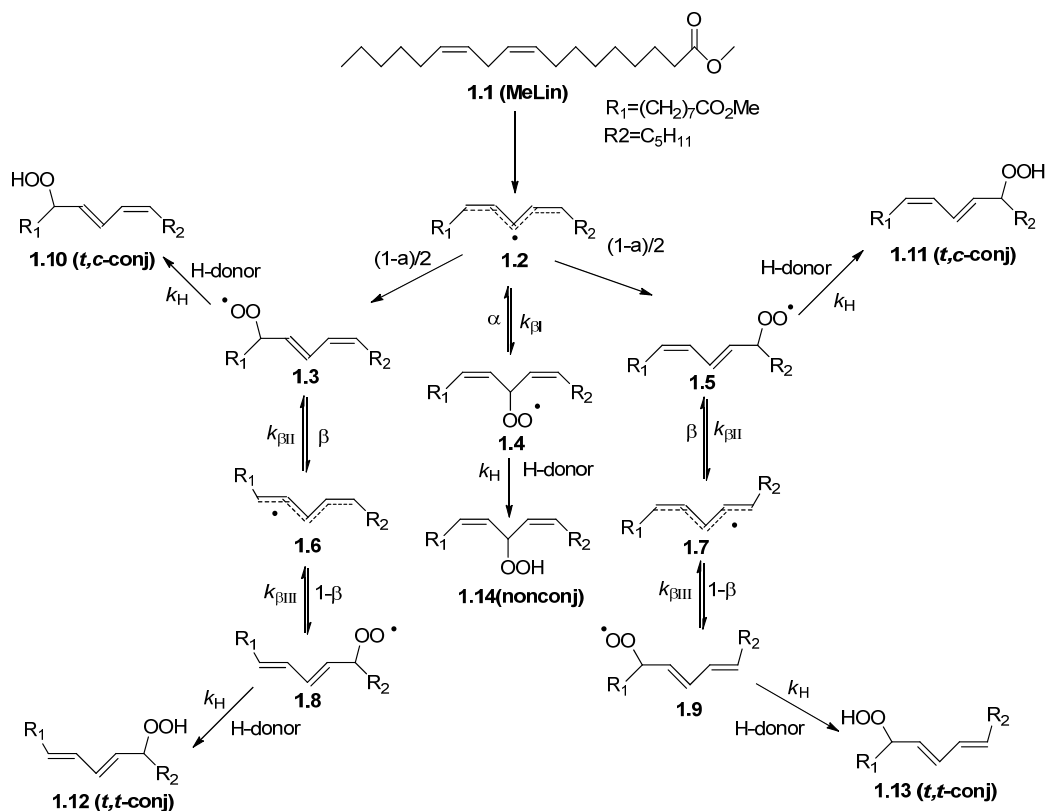
**Scheme 1.2** The pentadienyl radical intermediate arising in polyunsaturated lipid peroxidation

The chemical species that initiate the peroxidation of lipids in biological systems are often referred to as reactive oxygen species (ROS), most relevant of which are the hydroxyl radical (HO•) and the hydroperoxyl radical (HOO•), the conjugate acid of

the superoxide radical anion ( $O_2^{\bullet-}$ ). These species are unavoidable byproducts of cellular respiration; electrons passing "down" the electron transport chain 'leak' from the main path (especially as they pass through ubiquinone) and go directly to reduce oxygen molecules to the superoxide anion. Furthermore, they are produced directly by dedicated enzymes (e.g. NADPH oxidase) in phagocytic cells of the immune and inflammatory systems, such as neutrophils and macrophages.

The products of lipid peroxidation have toxic effects on cell structure, development and survival, and are implicated in various pathological conditions. For example, the oxidation of cholesterol esterified polyunsaturated acids in low-density lipoprotein (LDL), which circulates cholesterol in the bloodstream, is believed to be the initiating event in the development of atherosclerosis. Another example of the deleterious effects of lipid peroxidation involves membrane phospholipids; their oxidation results in increased mitochondrial permeability and release of cytochrome c, which leads to a disturbance of mitochondrial electron transport and initiates cell apoptosis – suggested to be an important factor in ageing. Furthermore, although not yet proven unequivocally, mounting evidence strongly implicates that the accumulation of oxidative damage to brain lipids in the pathogenesis of neurodegenerative diseases such as Alzheimer's Disease (AD).

The mechanism of peroxidation of unsaturated lipids is well understood.<sup>[11],[12]</sup> It is illustrated in Scheme 1.3 using methyl linoleate as an example.<sup>[13]</sup>



**Scheme 1.3** Mechanism of peroxidation of methyl linoleate, where  $k_{\beta\text{I}} = 2.4 \times 10^6 \text{ s}^{-1}$ ,  
 $k_{\beta\text{II}} = 27 \text{ s}^{-1}$ ,  $k_{\beta\text{III}} = 430 \text{ s}^{-1}$ .<sup>[13]</sup>

The autoxidation of **1.1** proceeds by the series of free-radical reactions introduced in Scheme 1.1: Firstly, a pentadienyl radical is formed upon hydrogen atom abstraction from the bis-allylic position of **1.1**. This is followed by oxygen insertion at one of the three different positions that bears the unpaired electron spin density (as in Scheme 1.2) to generate cis,trans conjugated dienylperoxyl radicals **1.3** and **1.5**, as well as the cis,cis non-conjugated dienylperoxyl radical **1.4** which can each oxidize another molecule of methyl linoleate to yield the corresponding hydroperoxides **1.10**, **1.11** and **1.14**. Bond rotation followed by  $\beta$ -fragmentation and re-addition of  $\text{O}_2$  leads to the isomerization of **1.3** and **1.5** to the thermodynamically-favoured trans,trans dienylperoxyls **1.8** and **1.9** which lead to the

corresponding hydroperoxides **1.12** and **1.13**.

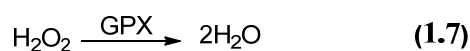
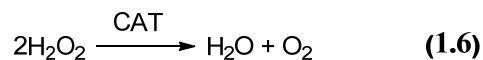
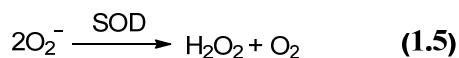
The observed product distribution is highly dependent on the rate of reduction of the intermediate peroxy radicals, which is dependent on both the concentration and kinetics of H-atom transfer from the hydrogen atom donor present in solution.

In the absence of an added H-donor or in the presence of a weak H-donor that can't compete with  $k_{\beta I}$ , the trans,trans diene hydroperoxides **1.12** and **1.13** are the major products. On the other hand, when there is a good H-donor available, the cis,trans dienyloxy radicals **1.3** and **1.5** will be trapped before they can isomerize and generate the cis,trans diene hydroperoxides **1.10** and **1.11** as the major products. The non-conjugated hydroperoxide **1.14** is observed only in the presence of high concentrations of a very good H-atom donor (e.g.  $\alpha$ -tocopherol, see section 1.3).

### **1.3 Antioxidants**

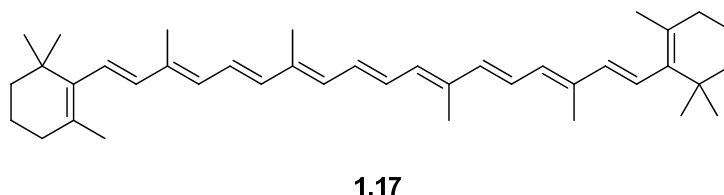
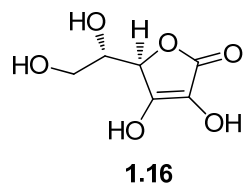
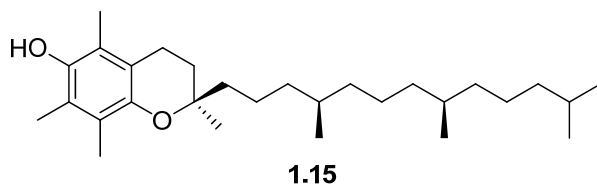
Antioxidants slow the rate of oxidation of the hydrocarbons to which they are added. They are typically separated into two classes: preventive antioxidants and chain-breaking antioxidants. Preventive antioxidants slow the rate of initiation, whereas chain-breaking antioxidants slow the rate of propagation. In biological systems, the key preventive antioxidants are those that eliminate reactive oxygen species that can initiate lipid peroxidation. The antioxidant enzymes superoxide dismutase (SOD), catalase (CAT) and glutathione peroxidase (GPx) are the most important examples, and reduce superoxide, hydrogen peroxide and hydroperoxides

to hydrogen peroxide, water and alcohols, respectively (Eq. 1.5-1.7).<sup>[14]</sup>



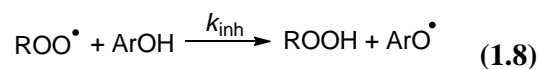
The oxidized glutathione is then recycled by another antioxidant enzyme -- glutathione reductase, which depends on the common reducing cofactor NAD(P)H.

Chain-breaking antioxidants are best exemplified by vitamin E. Vitamin E is a group of 8 related fat-soluble compounds that include both tocopherols (4) and tocotrienols (4); among them,  $\alpha$ -tocopherol (1.15) is the highest antioxidant activity.<sup>[15]</sup> Due to its inherently high reactivity towards radicals and its high solubility in fats, it is the key player in inhibiting lipid peroxidation in cell membranes and circulating lipoproteins. Vitamin C (1.16), also known as ascorbic acid, is a water-soluble chain-breaking antioxidant, and serves to both scavenge free radicals in the aqueous parts of the cell and surrounding media, and also serves to regenerate oxidized Vitamin E and work synergistically with vitamin E to quench free radicals.<sup>[16]</sup>  $\beta$ -Carotene (1.17), a precursor to Vitamin A, is only a moderately effective inhibitor of lipid peroxidation under most conditions, and arguably works best in quenching singlet oxygen.<sup>[17]</sup>



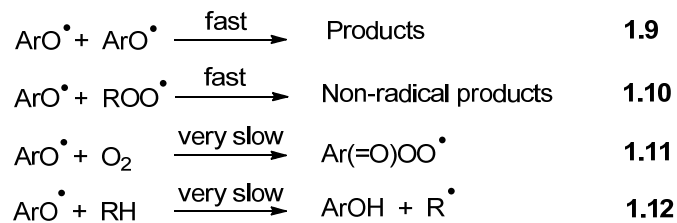
#### 1.4 Phenolic Antioxidants

It has been long known that phenolic compounds are effective antioxidants. Indeed, phenolic compounds have been used for decades as industrial antioxidants. Phenolic antioxidants are chain-breaking antioxidants, and inhibit autoxidation by transferring their phenolic H-atom to a chain-carrying peroxy radical (eq 1.8) at a rate (proportional to  $k_{inh}[ArOH]$ ) faster than that of chain propagation (proportional to  $k_p[L-H]$ ).



Afterwards, the formed phenoxy radical will react with another chain-carrying peroxy radical or with another phenoxy radical to form non-radical species. These reactions are much faster than the reactions of phenoxy radicals with  $O_2$  or the hydrocarbon – which would result in continuation of the radical chain reaction.





The mechanism of the reaction in eq 1.8 has long been thought to be a H-atom transfer (HAT) process, but more recent quantum chemical calculations suggest that the reaction is more appropriately described as a proton-coupled electron transfer (PCET).<sup>[18]</sup> In the PCET mechanism (Fig 1.1), the proton will move from the phenol to the lone pair on peroxy radical within a H-bonded complex. Concerted with the proton movement is the electron transfer from the 2p-type lone pair of the phenolic oxygen to the  $\pi^*$  orbital containing the unpaired electron on the peroxy radical.

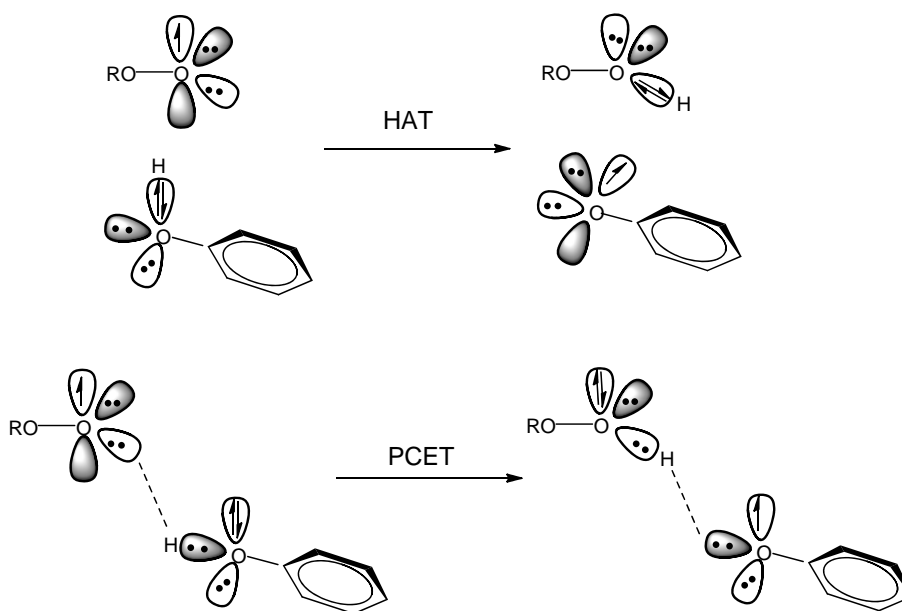


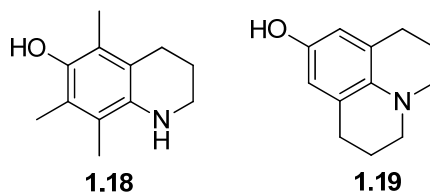
**Figure 1.1** Illustration of the H-atom transfer (HAT) and proton-coupled electron transfer (PCET) mechanisms for the reaction of a phenol and a peroxy radical.<sup>[18]</sup>

The reactivity of a phenolic antioxidant is mainly determined by its O-H bond dissociation enthalpy (BDE). The lower the BDE, the easier it is for the phenolic antioxidant to give up its H-atom to a chain-carrying peroxy radical. Electron-donating substituents at the ortho and para positions relative to the hydroxyl group stabilize the corresponding phenoxyl radical and thus effectively decrease the O-H BDE.<sup>[19]-[21]</sup> For example, p-methoxyphenol has an O-H BDE of  $82.8 \pm 0.8$  versus  $88.3 \pm 0.2$  for phenol itself.<sup>[22]</sup>

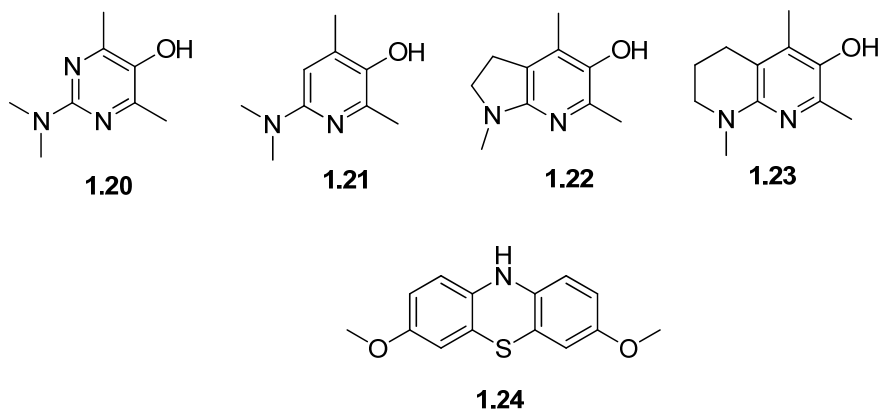
$\alpha$ -Tocopherol (**1.15**), the most potent form of Vitamin E and the major lipid-soluble antioxidant found in nature,<sup>[23],[24]</sup> has a very low O-H BDE of  $78.3 \pm 0.3$  kcal/mol<sup>[25]</sup> due to the combination of the para ring oxygen and the alkyl substitution on the ring, leading to an inhibition rate constant of  $3.2 \times 10^6 \text{ M}^{-1}\text{s}^{-1}$ .<sup>[25]</sup>

### 1.5 Improving Antioxidant Activity

Efforts to design new phenolic antioxidants with increased rates of H-atom transfer to peroxy radicals have been largely unsuccessful because the substitution of phenols with increasingly ED groups (e.g.,  $-\text{NH}_2$  and  $-\text{NR}_2$ ) to decrease their O-H BDEs also decreases their ionization potentials (IPs) such that they react directly with oxygen. For example, an aza-analogue of  $\alpha$ -TOH (**1.18**)<sup>[26]</sup> and 9-hydroxyjulolidine (**1.19**)<sup>[27]</sup> were both found to be useless as antioxidants because they were unstable in air.



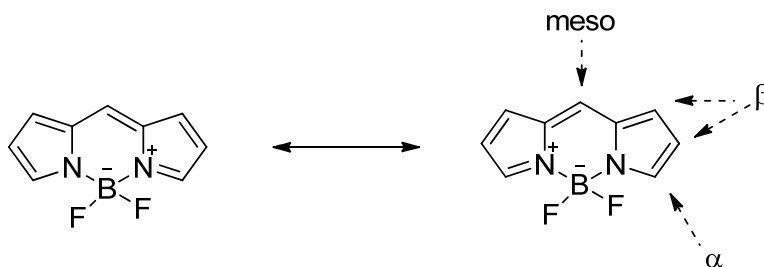
Within the last decade, our research group has developed a strategy to stabilize electron-rich phenols to autoxidation, such that compounds with peroxy radical-trapping activities far superior to  $\alpha$ -tocopherol could be developed. These compounds, pyrimidinols and pyridinols, are aza-analogs of phenols, and are so effective because the incorporation of nitrogen atoms at the 3- and/or 5-positions of the phenolic ring significantly raises the IP and greatly improves the stability of the compound in air while only minimally increasing the O-H BDE.<sup>[25]</sup> For example, pyrimidinol **1.20** and pyridinol **1.21** are 2- and 5-fold more effective peroxy radical-trapping antioxidants than  $\alpha$ -TOH based on the absolute inhibition rate constants derived from O<sub>2</sub>-uptake experiments. The vacant 5-position on the pyridine ring of the latter compound allows for fusion of an additional aliphatic ring, a substitution that further lowers the O-H BDE. In the end, the pyridinols **1.22** and **1.23** are, to the best of our knowledge, the fastest peroxy radical-trapping chain-breaking antioxidants ever reported (previously 3,7-dimethoxyphenothiazine (**1.24**) with  $k_{inh} = 5.5 \times 10^7 \text{ M}^{-1} \text{ s}^{-1}$ ).<sup>[28]</sup> The air-stability of **1.22** is moderate, but its  $k_{inh}$  exceeds  $10^8 \text{ M}^{-1} \text{ s}^{-1}$ , making it exclusively entropy-controlled.



Lipophilic derivatives of **1.23** have shown unprecedented efficacy in suppressing the oxidation of the cholesterol esterified polyunsaturated fatty acids. However, further studies in biological model systems or *in vivo* have been hampered by the lack of good tools to monitor their effects.

## 1.6 BODIPY

BODIPY, short for boron-dipyrromethene, is a class of fluorescent dyes. It is composed of dipyrromethene complexed to a disubstituted boron atom – typically a ‘BF<sub>2</sub>’ unit. BODIPY dyes tend to be strongly UV-absorbing small molecules that emit relatively sharp fluorescence peaks with high quantum yields.<sup>[29]</sup> They are relatively insensitive to the polarity and pH of their environment and are reasonably stable to physiological conditions. Furthermore, substitutions to the BODIPY core structure (Scheme 1.4) enable tuning of their spectroscopic characteristics; consequently, these dyes are widely used in analytical chemistry (e.g. ion detection) and biochemistry (e.g. protein labeling).



**Scheme 1.4** The dipyrromethene core structure of BODIPY fluorophores.<sup>[29]</sup>

The introduction of substituents at the meso-position of the BODIPY core can change its fluorescence properties. Some of such substituents, depending on their oxidation potentials relative to the excited state of the BODIPY core, can act as electron donors or acceptors. If electron transfer occurs, then the fluorescence is diminished when the excited state of the BODIPY core is reduced. This is sometimes referred to as reductive-PeT (PeT = photoinduced electron transfer), or a-PeT (“a” for acceptor; **Fig 1.2b**). However, if the energy states are such that the excited-state of the BODIPY can donate electrons to the substituent LUMO, then oxidative-PeT, or d-PeT, occurs (“d” for donor; **Fig 1.2c**).

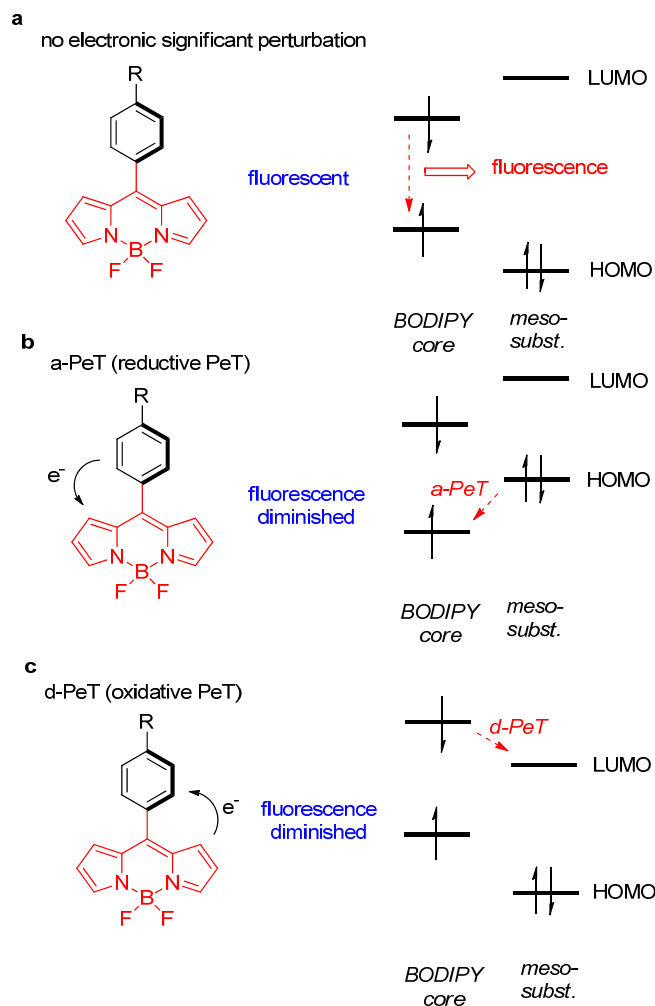


**Figure 1.2** General mechanism of reductive PeT and oxidative PeT.<sup>[29]</sup>

By applying these principles, various detecting and monitoring probes have been designed using substituted BODIPY. For example, Cosa's group<sup>[30]</sup> has made a BODIPY- $\alpha$ -TOH adduct which can be used as an off/on fluorescent antioxidant indicator in monitoring the antioxidant depletion and the onset of radical-mediated oxidation through emission enhancement over time. The fluorescence of B-TOH (**1.25**) is quenched by reductive-PeT between BODIPY and  $\alpha$ -TOH, but upon reaction of the  $\alpha$ -TOH (reporter) moiety with peroxy radicals, this can no longer occur and a ten-fold increase in fluorescence intensity is observed.

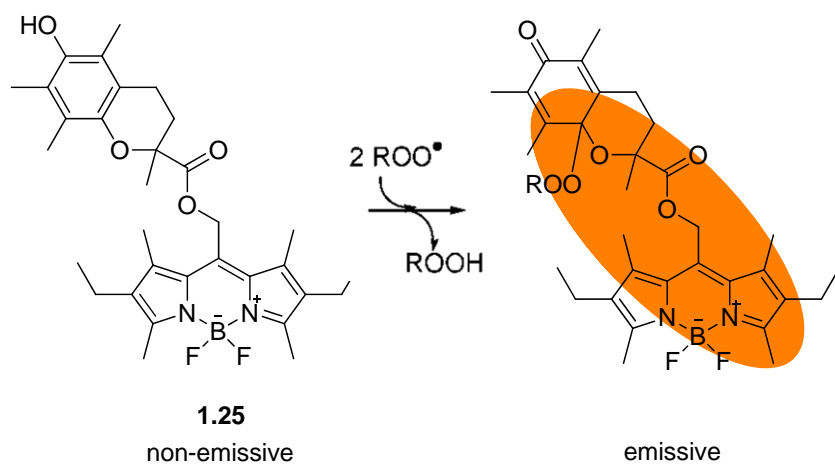
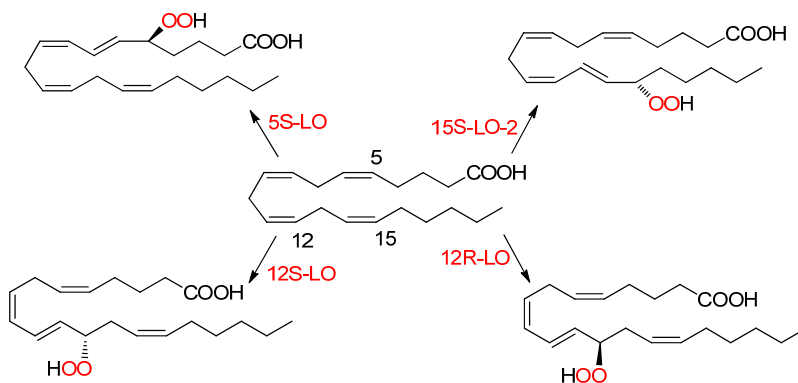


**Figure 1.3** B-TOH and its reaction with peroxy radicals.<sup>[30]</sup>

### 1.7 Lipoxygenases

Lipoxygenases are a family of iron-containing enzymes that catalyse the dioxygenation of polyunsaturated fatty acids in lipids containing a *cis,cis*-1,4-pentadiene structure. There are five LOX isoforms in humans that are active on arachidonic acid, and they catalyze four distinct reactions (5S, 12R, 12S, or 15S dioxygenation); the immediate products being individual fatty acid hydroperoxides (Scheme 1.5).



**Scheme 1.5** Different hydroperoxides derived from arachidonic acid catalyzed by

different LOXs.<sup>[35]</sup>

There are also numerous LOX enzymes found in plants, nearly all of which have evolved to utilize linoleic or linolenic acid as substrates, and many of which are quite specific for these fatty acids.<sup>[31],[32]</sup>

The proteins are highly homologous, and consist of a single polypeptide chain that is folded into two domains; a small N-terminal beta-barrel domain, which binds to the cell membrane and a major C-terminal, mostly alpha-helical, catalytic domain which contains the active site (**Fig 1.4**).<sup>[33]</sup> As a consequence, only the catalytic iron and three out of the five amino acids (Leu and Phe/Tyr) that serve as iron ligands are absolutely conserved within the LOX gene family.

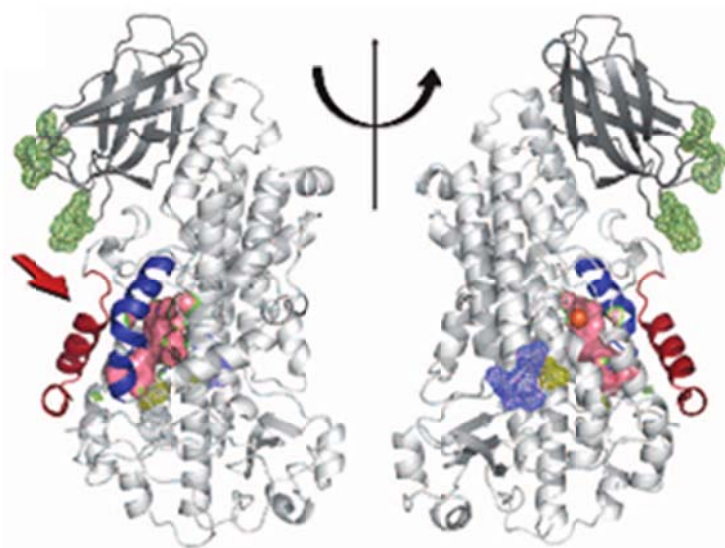
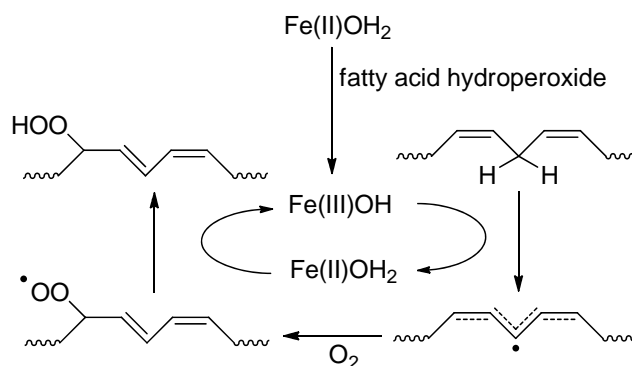


**Figure 1.4** The structure of Stable-5LOX. The N-terminal C2-like domain is in dark gray, and the catalytic domain in light gray. The distinctive arched helix is in blue, and helix  $\alpha 2$  in red. The internal cavity, generated with CastP (32), is in pink, and the Fe is an orange sphere. The positions of the mutated amino acids are indicated in mesh rendering: green, putative membrane insertion residues; yellow, proximal



cysteines; and blue, the KKK to ENL substitution.<sup>[33]</sup>

Though the structure of the products vary, the oxygenations that are catalyzed by LOX are all conducted on the similar *cis,cis*-1,4-pentadiene moiety in the substrates' structures, which implies that they share a common mechanism (Scheme 1.6).



**Scheme 1.6** General mechanism of polyunsaturated fatty acid dioxygenation catalyzed by lipoxygenases

The catalytically active form of the enzyme has an active site Fe(III)-hydroxyl species that generally needs to be generated via oxidation of the Fe(II)-water form of the resting (isolated) state of the enzyme by trace amounts of fatty acid hydroperoxide that are formed by autoxidation.<sup>[34]</sup> The enzyme is then capable of abstracting an H-atom from the substrate to form a pentadienyl radical which is capable of reaction with molecular oxygen to form a peroxy radical. The enzyme will then restore to its catalytically form by reduction of the peroxy radical to form a hydroperoxide product. The regioselectivity of dioxygenation of the different isoforms of LOX must then be based on how the substrate is bound in the active site and/or how oxygen is directed

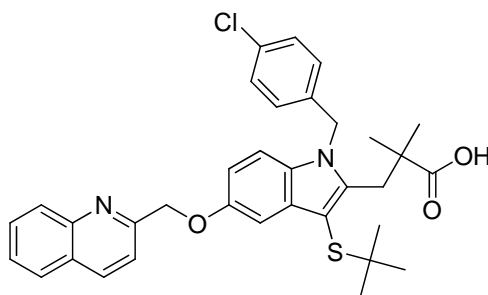
toward a specific face of a specific carbon atom of the intermediate pentadienyl radical. Unfortunately, to date there are no three dimensional (x-ray) crystallographic structures of lipoxygenases with the substrate (or an appropriate analog) bound, such that some insight into the regiochemical control could be provided. In fact, until very recently, no human lipoxygenases had been crystallized – even in the absence of substrate or inhibitors.

### **1.8 Lipoxygenase Inhibitors**

The lipid hydroperoxides produced by lipoxygenase action on arachidonic acid play major roles in the control of inflammation and various other cellular processes. These powerful signaling molecules are often referred to generally as ‘eicosanoids’ since they are derived from arachidonic acid (eicosatetraenoic acid) and have been implicated in respiratory and cardiovascular diseases and cancer, making them targets for drug development.<sup>[35]</sup> The biosynthesis of these hydroperoxides first requires that arachidonic acid is released from membrane phospholipids by the action of phospholipase A<sub>2</sub> (PLA<sub>2</sub>), such that it can then be metabolized by lipoxygenase (aided by the 5-LO-activating protein – or FLAP – in case of 5-LOX). Thus, in order to intervene with cellular LOX product synthesis, three pharmacological strategies can be basically pursued: inhibition of PLA<sub>2</sub>, antagonism of FLAP (in the case of 5-lipoxygenase-derived products) and inhibition of the LOX directly.

Suppression of PLA<sub>2</sub> enzymes (e.g., by glucocorticoids) would prevent the formation of all eicosanoids, which will cause lung injury, ischemia-reperfusion injury and other tissue injury as severe side effects, making this the least desirable strategy.<sup>[36]</sup>

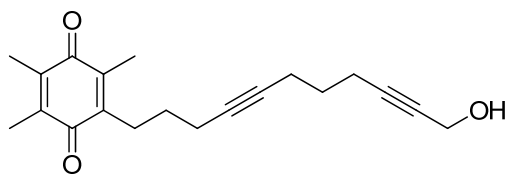
FLAP is an integral protein within the nuclear membrane and functions as a membrane anchor for 5-lipoxygenase. FLAP inhibitors may act as antagonists of FLAP by interfering with arachidonic acid substrate transfer, resulting in the reduced availability of arachidonic acid for 5-LOX at the membrane. MK0591 (**1.26**)<sup>[37]</sup> is an example of these class of inhibitors. While they are highly efficient in intact cells, their efficacy is greatly impaired in serum; MK0591 is 200-fold less potent in whole blood assays than in isolated leukocytes, possibly due to plasma protein binding of the drugs and/or competition with arachidonic acid and other cis-unsaturated fatty acids present in plasma. Another problem is the selectivity of these compounds for FLAP in cells and/or tissues where the 5-lipoxygenase cascade is to be inhibited. Since FLAP is also found at high levels in some cells lacking LOX, these inhibitors may also suppress signaling activities in these other cells, leading to undesirable side effects.



**1.26**

Inhibitors that target LOX directly can be categorized according to the inhibitory mode of action: i) redox-active LOX inhibitors, which act by reducing the active site iron, maintaining it in a reduced state that is incapable of substrate oxidation; ii) iron ligand inhibitors, containing hydroxamic acid or N-hydroxyurea groups that chelate the active site iron, altering its redox properties and interfering substrate binding; iii) non-redox inhibitors that compete with arachidonic acid for binding to LOX.

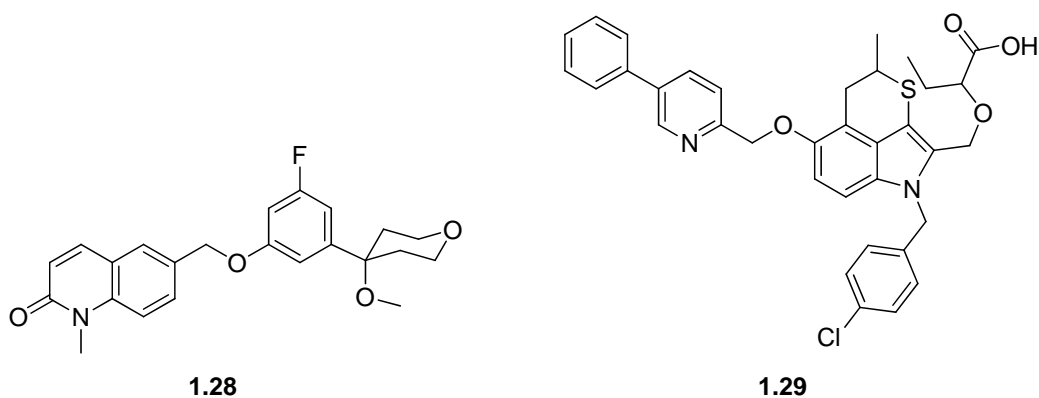
Redox-active inhibitors comprise lipophilic reducing agents including many natural plant-derived (e.g., nordihydroguaretic acid, caffeic acid, flavonoids, coumarins and several polyphenols) and synthetic compounds, such as AA-861 (**1.27**).<sup>[38]</sup> These types of inhibitors usually exhibit high activity towards LOX both in vitro and in vivo, however, generally have poor selectivity for LOX and exert severe side effects (e.g. methemoglobin formation) due to interference with other redox activity in the cell, or by the production of reactive oxygen species. These detrimental features prevent them from further clinical study and application.



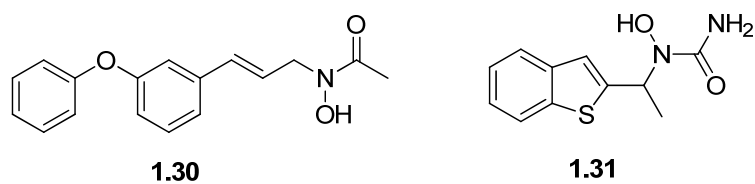
**1.27**

Non-redox inhibitors compete with arachidonic acid for binding to LOX. Such inhibitors are devoid of redox properties, and usually exhibit better selectivity than the redox inhibitors. Several examples are: ZD 2138 (**1.28**),<sup>[39]</sup> thiopyranoindole

L-699,333(**1.29**),<sup>[42]</sup> These types of inhibitors usually present high inhibition activity towards 5-LOX, however, elevated peroxide levels and/or phosphorylation of LOX by MK-2 and/or ERKs strongly impair the potency of some nonredox type LOX inhibitors in activated polymorphonuclear leukocyte.<sup>[43]</sup>



Iron ligand inhibitors represent hydroxamic acids or N-hydroxyurea derivatives that chelate the active site iron but also possess weak reducing properties. BWA4C (**1.30**) and Zileuton (**1.31**)<sup>[40],[41]</sup> are examples of such drugs. Zileuton is the first FDA approved 5-LOX inhibitor that entered into the market as a treatment for asthma. The main shortcoming for these drugs is that they have poor pharmacokinetics, necessitating that they be administered in high doses.

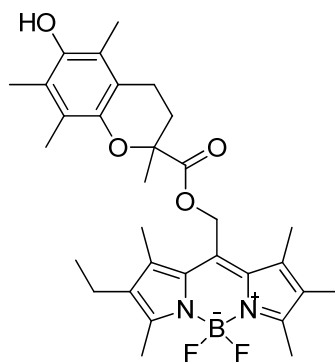


## **1.9 Research Objectives**

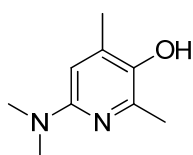
### **1.9.1 Synthesis and Study of Pyri(mi)dinol-Based Fluorescent Antioxidant Indicators**

Despite firm evidence relating lipid oxidation product levels and degenerative disease onset and progression, it remains unclear as to whether they are cause or consequence of the pathologies in question. This is confounded by the results of a number of international clinical trials designed to assess the preventive and/or therapeutic potential of the radical-trapping antioxidants Vitamin C, Vitamin E and beta-carotene, which have yielded dubious results. However, it must be pointed out that these compounds suffer from some relevant shortcomings as radical-trapping antioxidants. Ascorbate (Vitamin C) is water soluble, and is only an effective inhibitor of lipid oxidation in concert with a lipid-soluble inhibitor with which it can act synergistically. Moreover, it is such an effective one-electron reductant, that it can be a pro-oxidant under some physiological conditions.  $\alpha$ -Tocopherol, although lipid-soluble, can also be a pro-oxidant, as it has been shown to mediate the peroxidation of cholesterol esters in low-density lipoprotein under various conditions. Perhaps worst of the trio,  $\beta$ -carotene oxidizes readily, giving rise to a variety of peroxidic and carbonyl-containing products that are highly cytotoxic. Given the outcomes of these trials and what we know of the chemistry of the compounds, in lieu of dismissing the idea of using radical-trapping antioxidants as part of a preventive and/or therapeutic strategy to combat degenerative disease, perhaps we should instead ask the question: are we studying the right compounds?

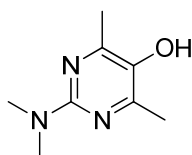
Addressing this question would be greatly enabled by a real-time imaging system capable of monitoring the extent of lipid peroxidation *in vivo*, and the effects of radical-trapping antioxidants, on this process. Cosa's BODIPY- $\alpha$ -Tocopherol (B-TOH) conjugates are a step toward that end, but suffer from low resolution owing to the relative small fluorescence enhancement upon oxidation, and reactivity that is no greater than  $\alpha$ -tocopherol itself. More reactive compounds that better quench the fluorescence of the BODIPY chromophore would be a significant improvement here – especially if they could be conjugated to chromophores with different colours. Over the last 10 years, our group has demonstrated that the incorporation of nitrogen into phenolic compounds in particular locations can lead to air-stable compounds that react at rates up to two orders of magnitude more quickly with autoxidation chain-carrying peroxy radicals. For example, **1.34**, **1.33** and **1.35**<sup>[14]</sup> are 2-, 5- and 28-fold more reactive antioxidants, respectively, than  $\alpha$ -TOH. Hence, we propose to conjugate **1.34**, **1.33** and **1.35** to BODIPY dyes in order to generate antioxidant indicators that are much more reactive than the native  $\alpha$ -TOH that is present *in vivo*. As such, we can monitor the reactions of **1.34**, **1.33** and **1.35** with peroxy radicals in real time within liposomes, lipoproteins and eventually, cells.



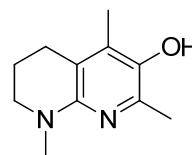
**1.32**



**1.33**



**1.34**



**1.35**

### **1.9.2 Preliminary Studies of Cyclopropanated Lipids as Substrates of Autoxidation and Enzyme-Catalyzed Oxygenation.**

Despite the central importance of lipoxygenases and their reaction products in human health and degenerative disease pathogenesis, the enzymes remain relatively poorly understood. One particular problem is the lack of three-dimensional structural information available for the six known human isoforms, which is essential to the design and development of specific inhibitors as potential therapeutics. While the recent x-ray crystallographic structure of human 5-lipoxygenase is a tremendous advance in this area,<sup>[42]</sup> it remains unclear as to whether the structure represents an active conformation, and further, how the polyunsaturated fatty acid substrate binds to the active site for conversion to products. A non-oxidizable substrate analog that could be co-crystallized with the enzyme would be useful in aiding to address these issues.



We propose to prepare cyclopropanated analogs of the polyunsaturated fatty acid (ester) linoleic acid and to undertake some preliminary studies to determine whether they may be good inhibitors and/or substrate analogs for lipoxygenases. These studies include peroxy radical clock experiments aimed at quantitating the effect of replacing one or both of the double bonds in linoleic acid with cyclopropane rings on the oxidation kinetics of the fatty acid and its derivatives, and also an evaluation of these compounds as substrate analogs and/or inhibitors of plant lipoxygenases, which use linoleic acid as their native substrates. We anticipate that insight gleaned from these studies may be useful in structural studies aimed at a better understanding of lipoxygenase catalysis and its inhibition by small molecules.

### 1.10 References

- (1) de Saussure, N. T.; *Recherches Chimiques sur laVégétation.V.Nyon* **1804**, 153-155
- (2) Hammond, E. G.; White, P. G. *Journal of the American Oil Chemists' Society* **2011**, 88, 891
- (3) Stephen, H. N.; *J. Am. Chem. Soc.* **1928**, 50, 568
- (4) Criegee, R.; Pilz, H.; Flygare, H. *Abteilung B* **1939**, 72B, 1799
- (5) Bolland, J. L. *Quarterly Reviews* **1949**, 3, 1-21.
- (6) Lundberg, W. O.; Chipault, J. R.; Hendrickson, M. J. *Journal of the American Oil Chemists Society* **1949**, 26, 109-115.
- (7) Ingold, K. U. *Science* **1967**, 158, 248-&.

- (8) Ingold, K. U. *Acc. Chem. Res.* **1969**, 2, 1-&.
- (9) Russell, G. A. *Angew. Chem. Int. Ed.* **1957**, 69, 688-688.
- (10) Russell, G. A. *J. Am. Chem. Soc.* **1957**, 79, 2977-2978.
- (11) Porter, N. A.; Weber, B. A.; Weenen, H.; Khan, J. A. *J. Am. Chem. Soc.* **1980**, 102, 5597-5601.
- (12) Porter, N. A. *Acc. Chem. Res.* **1986**, 19, 262-268.
- (13) Roschek, B.; Tallman, K. A.; Rector, C. L.; Gillmore, J. G.; Pratt, D.A.; Pumta, C. *J. Org. Chem.* **2006**, 71, 3527-3532.
- (14) Weydert, C. J.; Cullen, J. J. *Nature Protocols* **2010**, 5, 51 - 66
- (15) Traber, M.G.; BRIGELIUS-FLOHÉ, R.; *The FASEB Journal*. **1999**, 13, 1145-1155
- (16) Igarashi, O.; Yonekawa, Y.; Fujiyama-Fujihara, Y. *J. Nutr Sci Vitaminol* **1991** 37, 359-69.
- (17) DiMascio, P. et al. *Archives Biochimica et Biophysica* **1989**, 274, 532-538.
- (18) Mayer, J. M.; Hrovat, D. A.; Thomas, J. L.; Borden, W. T., *J. Am. Chem. Soc.* **2002**, 124, 11142-11147.
- (19) Lucarini, M.; Pedulli, G. F.; Cipollone, M. *J. Org. Chem.* **1994**, 59, 5063-5070.
- (20) Wayner, D. D. M.; Lusztyk, E.; Ingold, K. U.; Mulder, P. *J. Org. Chem.* **1996**, 61, 6430-6433.
- (21) Lucarini, M.; Pedrielli, P.; Pedulli, G.F.; Cabiddu, S.; Fattuoni, C. *J. Org. Chem.* **1996**, 61, 9259.
- (22) Pratt, D. A.; DiLabio, G. A.; Brigati, G.; Pedulli, G. F.; Valgimigli, L. *J.*

- Am.Chem.Soc.* **2001**, *123*, 4625-4626
- (23) Burton, G. W.; Ingold, K. U. *J. Am. Chem. Soc.* **1981**, *103*, 6472;
- (24) Bowry, V. R.; Ingold, K. U. *Acc. Chem. Res.* **1999**, *32*, 27.
- (25) Wijtmans, M.; Pratt, D. A.; Valgimigli, L.; DiLabio, G.A.; Pedulli, G. F.; Porter, N. A. *Angew. Chem. Int. Ed.* **2003**, *42*, 4370–4373
- (26) Burton, G. W.; Doba, T.; Gabe, E. J.; Hughes, L.; Lee, F. L.; Prasad, L.; Ingold, K. U. *J. Am. Chem. Soc.* **1985**, *107*, 7053-7065.
- (27) Wright, J. S.; Pratt, D. A.; DiLabio, G. A.; Bender, T. P.; Ingold, K. U. *Cancer Detect. Prev.* **1998**, *22*, 204.
- (28) Lucarini, M.; Pedrielli, P.; Pedulli, G. F.; Valgimigli, L.; Gimes, D.; Tordo, P. J. *J. Am. Chem. Soc.* **1999**, *121*, 11546.
- (29) Loudet, A.; Burgess, K. *Chem. Rev.* **2007**, *107*, 4891-4932
- (30) Oleynik, P.; Ishihara, Y.; Cosa, G. *J. Am. Chem. Soc.* **2007**, *129*, 1842–1843
- (31) Liavonchanka, A.; Feussner, I. *J. Plant Physiol.*, **2006**, *163*, 348–357.
- (32) Feussner, I.; Wasternack, C. *Annu. Rev. Plant Biol.*, **2002**, *53*, 275–297.
- (33) Gilbert, N. C.; Bartlett, S. G.; Waight, M. T.; Neau, D. B.; Boeglin, W. E.; Brash, A. R.; Newcomer, M. E. *Science* **2011**, *331*, 217
- (34) Scarrow, R. C.; Trimitsis, M. G.; Buck, C. P.; Grove, G. N.; Cowling, R. A.; Nelson, M. J. *Biochemistry* , **1994**, *33*, 15023–15035.
- (35) Schneider, C.; Pratt, D. A.; Porter, N. A.; Brash, A. R. *Chemistry & Biology*, **2007**, *14*, 473-488.
- (36) Nagase, T.; Uozumi, N.; Aoki-Nagase, T., et al. *Am J Physiol Lung Cell Mol*

*Physiol* **2003**; 284, L720-6

(37) Carlos, H. S.; Joao, H. P.; Momtchilo, R.; et al. *J.Immun.*, **2006**, 177, 3201-3208

(38) Tsukada, T.; Nakashina, K.; Shirakawa, S.; *Biochem Biophys Res Commun*,  
**1986**, 140, 832-836.

(39) Crawley, G. C.; Dowell, R. I.; Edwardo, P. N.; et al. *J.Med.Chem* **1992**, 35,  
2600-2609

(40) Werz, O. *Curr Drug Targets Inflamm Allergy* **2002**, 1, 23-44

(41) Werz, O, Steinhilber, D. *Exp Opin Ther Patents* **2005**, 15, 505-19

(42) Pergola, C.; Werz, O.; *Expert Opin Ther Pat.* **2010**, 20, 355-75.

(43) Werz, O.; Szellas, D.; Henseler, M.; Steinhilber, D. *Molecular Pharmacology*  
**1998**, 54, 445-451

**Chapter 2**  
**Towards Highly-Reactive Pyri(mi)dinol-Based**  
**Fluorescent Antioxidant Indicators**

## 2.1 Introduction

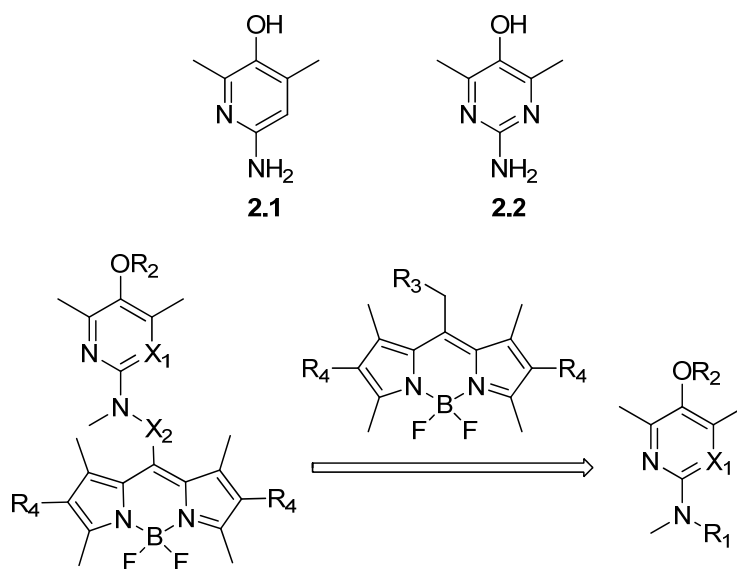
The aminopyridinol and aminopyrimidinol antioxidants developed in our group (Chapter 1.9.1) show better antioxidant activity than  $\alpha$ -TOH by comparing their inhibition rate constants, which are derived from O<sub>2</sub> uptake experiment in solution. Although these compounds are far better antioxidants than  $\alpha$ -TOH in solution, we cannot say they will exhibit the similar antioxidant efficiency in cells as well, since the heterogeneous environment of the cell is much more complicated than that of a homogenous organic solution. To determine whether these pyridinol and pyrimidinol compounds act in the same way in cells as they do in solution, a suitable indicator for the direct visualization of the antioxidant status and/or level of lipid peroxidation in cell membranes would be highly useful.

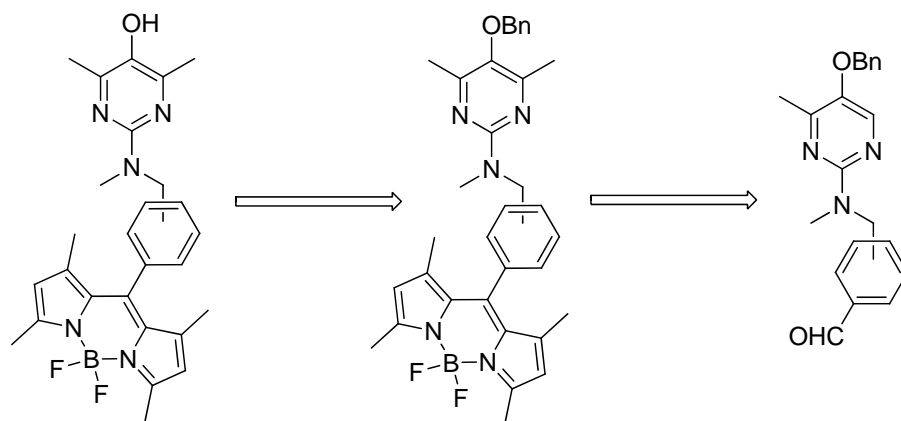
Such an indicator, wherein the fluorogenic dye 'BODIPY' was conjugated to the reactive chromanol group of  $\alpha$ -TOH, has been developed by Cosa (Chapter 1.9.1). This indicator, referred to as 'B-TOH' exhibits a 10-fold fluorescence enhancement upon scavenging the peroxy radicals in homogenous solution, and a 4-fold enhancement in cell membranes, which allows a real time monitoring of  $\alpha$ -TOH's oxidative status in cell. However, the difference between on/off states of such indicator is not as big as would be ideal for meaningful measurements, and the ester linkage in the indicator is also subjected to hydrolysis; limiting its potential applications. Our aminopyri(mi)dinol antioxidants both have lower oxidation potentials than does  $\alpha$ -TOH, which will make the intramolecular PeT responsible for BODIPY quenching more exergonic, and result in a better enhancement upon

oxidation of the pyri(mi)dinol. Meanwhile, it's also desirable to replace the ester linkage linking the BODIPY and antioxidant moieties as in B-TOH with more stable linkage such as either alkyl, ether or amine linkages. The resulting indicators should be not only able to monitor the pyri(mi)ridinol's antioxidant efficacy in cells, but they should also exhibit better resolution and be more stable in the cell environment.

### 2.1.1 Potential Approaches to Pyri(mi)dinol BODIPY Conjugates

Based on the well-precedented access to the structure of aminopyridinol **2.1** and aminopyrimidinol **2.2** established in our group<sup>[1]</sup>, it seemed that these were logical starting materials for conjugation. We envisioned alkylations of the amino group by BODIPY fluorophores containing an electrophilic handle at the meso position, or alkylations of the amino group to introduce an electrophile that could subsequently be reacted with BODIPY fluorophores containing a nucleophilic handle at the meso position. The strategies are outlined in the Scheme 2.1.





$R_1 = \text{CH}_2\text{COOH}, (\text{CH}_2)_4\text{NH}_2, (\text{CH}_2)_5\text{OH}, \text{CH}_2\text{OH}, \text{H}, \text{CH}_2\text{CH}=\text{CH}_2$ ;  $R_2 = \text{Bn}, \text{H}$

$R_3 = \text{OH}, \text{I}, \text{OTf}, \text{CH}_2\text{COOH}, \text{CH}_2\text{CH}=\text{CH}_2$ ;  $R_4 = \text{H}, \text{CH}_2\text{CH}_3, \text{Cl}$ ;

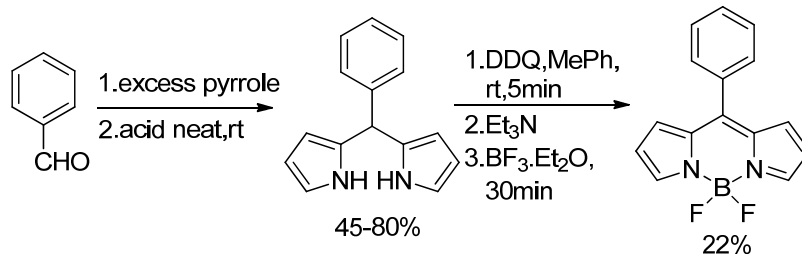
$X_1 = \text{C}, \text{N}$ ;  $X_2 = \text{CH}_2\text{COO}, (\text{CH}_2)_4\text{NHCH}_2, (\text{CH}_2)_5\text{OH}, \text{CH}_2\text{OOC}(\text{CH}_2)_2, \text{CH}_2$

**Scheme 2.1** Potential approaches to pyri(mi)dinol BODIPY conjugates

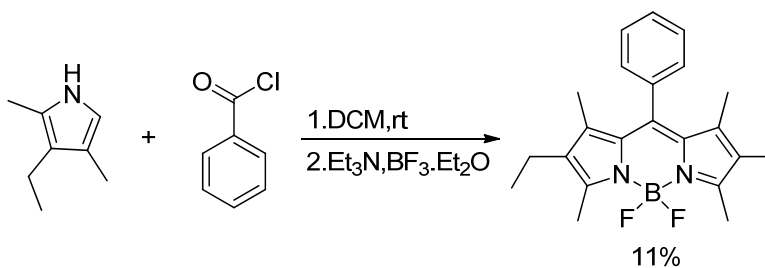
### 2.1.2 Aryl-Linked Pyri(mi)dinol-BODIPY-Conjugates

BODIPY fluorophores are typically prepared by treating a dipyrromethene precursor with boron trifluoride etherate in the presence of a tertiary amine.<sup>[2]</sup> Dipyrromethenes can be accessed from the corresponding pyrroles by several methods. Normally, one of the alpha positions in the employed pyrroles is substituted and the other is free. Condensation of such pyrrole, often available from Knorr pyrrole synthesis, with an aromatic aldehyde (to the best of our knowledge, aliphatic aldehydes have not been reported in this reaction) in the presence of TFA gives dipyrromethane, which is oxidized to dipyrromethene using a quinone oxidant such as DDQ or p-chloranil (Scheme 2.2).<sup>[3]</sup> Alternatively, acid chlorides and anhydrides have been used, as shown in Scheme 2.3<sup>[4]</sup> and Scheme 2.4.<sup>[5]</sup> The low yields in these reactions are due to sterics and the instability of the generated dipyrromethene intermediates.

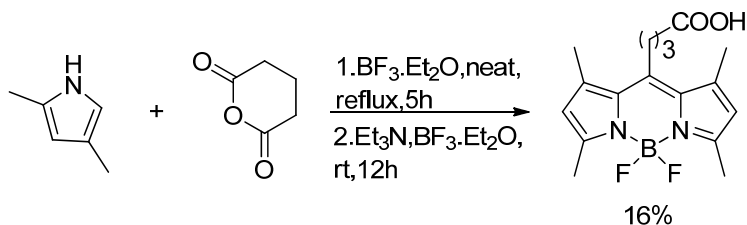




**Scheme 2.2** Synthesis of BODIPY using aromatic aldehyde as starting material



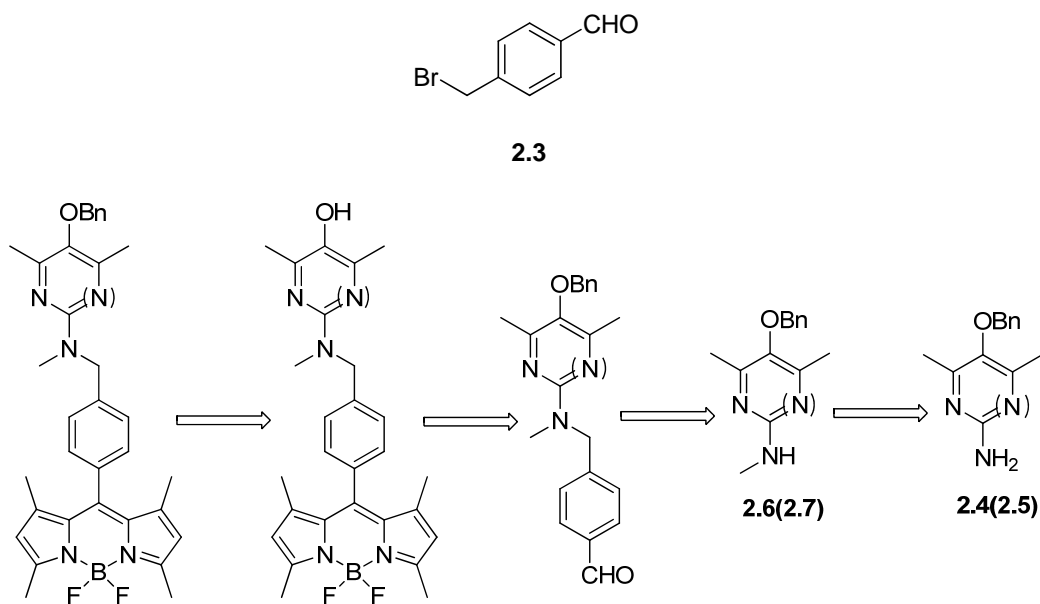
**Scheme 2.3** Synthesis of BODIPY using acid chloride as starting material



**Scheme 2.4** Synthesis of BODIPY using anhydride as starting material

Given that changes in the substitution of the BODIPY core can be introduced simply by changing the substituents on the aromatic aldehyde that is used as a precursor in the above route, one strategy to the desired conjugate is to attach our antioxidant to an aromatic aldehyde (**2.3**), which can be used as the electrophilic ‘methylene’ source for formation of BODIPY by condensation with suitable pyrroles.

The arylaldehyde can be obtained from the corresponding nitrile.<sup>[6]</sup> Since a dialkylamino group is the ideal substituent to afford the pyri(mi)dinol optimum activity, we will first attach one methyl group to the free amino group of pyri(mi)dyl starting material **2.4** or **2.5**, which can be synthesized according to reported procedures<sup>[7]</sup>. The mono-methylated pyri(mi)dyl compound (**2.6** or **2.7**) can be made following a procedure<sup>[8]</sup> that successfully transferred 2-amino-pyridine into mono-methyl-2-amino pyridine (Scheme 2.5).

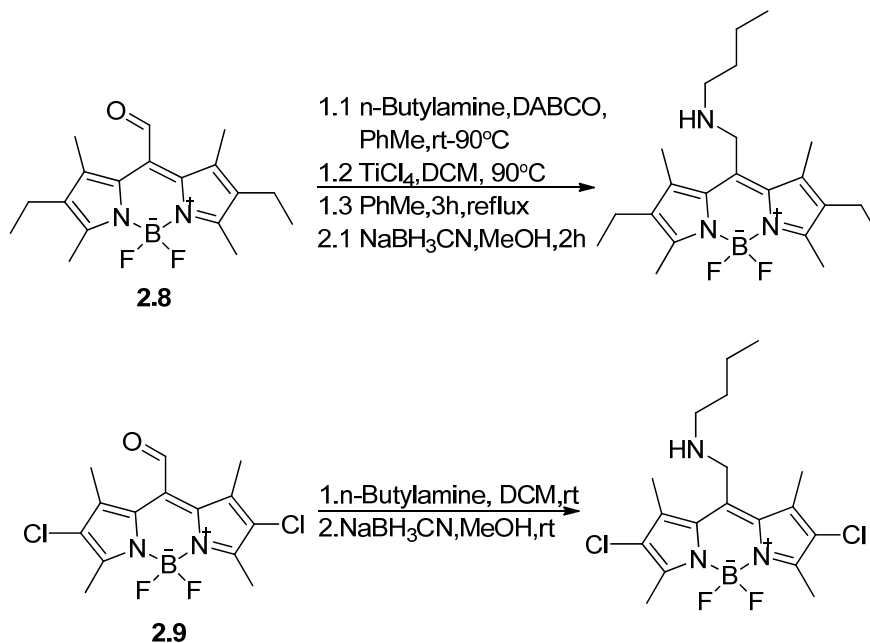


**Scheme 2.5** Retrosynthesis of aryl-linked pyri(mi)dinol-BODIPY-conjugates

### 2.1.3 Amine or Ether Linked Pyri(mi)dinol-BODIPY-Conjugates

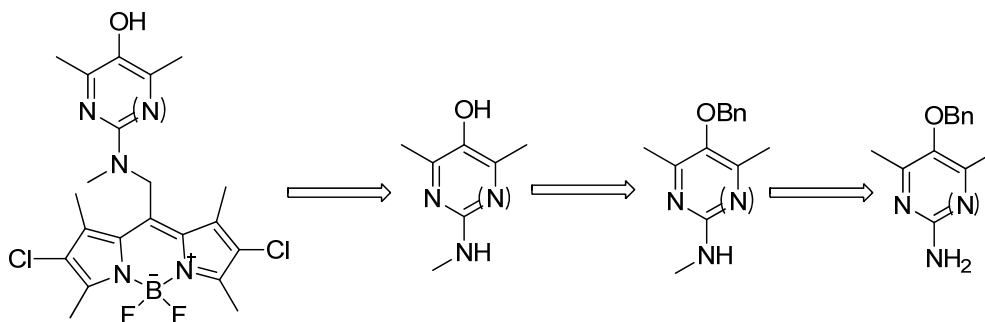
Perhaps the most straightforward approach to the desired conjugates is reductive amination of an aldehyde-substituted BODIPY with the aminopyridinol and/or aminopyrimidinol. Similar examples have been reported by Cosa's group (Scheme

2.6),<sup>[9]</sup> wherein the formylated BODIPY **2.8** has been found to react smoothly with amines in the presence of catalytic TiCl<sub>4</sub>. Moreover, when the 2- and 6-positions of the BODIPY core are substituted with electron donating groups (e.g. Cl, CN), the resulting BODIPY (**2.9**) reacts even in the absence of TiCl<sub>4</sub>.



**Scheme 2.6** Reductive amination of *meso*-formyl-BODIPY.<sup>[9]</sup>

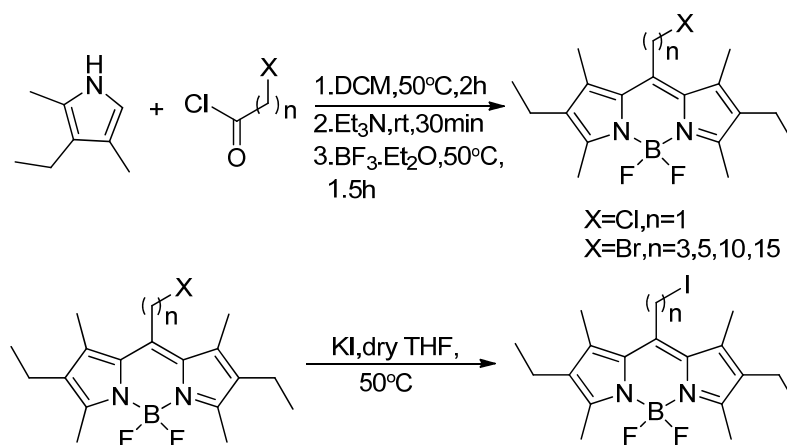
The retrosynthesis using this strategy is shown below (Scheme 2.7).



**Scheme 2.7** Retrosynthesis of pyri(mi)dinol-BODIPY-conjugates through reductive

## amination

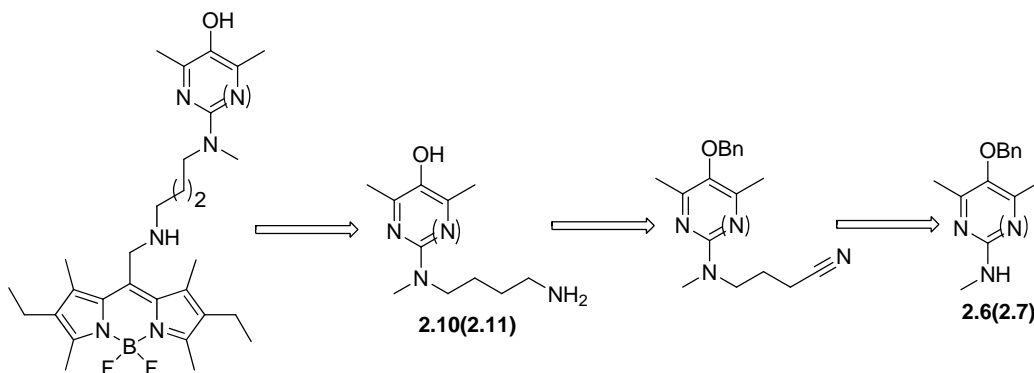
Another possibility is substitution of the amino group of the benzyl protected pyri(mi)dinol with BODIPY bearing an electrophilic alkyl halide moiety. Synthesis of such substituted BODIPYs have been well documented (Scheme 2.8).<sup>[10]</sup>



**Scheme 2.8** Synthesis of BODIPY bearing an alkyl halide at the meso position.<sup>[10]</sup>

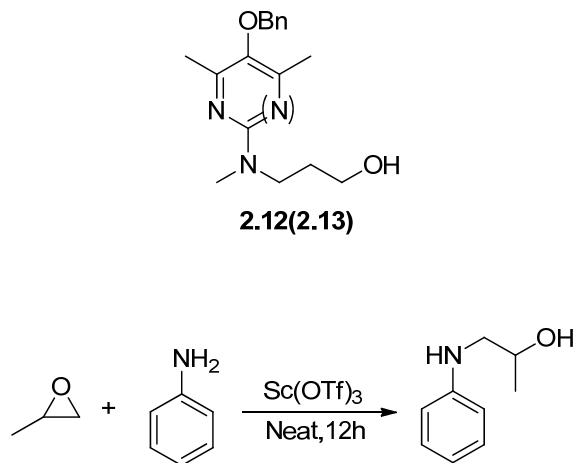
While these BODIPYs have frequently been used to alkylate free amines, the 2-aminopyridine and 2-aminopyrimidine moieties of our antioxidants are not very good nucleophiles. Since the BODIPY core is generally not very stable to higher temperatures, this may present a problem. To avoid harsh reaction conditions and increase the possibility of success for this reaction we will likely need to carry out a Finkelstein reaction to prepare the corresponding iodide.<sup>[11]</sup> To synthesize such compounds, we plan to first append an alkyl nitrile to compound **2.6** (**2.7**), and subsequently reduce the nitrile with LiAlH<sub>4</sub> to yield the expected pyri(mi)dylamine

**2.10(2.11)** for coupling as in Scheme 2.9.



**Scheme 2.9** Retrosynthesis of amine linked pyri(mi)dinol-BODIPY-conjugates

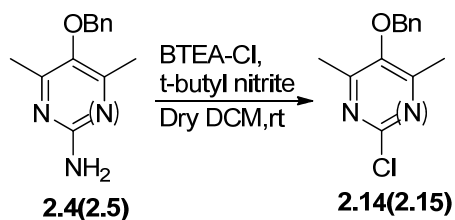
Alternatively, an ether linkage may be employed. The introduction of an aliphatic alcohol on the aminopyridinol or aminopyrimidinol will yield aminoalcohols such as **2.12** and **2.13**, which may react with BODIPY-I to generate an ether species which won't be protonated in buffer solutions. To make such compounds we plan to use an oxirane as the alkylating reagent. Similar reactions have been carried out with propylene oxide and aniline (Scheme 2.10).<sup>[12]</sup>



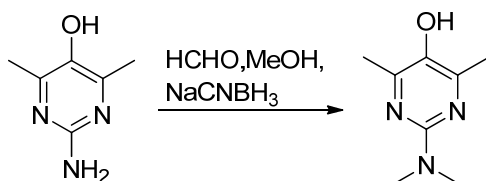
**Scheme 2.10** Alkylating benzylamine with oxirane.<sup>[12]</sup>

Another approach to the preparation of compounds **2.12** and **2.13** is by substitution of the pyri(mi)dyl chloride **2.14** (**2.15**) with an  $-\text{NH}_2(\text{CH}_2)_n\text{OH}-$  group and subsequent reductive amination with formaldehyde. Preparation of the chloride (Scheme 2.11) and reductive amination (Scheme 2.12) have been previously reported.

[13][14]

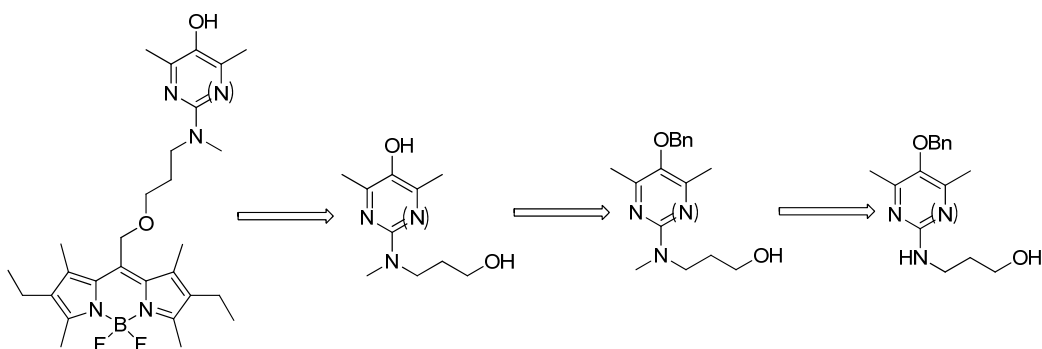


**Scheme 2.11** Nonaqueous chloro-de-diazonation of pyri(mi)dyl amines.<sup>[13]</sup>



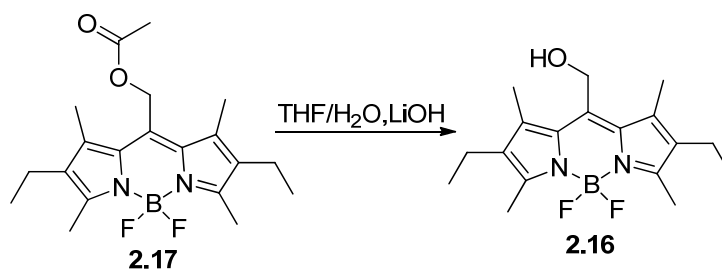
**Scheme 2.12** Reductive amination of pyrimidinol amine with formaldehyde.<sup>[14]</sup>

A retrosynthesis summarizing this strategy is shown below (Scheme 2.13).

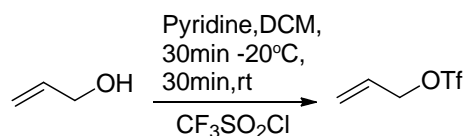


**Scheme 2.13** Retrosynthesis of ether linked pyri(mi)dinol-BODIPY-conjugates

An alternative to the use of a BODIPY bearing an alkyl halide pendant group is the activation of the BODIPY methylene alcohol, BODIPY-OH (**2.15**) – prepared easily by hydrolysis of its precursor PM650 (**2.16**) as in (Scheme 2.14),<sup>[15]</sup> – as a triflate (**2.17**) using trifluoromethanesulfonyl chloride. While the transformation of alkyl alcohols to their corresponding alkyl triflates is well documented (e.g. Scheme 2.15),<sup>[16]</sup> no similar reaction has been done on BODIPY derivatives.

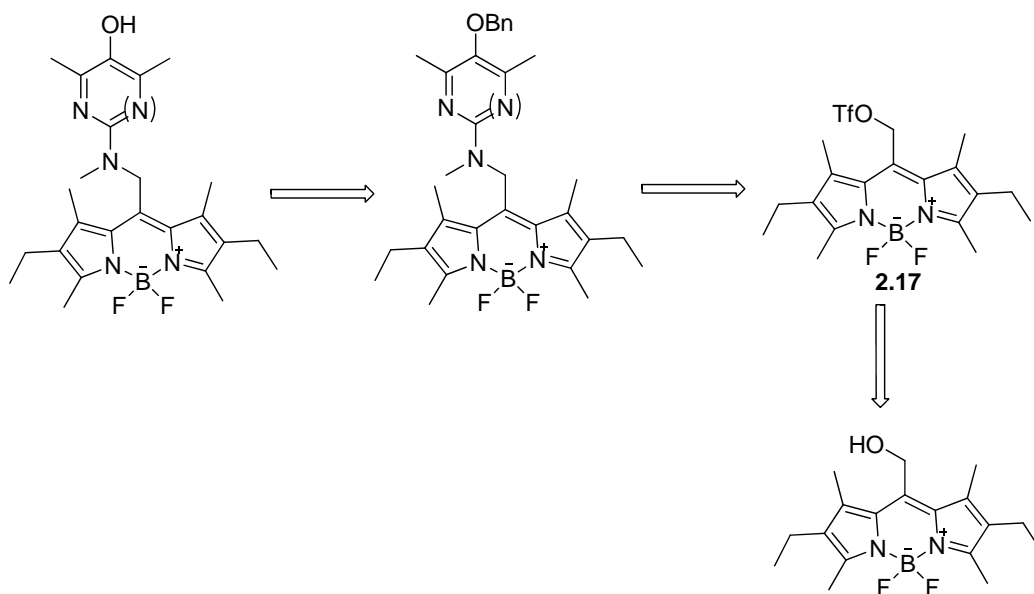


**Scheme 2.14** Hydrolysis of PM650.<sup>[15]</sup>



**Scheme 2.15** Transformation of alkyl alcohol to alkyl triflate.<sup>[16]</sup>

The retrosynthesis is shown below in **Scheme 2.16**.



**Scheme 2.16** Retrosynthesis of pyri(mi)dinol-BODIPY-conjugates through triflate activated BODIPY

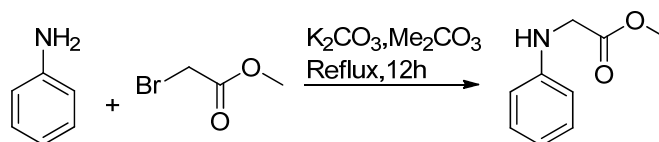
#### 2.1.4 Carboxyl- or Carbamoyl-Linked Pyr(imid)dinol-BODIPY Conjugates

Since BODIPY-OH (**2.16**) can be easily prepared by hydrolysis of its precursor PM650 (**2.17**) as in Scheme 2.14,<sup>[15]</sup> coupling approaches such as esterification become possible as long as our pyri(mi)dyl precursor **2.4** (**2.5**) have a carboxylate acid group installed. One approach of doing so is by oxidizing the alcohol species to the corresponding carboxylic acid. Oxidation of primary alcohol to carboxylic acid can be carried out by a variety of approaches, including Jones oxidation and PDC. Considering the susceptibility of the benzyl protecting group to strong acid



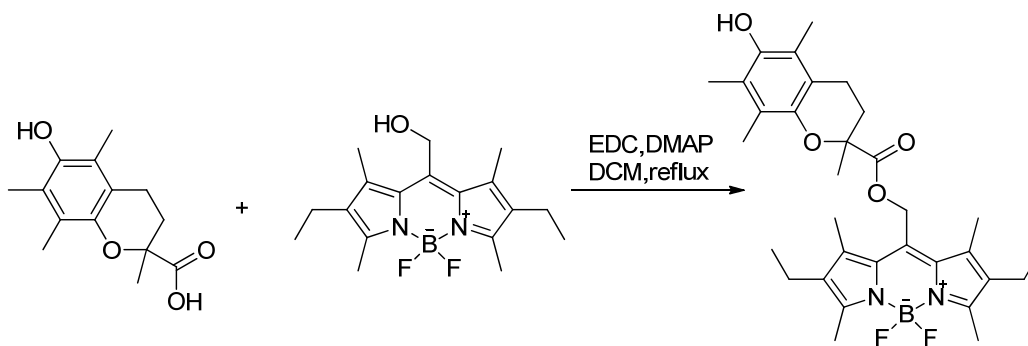
environment, we decided to adopt approaches with mild reaction conditions: PDC in DMF and periodic acid/PCC.<sup>[17][18]</sup>

Another approach of installing the carboxylic acid group is by substitution of compounds **2.6** (**2.7**) with methyl bromoacetate; subsequent hydrolysis of the resulting esters will generate the targeted carboxylic acids. Such an approach has been successfully applied on aniline (Scheme 2.17).<sup>[19]</sup>



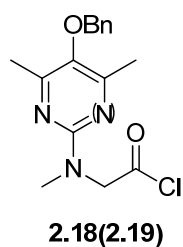
**Scheme 2.17** Alkylating aniline with methyl bromoacetate.<sup>[19]</sup>

The reaction conditions of esterification using BODIPY-OH as the substrate is reported in Cosa's work (Scheme 2.18),<sup>[15]</sup> where EDC is applied to activate the carboxylic acid and creates mild esterification conditions compatible with the BODIPY moiety in the system.

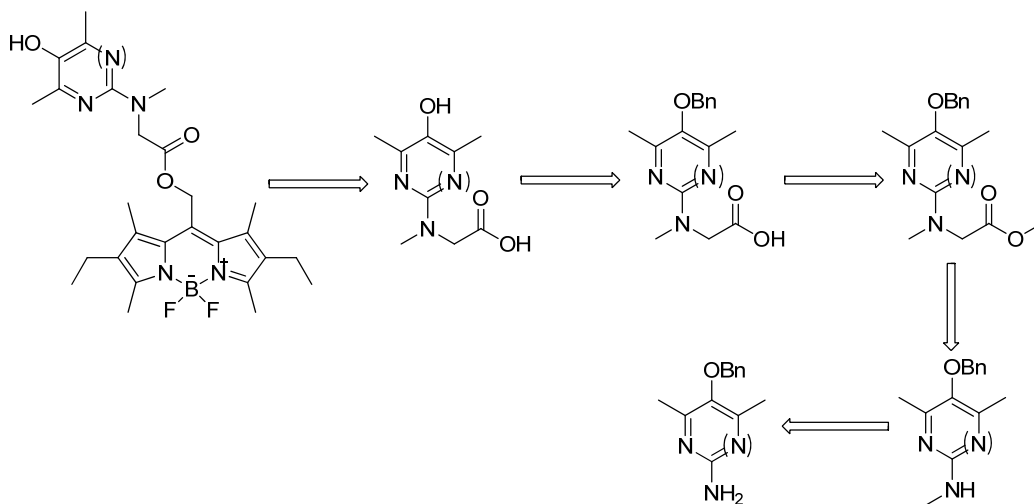


**Scheme 2.18** Esterification of PMOH with EDC activated trolox.<sup>[15]</sup>

We have also considered creating an acyl chloride group from the carboxylic acid species we designed. And then using this acyl chloride species (**2.18** or **2.19**) as electrophile to carry out the coupling reaction with the BODIPY-OH.



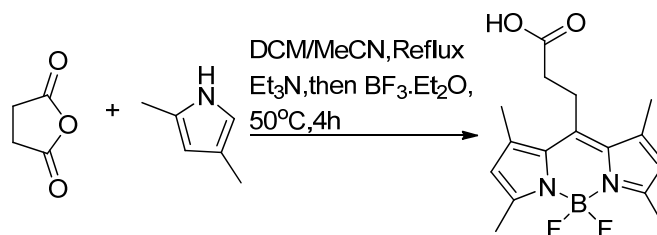
The corresponding retrosynthesis is shown below (Scheme 2.19).



**Scheme 2.19** Retrosynthesis of carboxyl-linked pyri(mi)dinol-BODIPY-conjugates using pyri(mi)dinol acid species

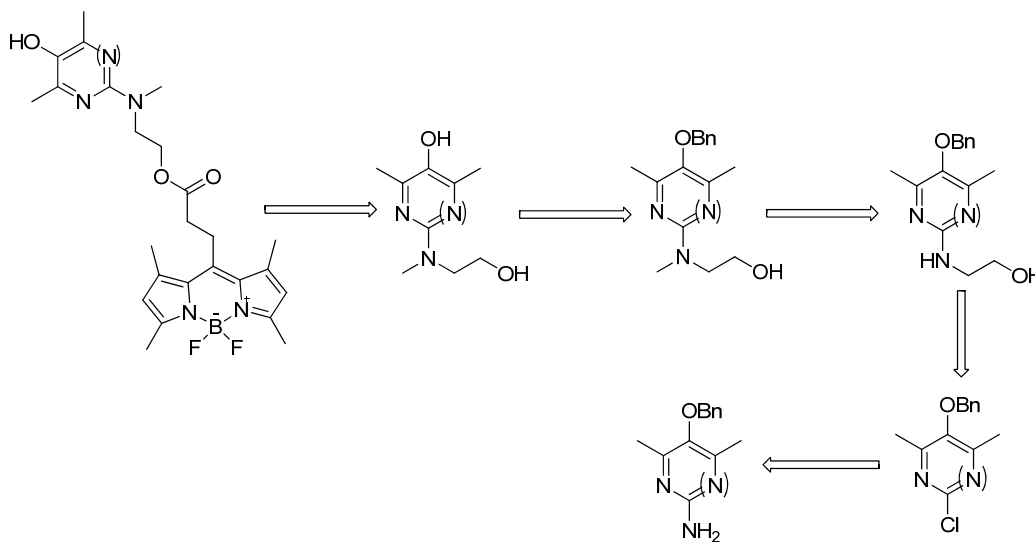
The esterification could also be attempted the other way around, by treating a carboxylated (e.g. BODIPY-COOH, **2.20**) with a pyri(mi)dyl alcohol (e.g. **2.12** or

2.13). The synthesis of BODIPY-COOH **2.20** is reported by condensation of 2,4-dimethylpyrroles with succinic anhydride (Scheme 2.20).<sup>[20]</sup>



**Scheme 2.20** Synthesis of BODIPY acid using anhydride as starting material.<sup>[20]</sup>

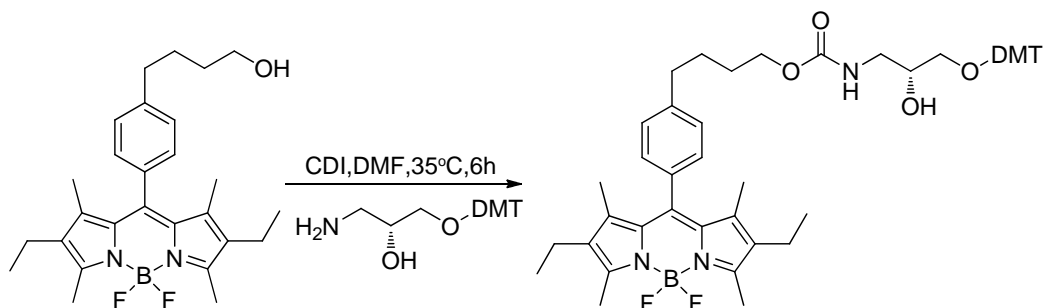
The approach is shown below in Scheme 2.21.



**Scheme 2.21** Retrosynthesis of carboxyl-linked pyri(mi)dinol-BODIPY-conjugates using BODIPY acid species

BODIPY-OH may also be activated by substances such as CDI, and the activated BODIPY can then react at mild condition with pyri(mi)dyl amines (**2.10** or **2.11**). A

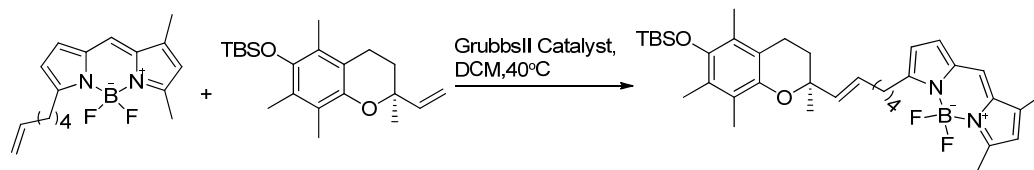
similar transformation has been reported as shown in Scheme 2.22, in which a carbamoyl-linkage is formed.<sup>[23]</sup>



**Scheme 2.22** Synthesis of carbamoyl-linked BODIPY conjugates using CDI activated BODIPY species.<sup>[23]</sup>

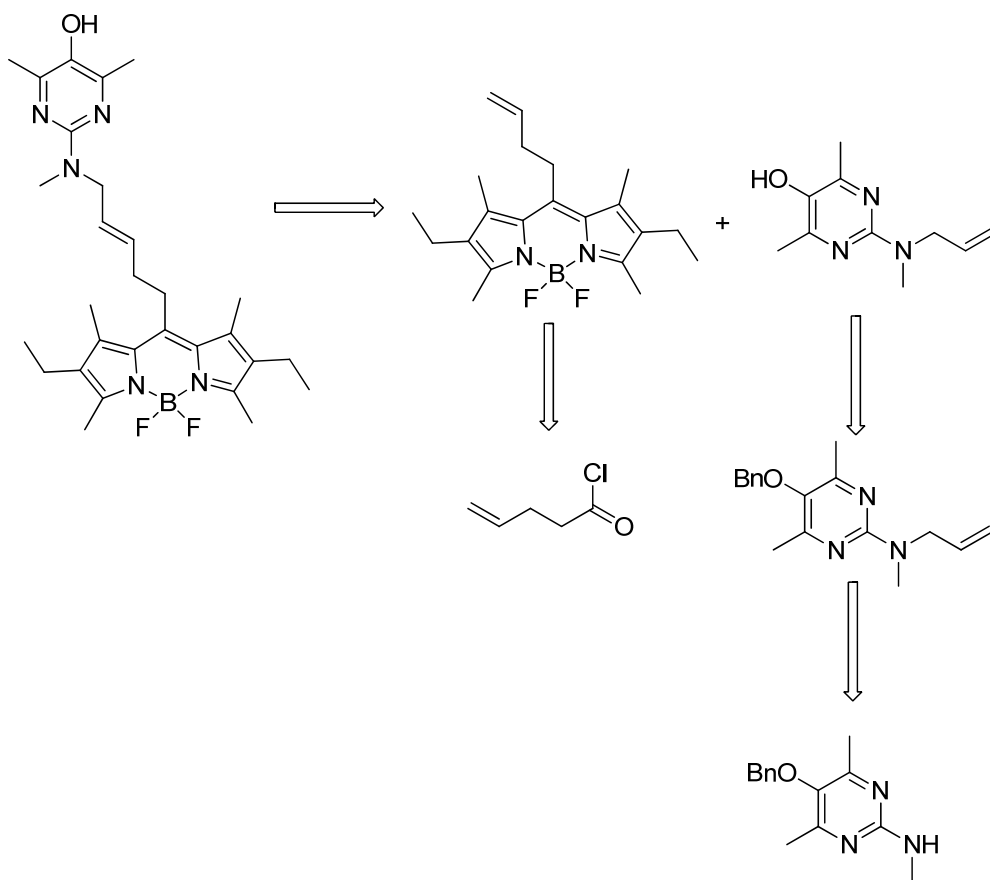
### 2.1.5 Alkene-Linked Pyri(mi)dinol-BODIPY Conjugates

The last approach we envisioned to prepare the desired conjugates is olefin metathesis. The metathesis of alkenylated BODIPY is reported in a few papers, such as the work by Atkinson's group (Scheme 2.23).<sup>[24]</sup>



**Scheme 2.23** Synthesis of alkene linked BODIPY conjugate through olefin metathesis.<sup>[24]</sup>

Retrosynthesis is shown below (Scheme 2.24).



**Scheme 2.24** Retrosynthesis of alkene-linked pyri(mi)dinol-BODIPY conjugates

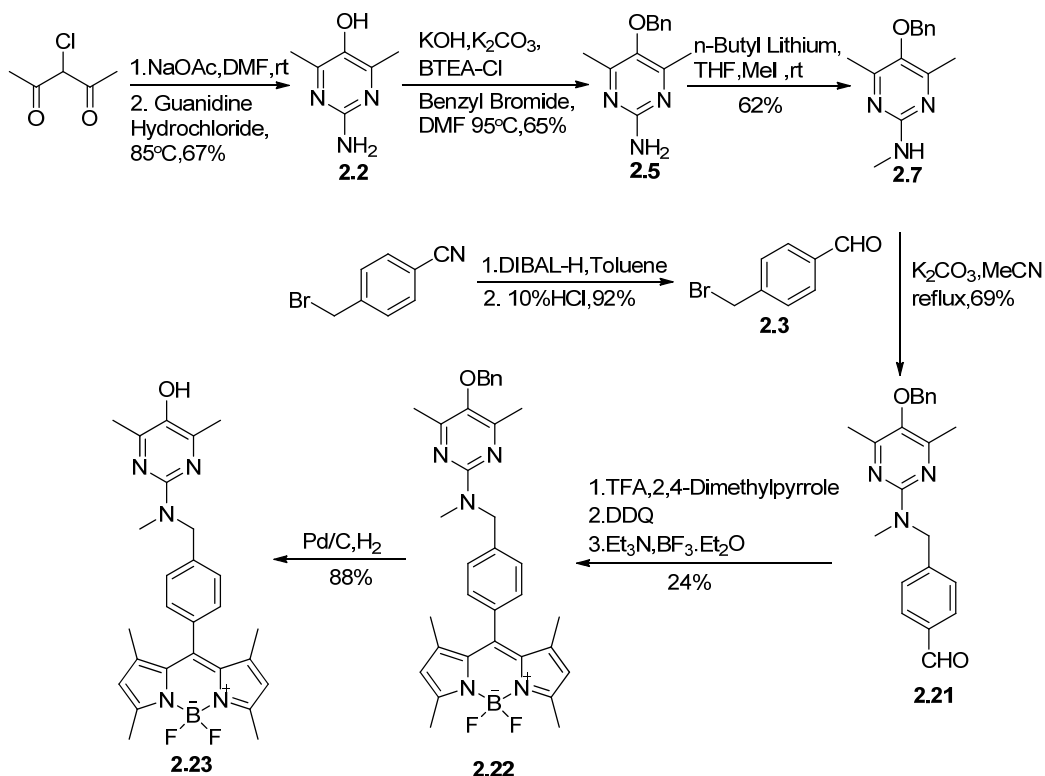
## 2.2 Results and Discussion

### 2.2.1 Formation of Aryl-Linked Pyrimidinol-BODIPY-Conjugates

#### 2.2.1.1 Para-Substitution

The approach we first took towards the preparation of pyrimidinol-BODIPY conjugates with an aryl linkage is shown in Scheme 2.25. We began by obtaining the 2,4-dimethyl-amino-pyrimidinol **2.2** from condensation of guanidine with 2,4-dioxopentan-3-yl acetate, which can be obtained quantitatively from 3-chloropentane-2,4-dione and sodium acetate. The hydroxyl group was then

protected by benzylation so that it would not interfere in subsequent substitution reactions.

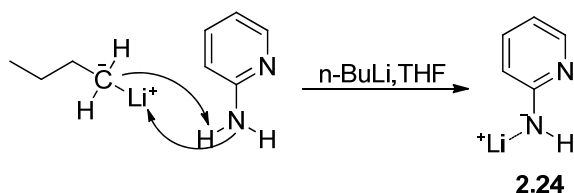


**Scheme 2.25** Synthesis of para-Pyrimidyl-BODIPY

The benzyl protected pyrimidinol **2.5** was then treated with n-BuLi and MeI, producing the mono-methylated aminopyrimidyl **2.7** in 62% yield. The mass balance was the di-methylated aminopyrimidyl compound, which was obtained in around 15% yield. It is generally difficult to carry out mono-methylation of an amine group simply by manipulation of the amount of methylating reagent (e.g. MeI) because once the mono-methylated amine is formed, the nucleophilicity of the amine is increased due to the electron donation from the attached methyl group, and it is a more reactive

reagent than the starting material.

The mechanism of mono-methylation of amines using n-butyl lithium is shown in Scheme 2.26, a highly reactive lithioamino anion (**2.24**) is believed to be formed first, with this species subsequently reacting with the methylating reagent. The amount of n-BuLi added (1.0 equivalent) is important in determining the yield, but the production of di-methylated compound seems unavoidable, since it likely arises since the monomethylated product can react with MeI competitively with the lithiated aminopyrimidine.



**Scheme 2.26** Mechanism of formation of mono-lithium amide in the reaction of pyridylamine with n-BuLi

Compound **2.7** was then treated with 4-bromomethyl benzaldehyde (**2.3**), which was obtained by reduction of 4-bromomethyl benzonitrile using DIBAL-H and 10% HCl. This reaction generated product **2.21** in 69% yield, along with 30% of unreacted starting material. Carrying out this reaction at high concentrations is essential in obtaining a good yield. In principle, the best yield could be obtained under neat conditions, but both of the starting materials are solid, so a minimum amount of MeCN is required to dissolve the starting materials.

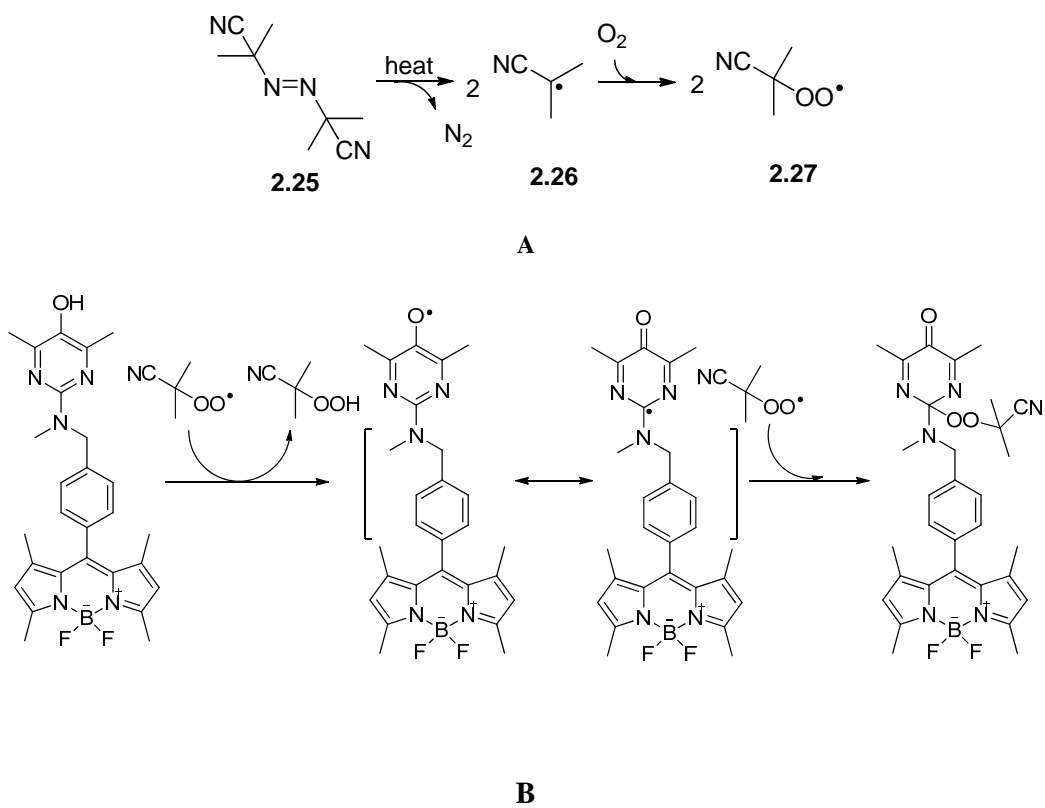
Compound **2.21** was then reacted with 2,4-dimethylpyrrole, following the classic procedures of synthesizing BODIPY. The condensation reaction is catalyzed by TFA and subsequent oxidation with DDQ generates a dipyrromethene species which is then deprotonated by triethylamine and coordinated to BF<sub>3</sub> etherate to generate product **2.22** in 24% yield. The yield isn't too bad in light of the reported yields for the preparation of such BODIPY species, which range from 10-30%; presumably due to the instability of the dipyrromethane and dipyrromethene intermediates.

The final step was deprotection of the benzyl ether group, which was carried out using Pd/C and H<sub>2</sub> to give the product **2.23** in 88% yield, with some decomposition shown on the baseline of TLC plate, which could not be characterized.

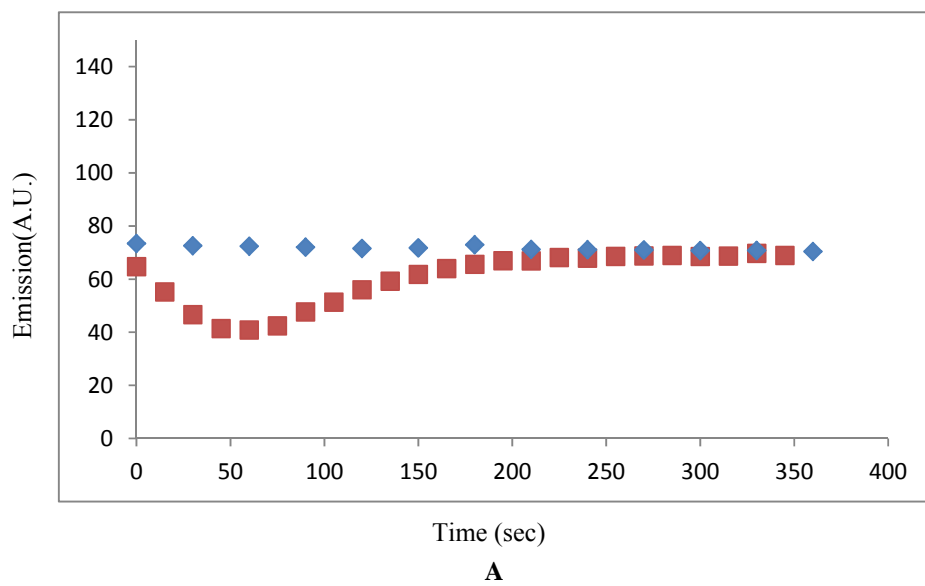
#### **2.2.1.2 Radical-Trapping Activity of para-Pyrimidyl-BODIPY**

With the para-Pyrimidyl-BODIPY conjugate **2.23** in hand, we examined its fluorescence in the presence of AIBN at 55°C. At this temperature, AIBN (**2.25**) decomposes smoothly to eliminate a molecule of nitrogen gas and two 2-cyanoprop-2-yl radicals (**2.26**) that yield peroxy radicals (**2.37**) in the presence of air (Scheme 2.27 A). These peroxy radicals will be reduced by rapid H-atom transfer from para-Pyrimidyl-BODIPY (**2.23**). Since it is expected that PeT between pyrimidinol and BODIPY quenches the fluorescence of the dye, the fluorescence will increase with time as **2.23** reacts with peroxy radicals, such as that of B-TOH.<sup>[15]</sup> However, the result we have obtained in this experiment (Figure 2.1) shows a different picture.





**Scheme 2.27 A.** Thermolysis of AIBN in the presence of Oxygen. **B.** Scavenging of AIBN derived peroxy radicals by para-Pyrimidyl-BODIPY.



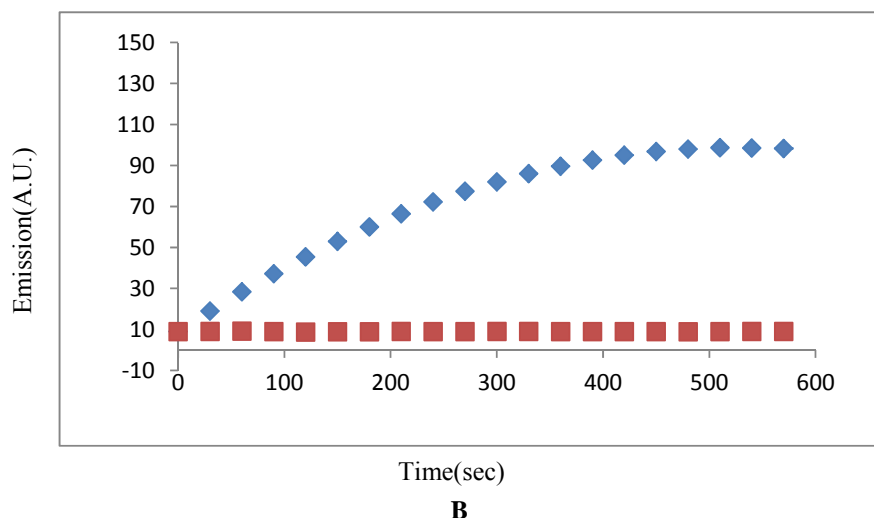
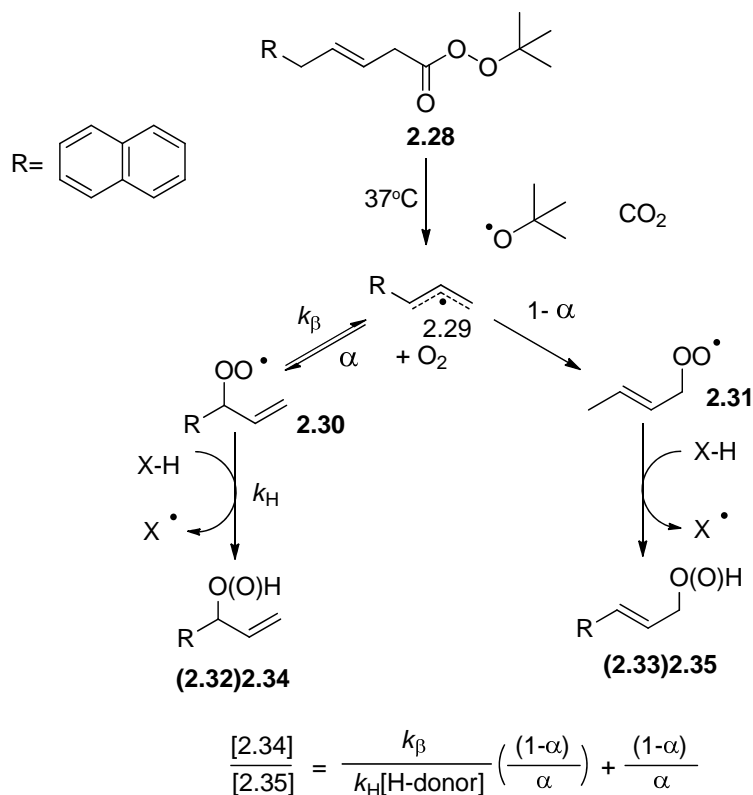


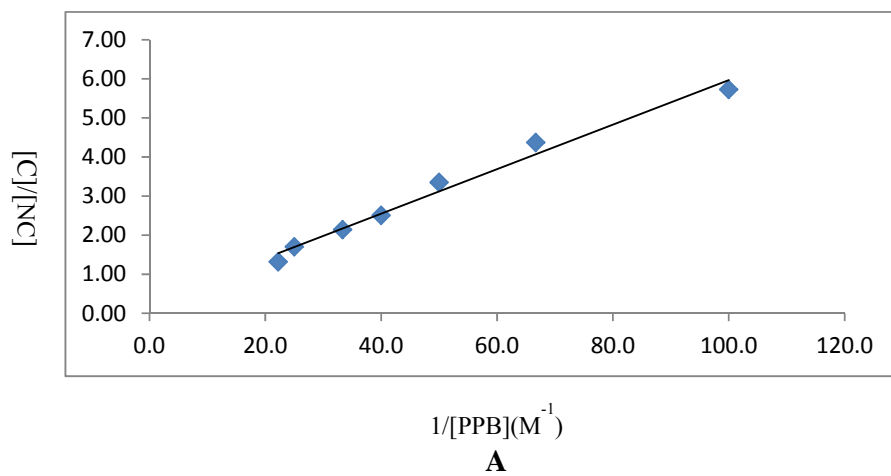
**Figure 2.1** Emission intensity time profiles for para-Pyrimidyl-BODIPY(A) incubated at 55°C with (■) or without (◆) AIBN and B-TOH (B) incubated at 55°C without (■) or with (◆) AIBN in toluene

These unexpected results lead us to doubt if the conjugation of BODIPY onto the pyrimidinol impaired its antioxidant activity. So, we carried out peroxy radical clock experiments aimed at determining the rate constant for the reaction of para-Pyrimidyl-BODIPY with peroxy radicals. The kinetic competition that arises in these experiments is shown in Scheme 2.28<sup>[25]</sup> and the results obtained with the para-Pyrimidyl-BODIPY(PPB)(**Fig 2.2 A**) yield a rate constant of  $6.1 \times 10^6 \text{ M}^{-1} \text{ s}^{-1}$  (incubated at 37°C in benzonitrile by perester **2.28** radical clock) which is close to that reported for the analogous 2,4-dimethyl amino-pyrimidinol lacking the BODIPY conjugate ( $6.5 \times 10^6 \text{ M}^{-1} \text{ s}^{-1}$ ).<sup>[27]</sup> The same clock experiment was carried out on B-TOH (**Fig 2.2 B**) and yielded a rate constant of  $2.8 \times 10^6 \text{ M}^{-1} \text{ s}^{-1}$ , in good agreement with the reported value for  $\alpha$ -TOH which is  $3.2 \times 10^6 \text{ M}^{-1} \text{ s}^{-1}$  (in benzene at

37°C by methyl linoleate radical clock).<sup>[27]</sup>



**Scheme 2.28** General mechanism for perester peroxy radical clock.<sup>[27]</sup>



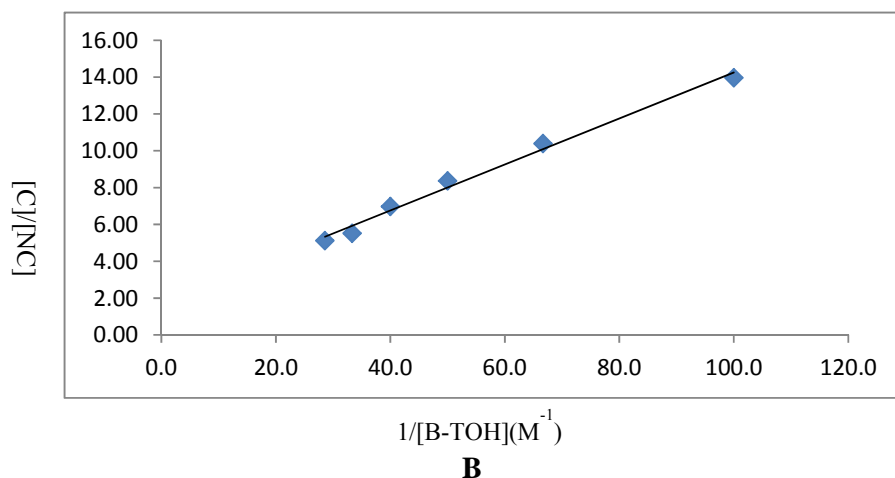


**Figure 2.2** Ratio of conjugated to non-conjugated products *versus* 1/[PPB] (**A**) and 1/[B-TOH] (**B**) obtained from peroxy radical clock experiments (incubated at 37°C in benzonitrile by perester **2.28** radical clock)

From these peroxy radical clock experiments, it is clear that the reactivity of the pyrimidinol moiety to peroxy radicals remains intact upon conjugation to BODIPY via the aryl linkage. Therefore, the lack of fluorescence enhancement upon reaction of para-Pyrimidyl-BODIPY with peroxy radicals must be due to inefficient quenching of the fluorescence of BODIPY by the pyrimidinol moiety. Upon comparing our dye (**2.23**) with the reported dye (B-TOH)<sup>[15]</sup>, it became clear that the more flexible linkage (**Fig 2.3 B**) that connects BODIPY and Trolox in B-TOH may permit greater interactions between the ‘donor’ and ‘acceptor’ moieties than in our dye, which is rigidly linked via the para-disubstituted aryl ring (**Fig 2.3 A**). The obvious solution to this problem is changing the linkage to more flexible ones such as ester, ether, amine linkages etc.

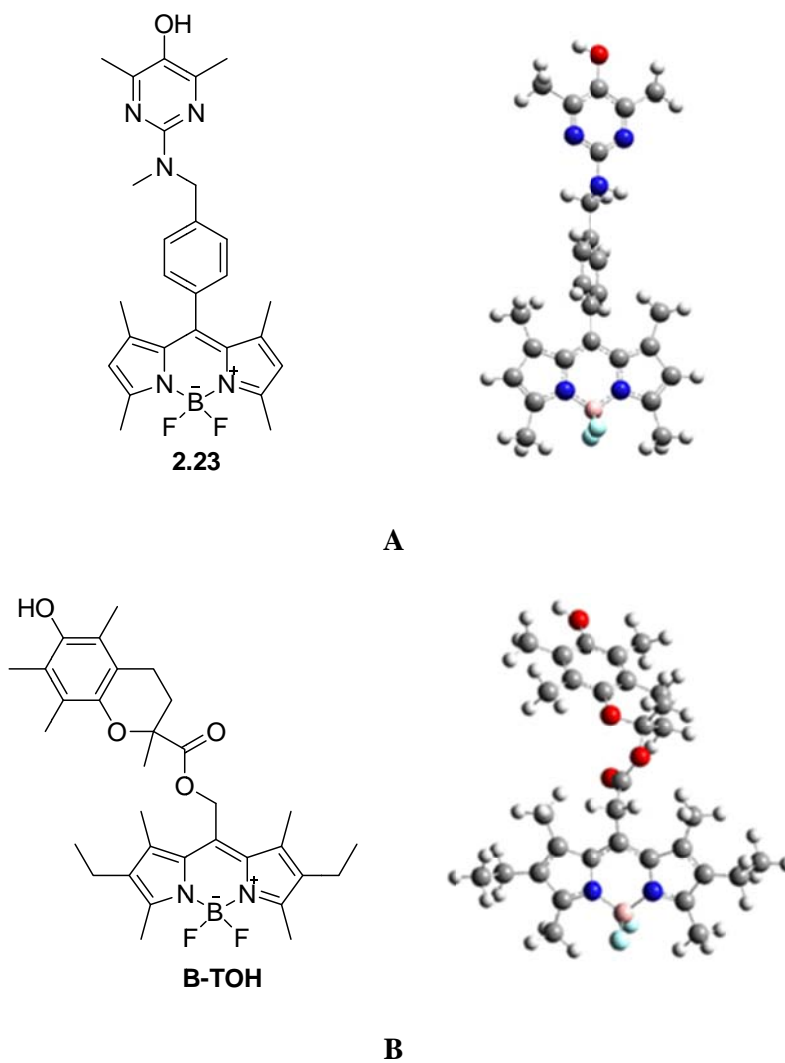
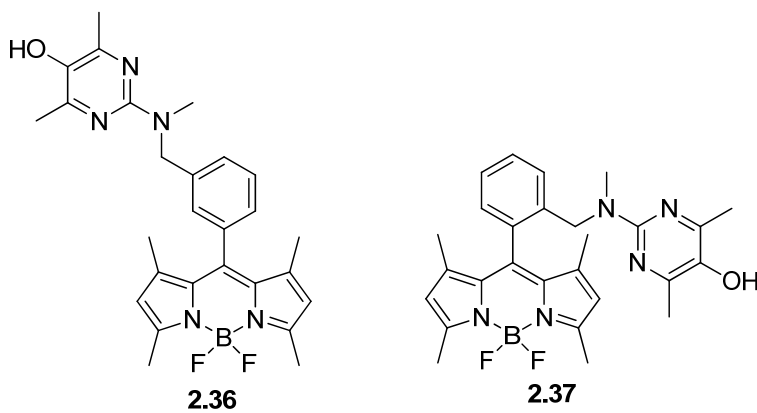


**Figure 2.3** Predicted three-dimensional structures of para-Pyrimidyl BODIPY **2.23** (A) and B-TOH (B)

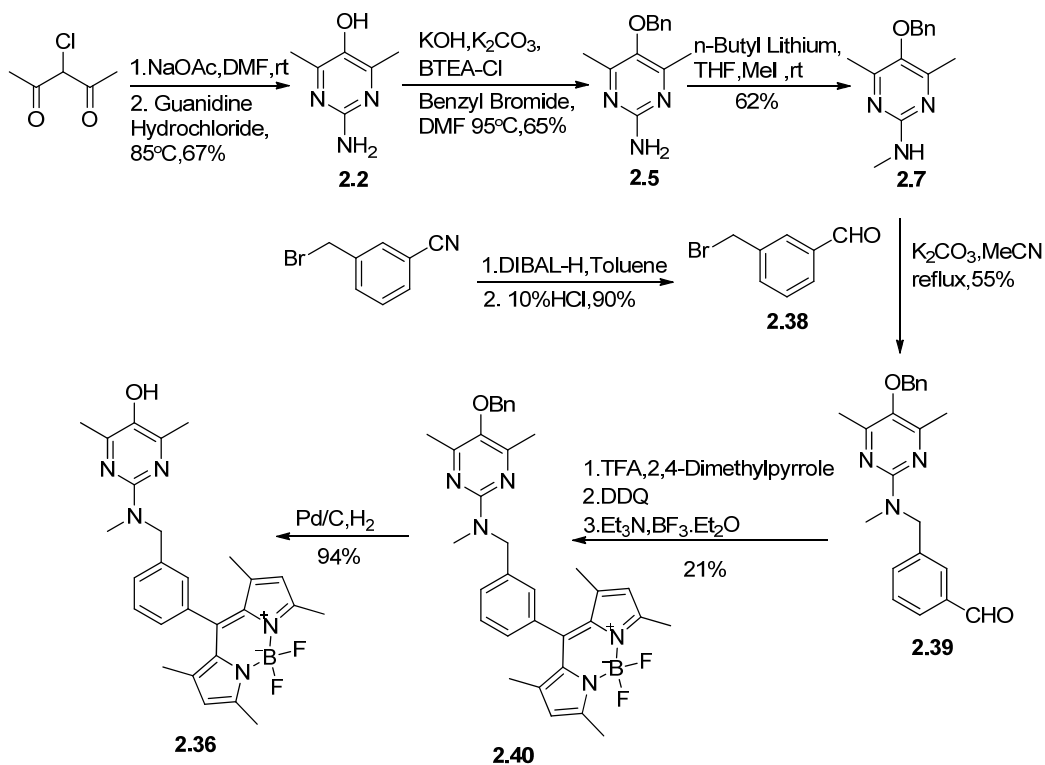
### 2.2.1.3 Synthesis, Fluorescent and Kinetic study of Meta, and Ortho-Pyrimidyl-BODIPY

Prior to trying to change the type of linkage, we wondered whether simply moving the pyrimidinol and BODIPY moieties closer together along the aryl linkage would improve the PeT necessary for fluorescence quenching. Thus, we attempted the

synthesis of the analogous meta-Pyrimidyl-BODIPY (**2.36**) and ortho-Pyrimidyl-BODIPY (**2.37**).

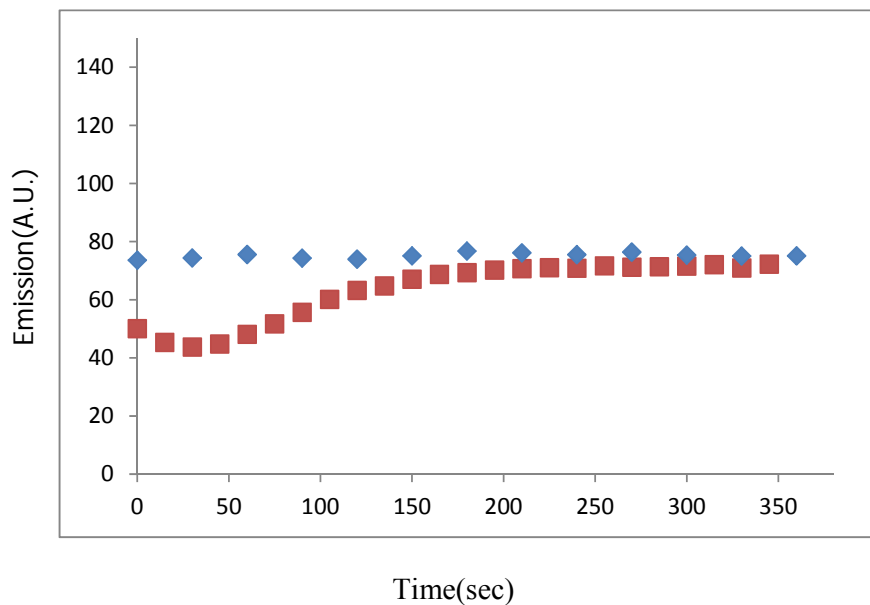


Compound **2.36** was prepared using the same procedures as those used to prepare compound **2.23**: the aminopyrimidinol **2.7** was alkylated with 3-bromomethylbenzaldehyde, and subsequent BODIPY formation and deprotection was carried out to give meta-Pyrimidyl-BODIPY **2.36**.

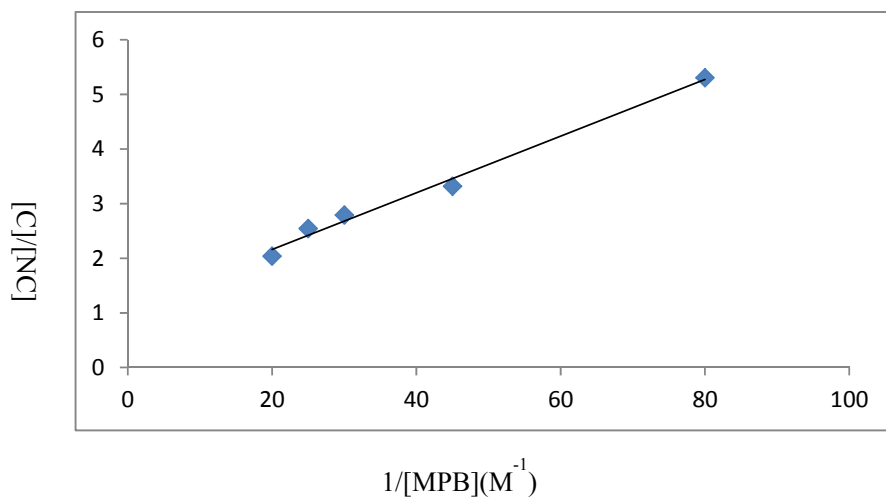


**Scheme 2.29** Synthesis of meta-Pyrimidyl-BODIPY **2.36**

Unfortunately, similar to the case with the para isomer, the meta-Pyrimidyl-BODIPY does not undergo a fluorescence enhancement upon reaction with AIBN-derived peroxy radicals. Again, we carried out peroxy radical clock experiments to verify that the pyrimidinol moiety remained highly reactive to peroxy radicals, finding a rate constant of  $5.8 \times 10^6 \text{ M}^{-1} \text{ s}^{-1}$  (Figure 2.4) – similar to compound **2.23** and the analogous pyrimidinol lacking the BODIPY fluorophore. This indicates that the distance between the ‘donor’ and ‘acceptor’ moieties is still too great for PeT to be effective.



**A**



**B**

**Figure 2.4** A. Emission intensity time profiles for Meta-Pyrimidyl-BODIPY incubated at 55°C with (■) and without(◆) AIBN in toluene. B. Clocking experiments, ratio of conjugated:nonconjugated products *versus* 1/[MPB] (incubated at 37°C in benzonitrile by perester **2.28** radical clock)



As a last ditch effort, we attempted to prepare the ortho-Pyrimidyl-BODIPY isomer (**2.37**), which would bring the pyrimidinol and BODIPY moieties to very close proximity (Figure 2.5).

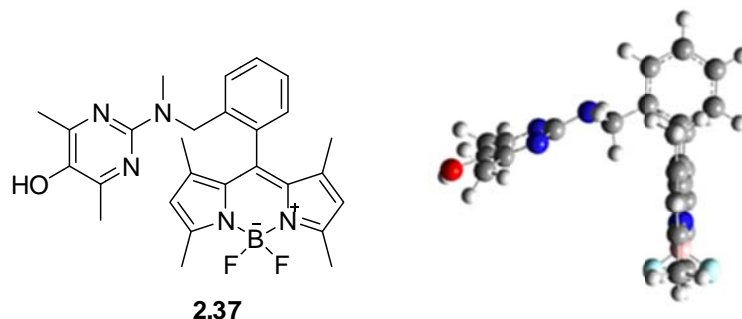
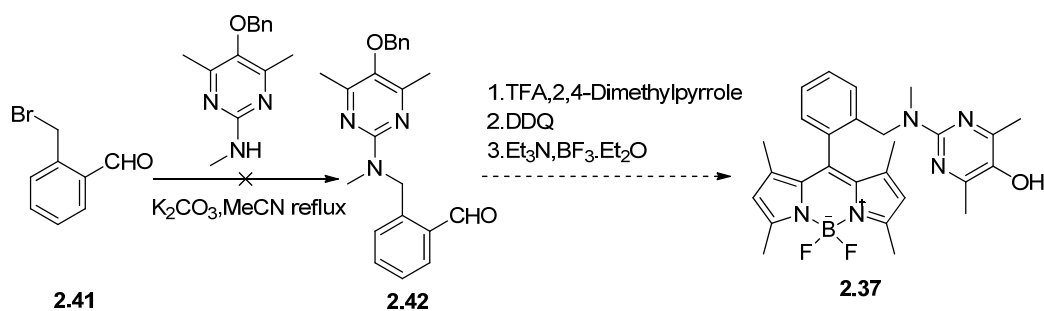


**Figure 2.5** Predicted three-dimensional structure of ortho-Pyrimidyl-BODIPY

Unfortunately, the synthesis of the ortho isomer failed (Scheme 2.30). Presumably, this is the result of the steric hindrance between the aldehyde and bromide as well as the poor nucleophilicity of py(ri)midyl compound. Despite extensive attempts, we were unable to find conditions to carry out the initial substitution. We tried to heat the reaction to up to 120°C, however, only very trace amount of byproduct was formed, and when the temperature was raised above 120°C, the starting aldehyde began to decompose. The use of stronger bases, such as NaH, was accompanied by the formation of many byproducts when the reaction was heated above 60°C. It is reasonable to further suggest that even if the substitution reaction was successful, the subsequent condensation with the pyrrole is going to be even more

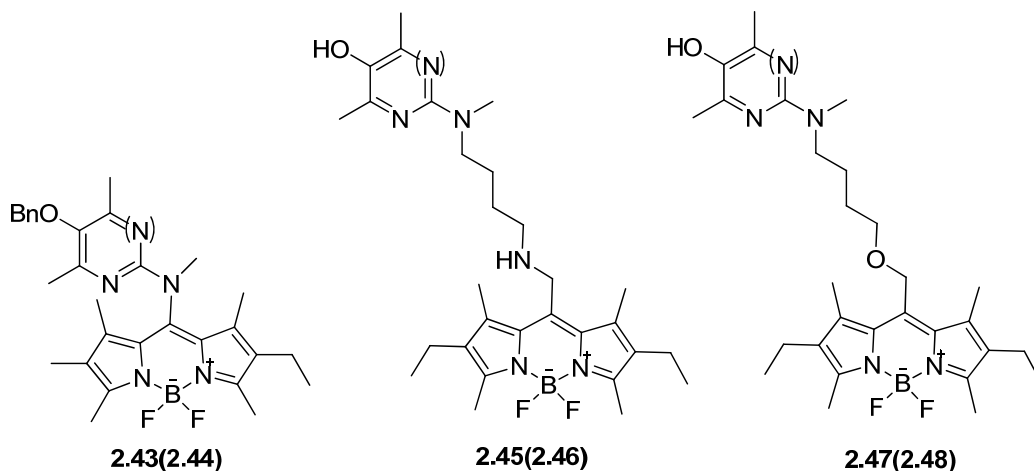
difficult owing to the steric demands of compound **2.42**. Thus, despite the ease with which the para and meta isomers can be prepared, the aryl linkage for the formation of pyrimidinol-BODIPY conjugates was abandoned.



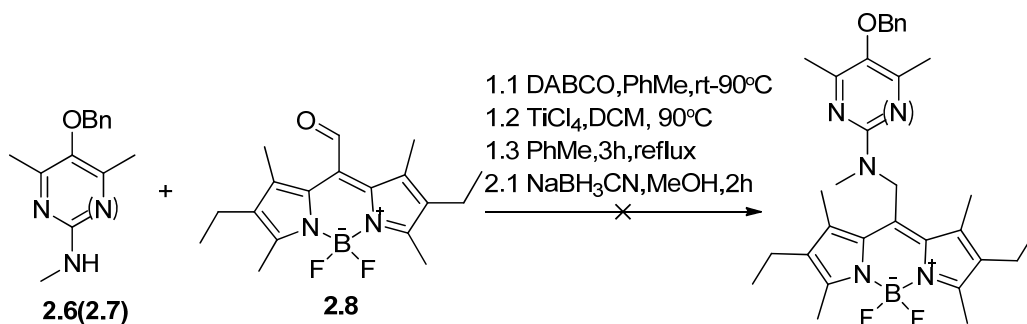
**Scheme 2.30** Attempted synthesis of ortho-Pyrimidyl-BODIPY.

### 2.2.2 Formation of Amine or Ether Linked Pyri(mi)dinol-BODIPY-Conjugates

We envisioned two accessible BODIPY-Pyri(mi)dinol conjugates containing amine linkages: compound **2.43** (**2.44**), which may be obtained through reductive amination of a formyl-BODIPY with an aminopyridinol (aminopyrimidinol); and compound **2.45** (**2.46**), which may be obtained through substitution of a halomethyl-substituted BODIPY with an aminated pyridinol (pyrimidinol).



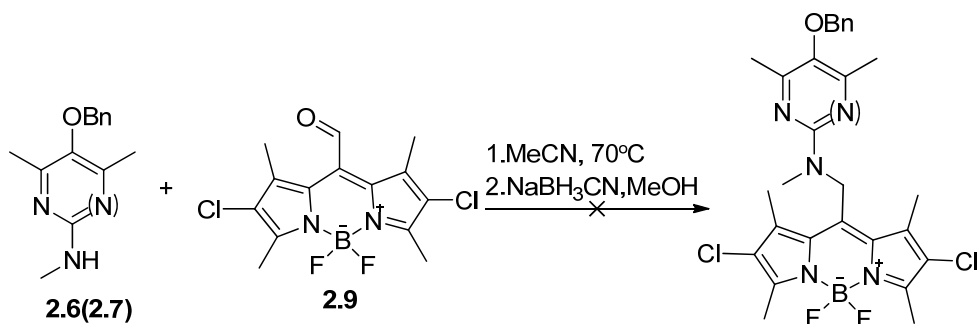
Pyri(mi)dinol compound **2.6(2.7)** is firstly tried in the reductive amination with BODIPY aldehyde **2.8(Scheme 2.31)**, similar reaction of compound **2.8** with butylamine needs  $\text{TiCl}_4$  as the catalyst, and such aldehyde activation is required because of the low reactivity of the aldehyde group and the bulkiness of the BODIPY core that attached to it. We tried the same condition, however, the reaction failed to form any imine compound, which could be due to the fact that  $\text{TiCl}_4$  coordinated with the nitrogen on pyrimidinol compound and thus got deactivated.



**Scheme 2.31** Attempted synthesis of pyri(mi)dinol-BODIPY-conjugates through

reductive amination using 2,6 diethyl-substituted BODIPY aldehyde

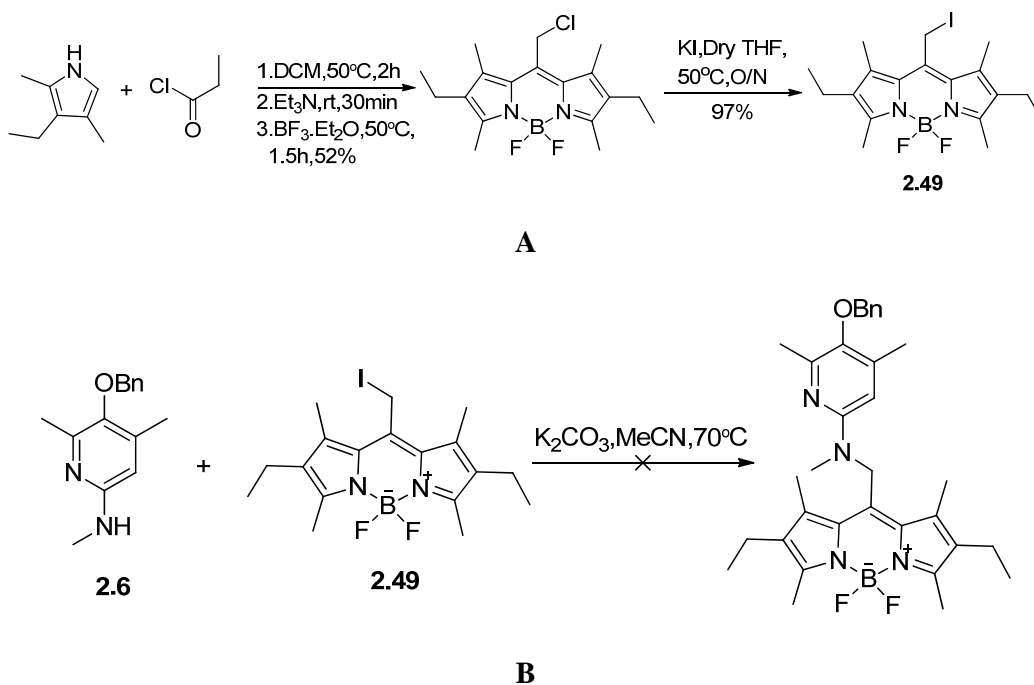
To avoid using such Lewis acid catalysts, we next utilized a more reactive BODIPY aldehyde **2.9**, whose aldehyde group is much more electrophilic than compound **2.8** due to the electron withdrawing effects of the two chlorine atoms substituted at the 2- and 6-positions of the BODIPY core. Unfortunately, when we treated compound **2.9** with pyri(mi)dinol **2.6** (**2.7**) in dry acetonitrile with heating up to 70°C (Scheme 2.32) no imine was formed; above 70°C the BODIPY began to decompose, despite our attempts to rigorously exclude oxygen from the system.



**Scheme 2.32** Attempted synthesis of pyri(mi)dinol-BODIPY-conjugates through reductive amination using 2,6 dichloro-substituted BODIPY aldehyde

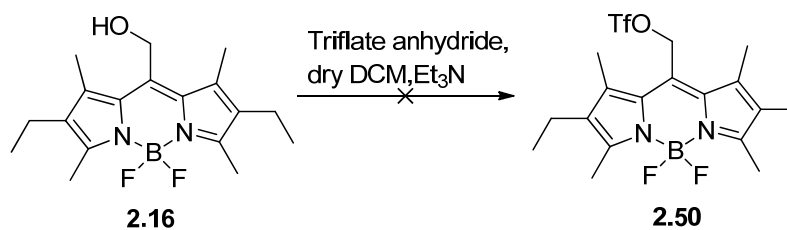
We also tried the substitution reaction (Scheme 2.33A) of BODIPY-I (**2.49**), with the aminopyridine **2.8**. The iodomethyl BODIPY was prepared as Scheme 2.33B under Finkelstein conditions by treating BODIPY-Cl with NaI in dry acetonitrile at 70°C containing K<sub>2</sub>CO<sub>3</sub> to react with the HI that can be generated during the reaction. However, the reaction didn't proceed at 70°C, and when we tried to rise up to a higher temperature, BODIPY decomposes rapidly. We suspect that both the reductive amination and amine substitution reactions have failed due to the low nucleophilicity

of the amino group on the aminopyri(mi)dinol as well as steric effects owing to the peri methyl groups on the BODIPY.



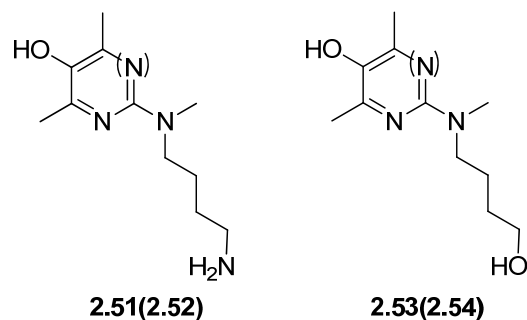
**Scheme 2.33 A.** Formation of BODIPY-I. **B.** Attempted synthesis of pyridinol-BODIPY-conjugate through alkylation with BODIPY-I

Finally, we also tried is to activate the BODIPY-OH (**2.16**) by transformation of the hydroxyl group to a triflate group, which is a much better leaving group than iodide. However, the reaction (Scheme 2.34) to form the BODIPY-triflate (**2.50**) failed due to the rapid decomposition of BODIPY by the triflic acid generated during the reaction, which cannot be prevented or slowed down by reaction at low temperature (-78°C) or addition of neutralizing reagent (e.g. Et<sub>3</sub>N).



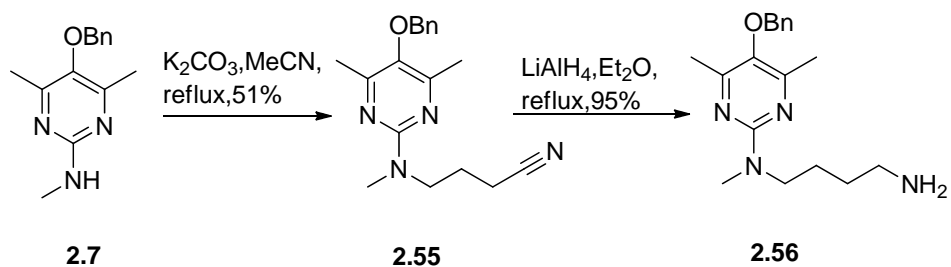
**Scheme 2.34** Attempted synthesis of triflate-activated BODIPY

An alternative way to increase the nucleophilicity of the pyri(mi)dyl moiety is by substituting the amino group with an alkyl amine (**2.51** or **2.52**) or alkyl hydroxyl group (**2.53** or **2.54**), which can be expected to more easily undergo reaction with BODIPY-I (**2.49**), however this would bring the problem of protonation of the resulting adduct in buffer solutions (pH=7.4), since the pKa of the product's analog diethylamine is around 10.28. This problem can be solved if the aliphatic linker is long enough so that its lipid solubility will be greatly increased and the protonation will be less likely to happen, however this would lead to another problem, as the longer the linker is the less likely the PeT would happen and the less likely the adduct will be an effective indicator.



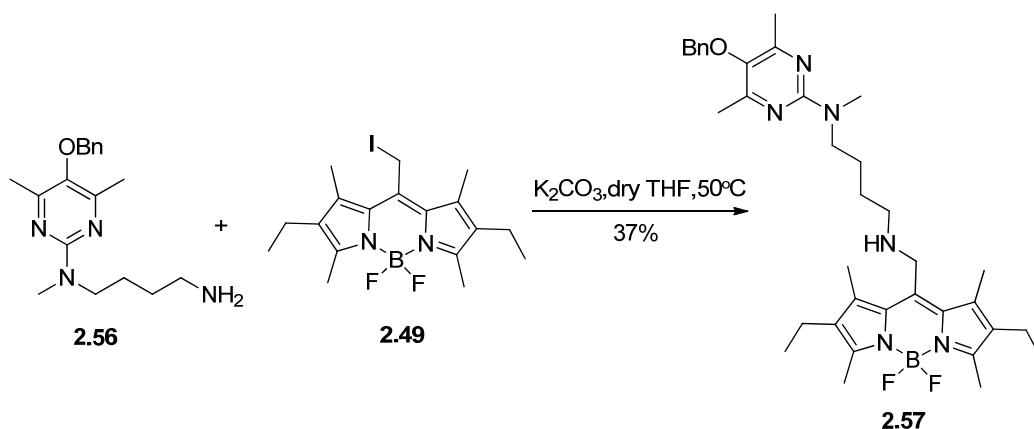
The synthetic route to make compound **2.52** is shown in Scheme 2.35.

Aminopyrimidine **2.7** was treated with 4-bromobutanenitrile and  $K_2CO_3$  in refluxing acetonitrile overnight, producing the corresponding nitrile (**2.55**) in 51% yield. Bromoalkyl nitriles with shorter chains were also subjected to the same reaction conditions, however, due to the strong electron withdrawing effect of the nitrile group, these reactions either failed or had very low yield (less than 5%). The resulting nitrile was then reduced using  $LiAlH_4$  in refluxing ether to generate the corresponding amine (**2.56**) in 95% yield.



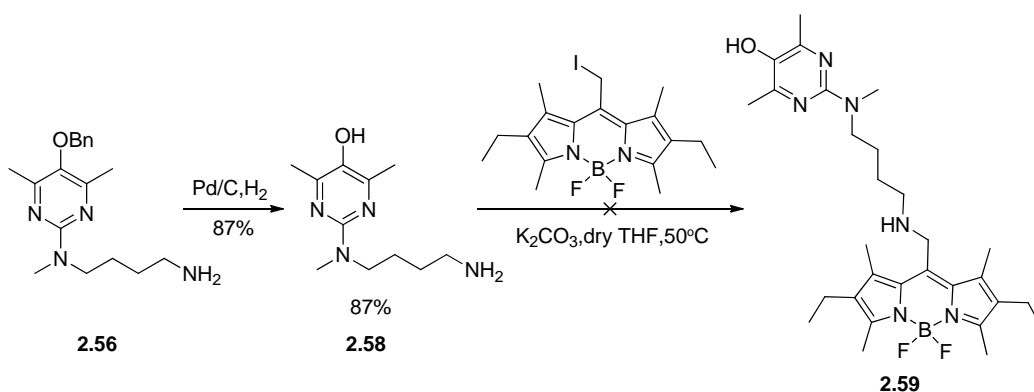
**Scheme 2.35** Installation of butylamine group onto pyrimidyl compound **2.7**

Amine **2.56** was then successfully used to displace iodide from BODIPY-I (**2.49**) in dry THF at  $50^\circ C$  to obtain the desired product **2.57** in 37% yield.



### Scheme 2.36 Synthesis of amine-linked pyrimidyl-BODIPY-conjugate

Once we had confirmed that the substrates are sufficiently reactive for substitution, we proceeded to deprotection of the benzyl group from compound **2.56** and then use the generated pyrimidinol compound **2.58** in the substitution reaction with BODIPY-I. This route (Scheme 2.37) was preferred since we anticipated that removal of the benzyl group from compound **2.57** by Pd/C-catalyzed hydrogenation conditions, would also reduce the double bond at the meso position of the BODIPY-core. This is in contrast to the debenzylation of para-Pyrimidyl-BODIPY (**2.23**) described above, which is successful due to the stability imparted to the double bond by the aryl ring at the meso position.



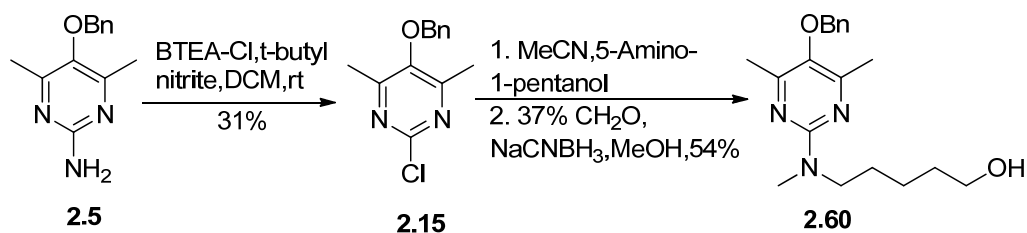
### Scheme 2.37 Attempted synthesis of amine linked pyrimidinol-BODIPY-conjugate

The reaction, however, failed to produce any desired product **2.55**. Instead, most of the BODIPY decomposed and formed a light red mess that would not migrate upon analysis of the reaction mixture by thin layer chromatography. There were two other



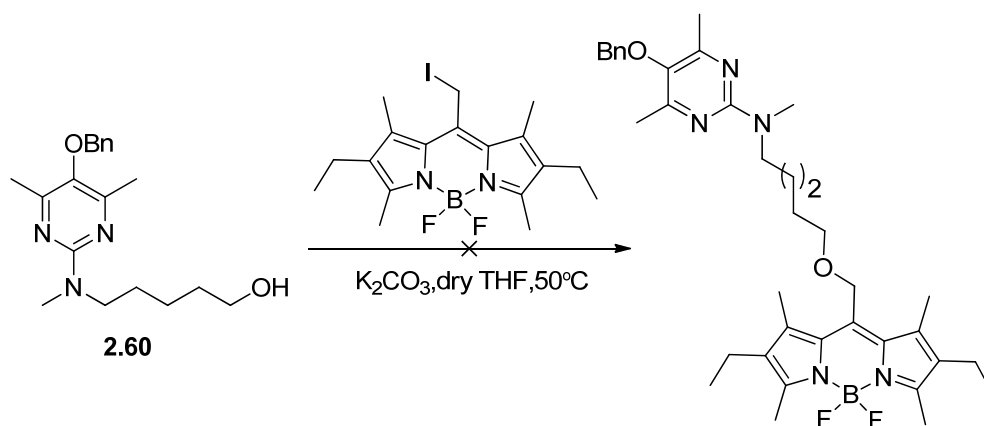
spots also visible on the TLC plate, but they were both obtained in very low yield (less than 5%) following separation by flash column chromatography, and could not be characterized by NMR.

The synthetic route to compound **2.60** is shown in Scheme 2.38. The pyrimidyl chloride **2.15**, which was obtained from the corresponding pyrimidyl amine by non-aqueous halo-de-diazonation, was combined with 5-amino-1-pentanol and refluxed in acetonitrile containing and  $K_2CO_3$ . The resultant pyrimidyl amino alcohol (**2.61**) was then reductively alkylated with formaldehyde and  $NaCNBH_3$  to give compound **2.60** in 54% overall yield.



**Scheme 2.38** Installation of pentanol group onto aminopyrimidine **2.5**

The pyrimidine amino alcohol **2.60** was then reacted with BODIPY-I in dry THF containing  $K_2CO_3$  (Scheme 2.39), but disappointingly, the BODIPY appeared to decompose completely.



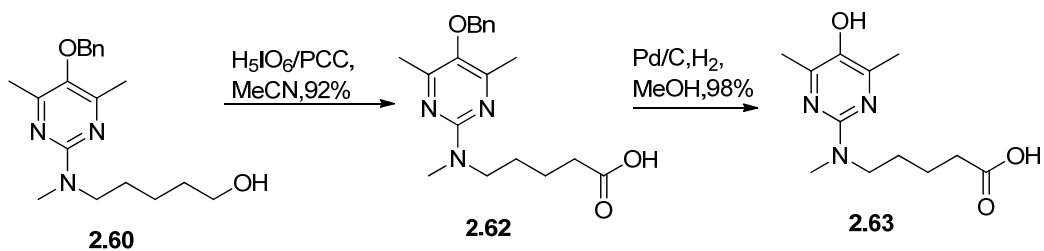
**Scheme 2.39** Attempted synthesis of ether linked pyrimidyl-BODIPY-conjugate

Failure of these substitution reactions may suggest that the free aryl alcohol in complicates the coupling reactions in some way – perhaps by competition, although this is highly unexpected. Future efforts to circumvent this problem should employ other protecting groups that are more compatible with the chemistry of the intact BODIPY fluorophore; trimethylsilyl group may solve this problem. Similar work, in which a TMS-protected phenol conjugated to BODIPY has been deprotected using HCl/methanol/THF, has been reported by Atkinson's group.<sup>[22]</sup>

### 2.2.3 Formation of Carboxyl- or Carbamoyl-Linked Pyri(mi)dinol-BODIPY Conjugates

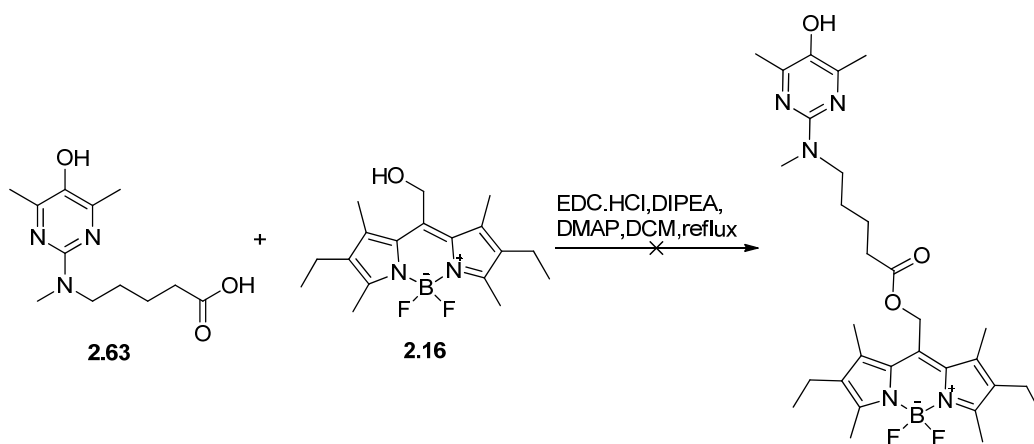
The preparation of a pyrimidyl carboxylic acid (Scheme 2.40) required for esterification to a BODIPY-derived alcohol began with the oxidation of amino alcohol **2.60** to the corresponding carboxylic acid **2.62**. This reaction proceeded smoothly in acetonitrile using  $\text{H}_5\text{IO}_6/\text{PCC}$  as oxidant, generating the pyrimidyl carboxylic acid in 92% yield. The subsequent hydrogenative debenzoylation catalyzed by Pd/C in MeOH

generated the pyrimidinol carboxylic acid **2.63** in essentially quantitative yield.

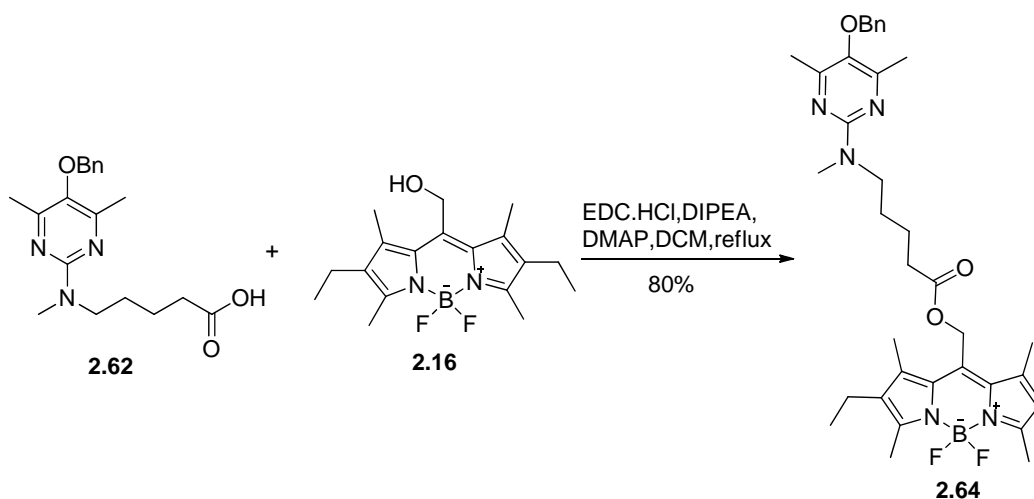


**Scheme 2.40** Installation of butyric acid group onto amino pyrimidinol.

The pyrimidinol carboxylic acid **2.63** and BODIPY-OH was then treated with EDC•HCl, DIPEA, and DMAP in refluxing dry DCM (Scheme 2.41), in a first attempt at the esterification based upon the protocol used to couple Trolox and BODIPY-OH **2.16** for the formation of B-TOH. To our surprise, and disappointment, the reaction was unsuccessful, and BODIPY-OH remained unreacted after more than a day. Switching solvents and increasing the temperature to  $60^\circ\text{C}$  (in dry THF) was equally disappointing, with the only observable change now being some decomposition of BODIPY-OH.



**Scheme 2.41** Attempted EDC coupling using BODIPY-OH and pyrimidinol-butylbutyric acid

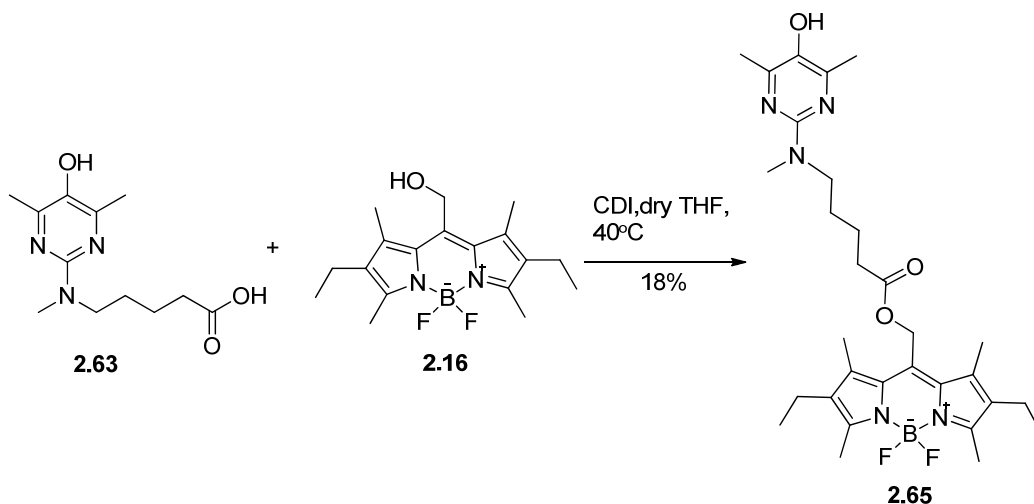


**Scheme 2.42** EDC coupling using BODIPY-OH and pyrimidinol-butylbutyric acid

The reaction of the benzyl-protected pyrimidinol compound **2.62** with BODIPY-OH (Scheme 2.42) under the same reaction condition worked well to yield the corresponding adduct (**2.64**) in 80% yield, but removal of the benzyl protecting group by a variety of methods was unsuccessful.

We then returned our focus to the coupling of the unprotected compound **2.63** and BODIPY-OH (Scheme 2.43). After surveying many possible reaction conditions

(not shown), we were able to successfully couple the two partners and obtain the conjugate in a disappointing 18% yield by treating compound **2.63** with 1 eq CDI first and subsequent addition of BODIPY-OH and heating to 40°C. The low yield is presumably due to the competitive self-reaction of the CDI-activated pyrimidinol.

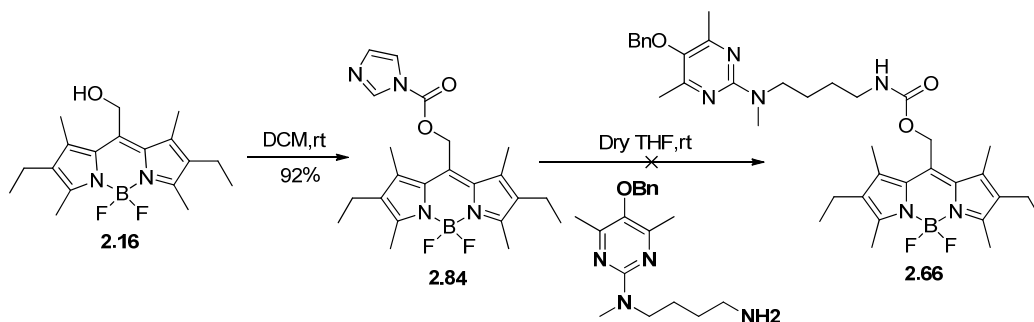


**Scheme 2.43** CDI coupling using PMOH and pyrimidyl-butyric acid.

While this was highly encouraging, we were then disappointed to see that the fluorescence of the BODIPY chromophore was not quenched following conjugation to the pyrimidinol (in each of toluene, EtOAc, hexanes and methanol). Again, since the oxidation potential of the pyrimidinol moiety is smaller than that of the Trolox moiety used in B-TOH, the only reason can be the distance between the pyrimidinol and BODIPY is still too long for efficient PeT to take place.

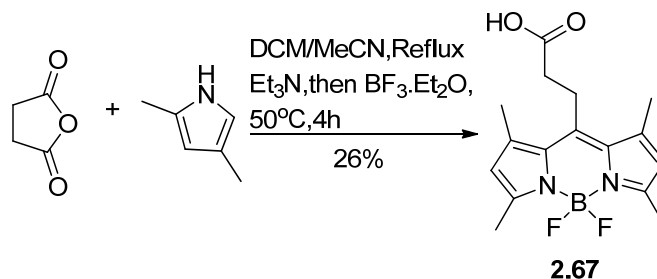
We also found, in the process of trying to use CDI as the activation reagent for pyrimidyl-carboxylic acid **2.63**, that BODIPY-OH can react with CDI to form compound **2.66** in 92% yield. We therefore hoped that this CDI-activated BODIPY

may be able to react with the pyrimidyl amine **2.58** to get carbamate **2.84** (Scheme 2.44). Unfortunately, such activated BODIPY proved to be unstable under the reaction conditions, where it decomposed completely.

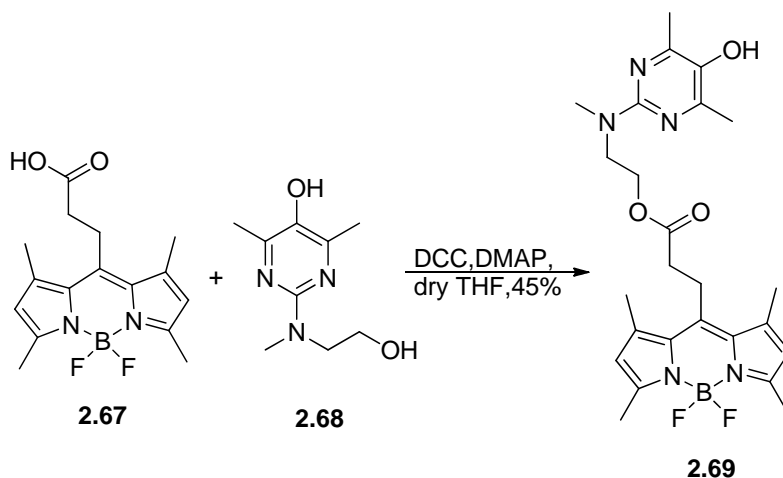


**Scheme 2.44** Attempted synthesis of carbamoyl-linked pyrimidyl-BODIPY conjugate using CDI activated BODIPY species

We then decided to exchange the handles on the two coupling partners, and attempted to couple the carboxy-substituted BODIPY **2.67**, obtained using a literature procedure as in Scheme 2.45,<sup>[20]</sup> with pyrimidyl compound **2.68** in the presence of DCC and DMAP in dry THF. The reaction gave the desired product **2.69** in 45% yield (Scheme 2.46).



**Scheme 2.45** Synthesis of BODIPY acid



**Scheme 2.46** DCC coupling using BODIPY acid with hydroxyethyl pyrimidinol **2.68**

Sadly, yet again, there appeared to be no quenching of the BODIPY fluorescence upon conjugation. Furthermore, incubation with AIBN as a source of peroxy radicals lead to increase in fluorescence with time (Figure 2.6), despite the fact that the linker between the BODIPY and pyrimidinol moieties in compound **2.69** is one methylene group shorter than in compound **2.65**.

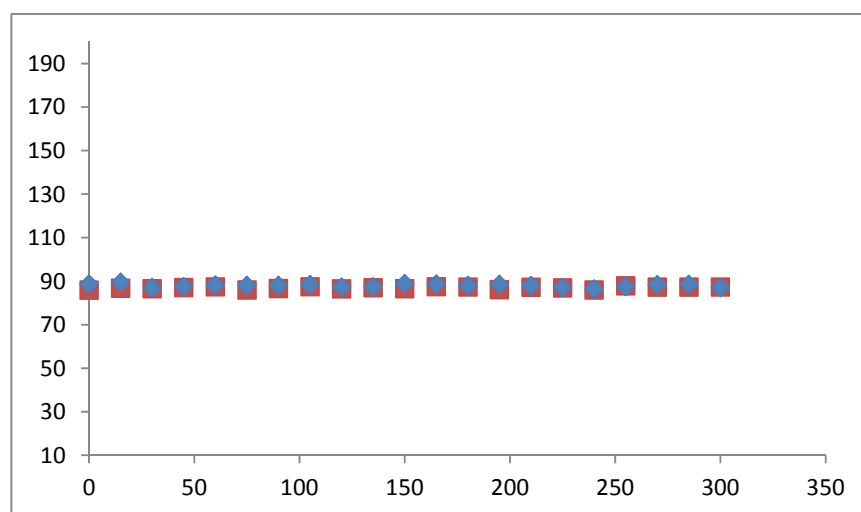
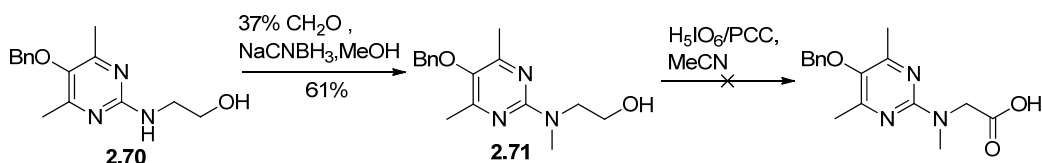


**Figure 2.6** Emission intensity time profiles for Dye 2.67 incubated at 55°C with (■)

and without(♦) AIBN in toluene

We next tried to shorten the linker as much as possible. In order to do so, we used the shortest  $\text{NH}_3(\text{CH}_2)_n\text{OH}$  compound – ethanolamine ( $n=2$ ) – in the substitution reaction with pyrimidyl chloride. The generated alcohol compound **2.70** then underwent reductive alkylation with formaldehyde and  $\text{Na}(\text{CN})\text{BH}_3$  to give compound **2.71**, which was then oxidized using  $\text{H}_5\text{IO}_6/\text{PCC}$  as in Scheme 2.47. Unfortunately, while the starting material (**2.71**) was completely consumed, a black mess at the baseline of TLC plate was observed a product, which was an inseparable mixture that could not be characterized by NMR. Neutralization prior to analysis by TLC did not promote movement of the spot on the plate, implying that the generated byproduct is not simply a protonated pyrimidyl species.



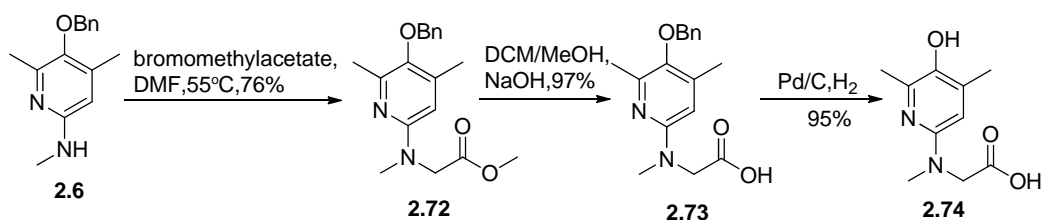
**Scheme 2.47** Attempted synthesis of pyrimidyl-acetic acid

We then attempted treating compound **2.71** with PDC in DMF, however, the reaction still would not provide any product.

Following these failures with the pyrimidyl alcohol compounds, we decided to alkylate the pyri(mi)dyl compound **2.6** (**2.7**) with methyl bromoacetate. Due to the attached bromide and carbonyl group, the methylene group in methyl bromoacetate is

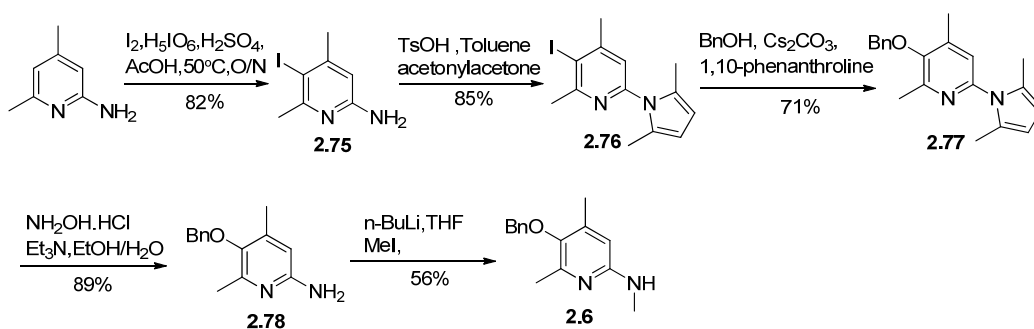


very electrophilic and as a result, in spite of the poor nucleophilicity of the amino group on the aminopyridine **2.6**, it still reacted at a relatively low temperature (50°C). The reaction, however, failed with the with pyrimidyl compound **2.7**. The subsequent hydrolysis of compound **2.73** using sodium hydroxide in MeOH/DCM solution and debenzoylation via Pd/C-catalyzed hydrogenation gave compound **2.74** as a colourless oil (Scheme 2.48).



**Scheme 2.48** Synthesis of pyridinol-acetic acid

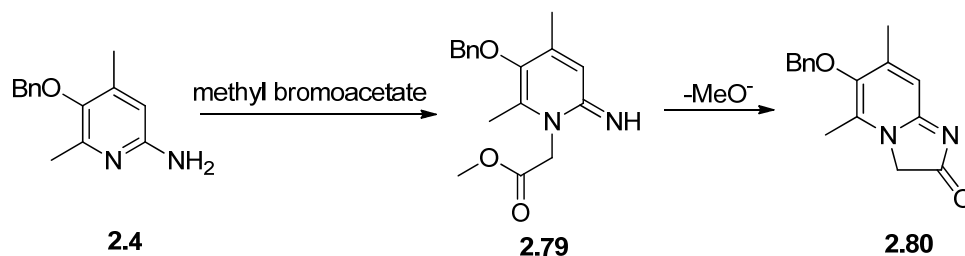
The synthesis of the aminopyridinol starting material is shown in Scheme 2.49.



**Scheme 2.49** Synthesis of compound **2.6**

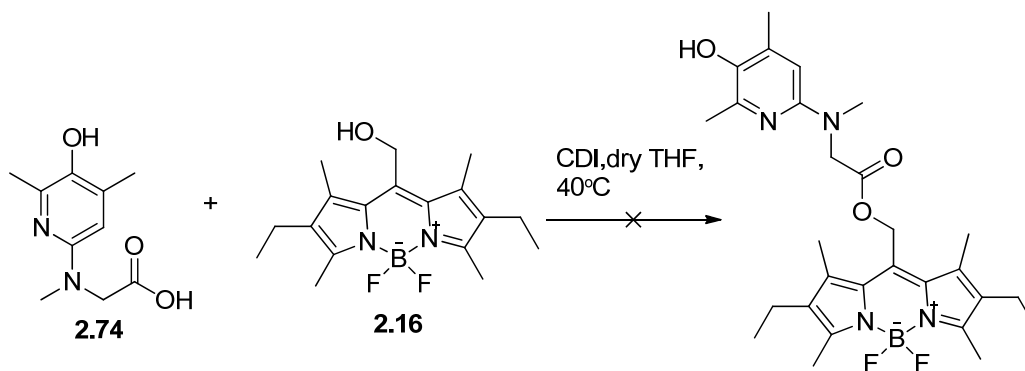
The direct alkylation of the exocyclic nitrogen of pyridyl compound **2.4** by methyl bromoacetate is known to occur at the ring nitrogen, giving the related

imidazo[1,2-a] (**2.79**) derivatives through the corresponding intermediate pyridone imines (**2.80**) as in Scheme 2.50.



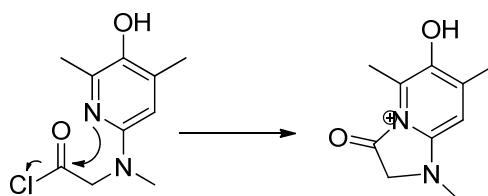
**Scheme 2.50** Mechanism of formation of pyridine imines from direct alkylation of pyridyl compound 2.6 with methyl bromoacetate

The pyridinol acetic acid **2.74**, however, wouldn't provide any coupling product (Scheme 2.51): upon activation by CDI, 3 new spots formed on TLC, and the subsequent reaction with BODIPY-OH failed. We try to analyze the CDI-activated intermediate but couldn't characterize it through NMR, presumably due to its inherent lability.



**Scheme 2.51** Attempted CDI coupling using BODIPY-OH and pyridinol acetic acid

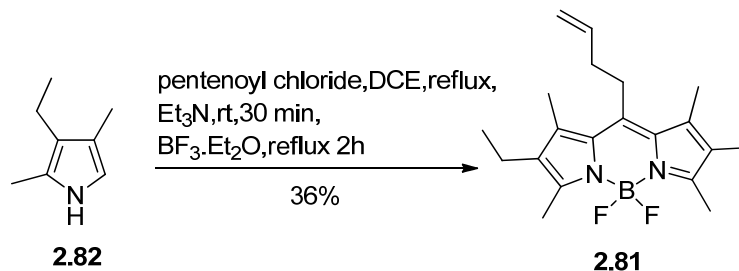
We have also tried activate acid **2.74** using thionyl chloride, however, as soon as the addition of thionyl chloride into the solution of **2.74** in acetonitrile, the solution turned to dark green and TLC showed several spots. The crude NMR of this reaction in DMSO shows that the methylene group in **2.74** is missing, which is difficult to explain. It seems reasonable to suggest the initial formation of an activated acyl pyridinium intermediate (Scheme 2.52), and it may be that this undergoes reactions indiscriminately with any nucleophiles available in solution.



**Scheme 2.52** Formation of putative acyl pyridinium ion intermediate

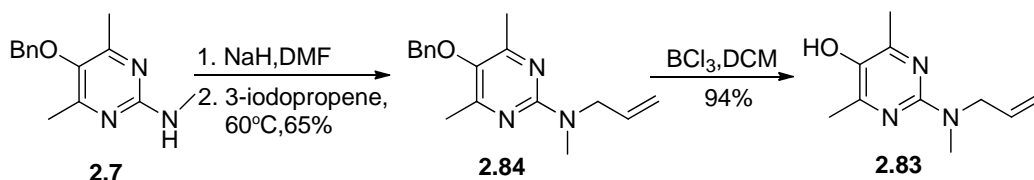
#### 2.2.4 Formation of Alkene-Linked Pyri(mi)dinol-BODIPY Conjugates

We have also tried olefin metathesis for the coupling of BODIPY and pyrimidyl moieties. The alkenylated BODIPY **2.81** can be synthesized as shown in Scheme 2.53. The synthesis is a one-pot reaction that starts with condensation of pentenoyl chloride with 3-ethyl-2,4-dimethylpyrrole (**2.82**), subsequent deprotonation with  $\text{Et}_3\text{N}$  and then coordination with  $\text{BF}_3 \cdot \text{Et}_2\text{O}$  in the usual way to generate **2.81** in 36% yield.



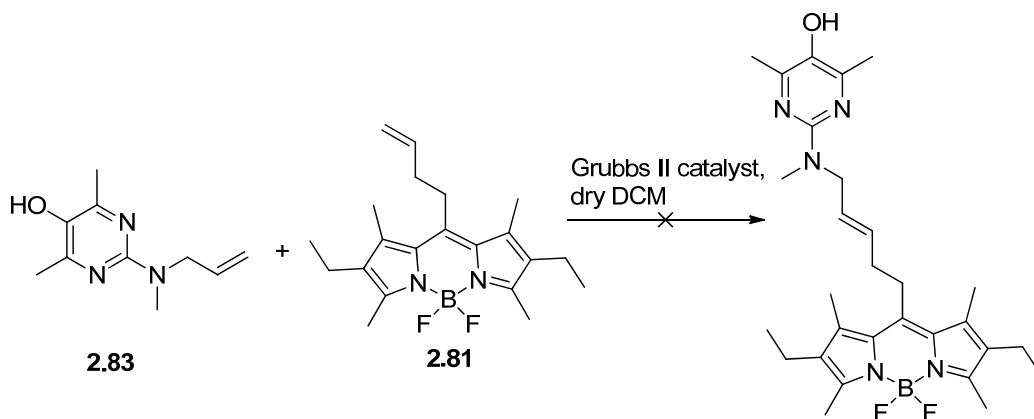
**Scheme 2.53** Synthesis of BODIPY-butene

The allylated pyrimidine **2.83** was synthesized as in Scheme 2.54. Deprotonation of pyrimidyl compound **2.7** with NaH, and then substitution on 3-iodopropene in dry DMF, and stirring at 60 °C for overnight, gave compound **2.84** in 65% yield. Subsequent hydrogenation afforded the allylated pyrimidinol **2.83** in 94% yield.

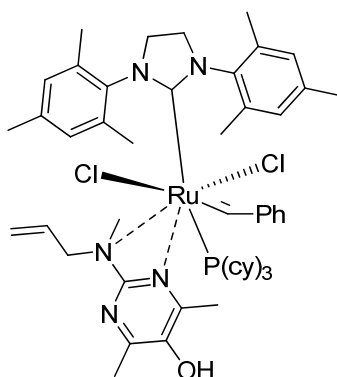


**Scheme 2.54** Synthesis of allylated pyrimidinol **2.83**

Unfortunately, despite attempts with both first- and second-generation Grubbs catalysts, metathesis with the allylate pyrimidinol **2.83** and the homoallylated BODIPY **2.81** failed (Scheme 2.55). We surmise that the nitrogen atoms in the aminopyrimidyl compound may coordinate to the Ru atom in Grubbs catalyst (Scheme 2.56). In future work, we plan to attempt incorporation of a proper Lewis acid in the reaction mixture in order to insure that the Grubbs catalyst can participate in metathesis rather than simple coordination chemistry.



**Scheme 2.55** Attempted metathesis of an allylated pyrimidinol and homoallylated BODIPY.



**Scheme 2.56** Coordination of Grubbs II catalyst with allylated pyrimidinol.

### 2.3 General Experimental Procedures.

**4,6-dimethyl-2-aminopyrimidinol (2.2).** To a stirred solution of 3-chloropentane-2,4-dione (1.34 g, 10 mmol) in DMF (10 ml) was added sodium acetate (1.6 g, 20 mmol), the reaction was let stirring at room temperature for 24 hours, until TLC shows complete consumption of starting material, and guanidine hydrochloride (950 mg, 10

mmol) was added to the reaction solution, and the reaction was heated up to 85°C, and kept stirring under argon for overnight. The resulting dark brown solution was evaporated under high vacuum to dryness and washed with methanol (10 ml) for 3 times, the methanol solution is then evaporated to dryness and the resulting dark brown solid is recrystallized in ethyl acetate/methanol solution to afford pure product as white solid in 67% yield. The spectral data is in accordance with literature values.<sup>[13]</sup>

**4-bromomethyl-benzaldehyde (2.3).** To a stirred solution of 4-bromomethyl-Benzonitrile (1.94 g, 10 mmol) in dry toluene (20 ml) cooled to 0°C under argon was added dropwise of DIBAL-H (14ml, 14mmol, 1.0M solution in toluene), the reaction was kept stirring for 1 hour and the temperature was kept under 5°C, the resulting solution was diluted with chloroform (30 ml) and quenched by 10% HCl (70 ml) in small portions while cooling, the resulting solution was kept stirring for 1 additional hour at room temperature. The resulting solution was extracted with ether for several times and the ether extraction solution was concentrated and yielding a white needle like solid (1.876g, 92%), which can be used in the next step without further purification. And the spectral data is in accordance with literature values.<sup>[6]</sup>

**5-benzyloxy-4,6-dimethyl-2-aminopyrimidinol (2.5).** To a stirred solution of potassium hydroxide (1.14g, 20 mmol), potassium carbonate (2.8 g, 20 mmol) and BTEA-Cl (2.27 g, 10 mmol) in DMF (20 ml) was added 4,6-dimethyl-2-amino

Pyrimidinol (**2.2**, 1.39g, 10 mmol), the solution was stirred under room temperature for 15 minutes and benzyl bromide (2.57g, 15mmol) was added, the reaction was then heated up to 95°C, and kept stirring under argon for 48 hours. The resulting dark brown solution was evaporated under high vacuum to dryness, and the resulting dark brown solid was dissolved in water and extracted several times using ethyl acetate. The resulting dark brown oil is purified using flash chromatography with 25% Hexanes/Ethyl acetate to afford pure product as a white solid (14.88g, 65%), the spectral data is in accordance with literature values.<sup>[13]</sup>

**5-benzyloxy-4,6-dimethyl-2-N-methylaminopyridinol (2.6)**. Same procedures as making compound **2.7**, yield a white solid (134mg, 55%). <sup>1</sup>H NMR (400 MHz, CDCl<sub>3</sub>): δ 2.20 (s, 3H), 2.35 (s, 3H) 2.83 (s, 3H), 4.40 (bs, 1H), 4.72 (s, 2H), 6.06 (s, 1H), 7.24-7.45(m, 5H) ppm. <sup>13</sup>C NMR (300 MHz, CDCl<sub>3</sub>): δ 16.50, 19.13, 29.83, 74.97, 104.50, 127.98, 128.08, 128.56, 137.47, 142.47, 144.52, 149.66, 155.76 ppm. HRMS (ES<sup>+</sup>) calcd (M) 242.1419, obsd 242.1405

**5-benzyloxy-4,6-dimethyl-2-N-methylaminopyrimidinol (2.7)**. To a stirred solution of 5-benzyloxy-4,6-dimethyl-2-aminopyrimidinol (**2.5**, 243 mg 1mmol) in dry THF cooled to -10°C under argon was added n-Butyl lithium (0.625 ml, 1mmol, 1.6 M in hexanes), the solution was kept stirring for 20 minutes and MeI (142mg, 1mmol) was added, the reaction solution was resume to room temperature and kept stirring for an additional hour. The resulting solution was quenched with sat. NH<sub>4</sub>Cl and extracted

with DCM, the DCM extraction solution is then concentrated the resulting yellow oil is purified through flash chromatography to afford pure compound **2.7** as white solid(150mg,62%). <sup>1</sup>H NMR (400 MHz, CDCl<sub>3</sub>): δ 2.29 (s, 6H), 2.93 (s, 3H) 4.70 (s, 2H), 5.45 (s, 1H), 7.36-7.38 (m, 5H) ppm. <sup>13</sup>C NMR (400 MHz,CDCl<sub>3</sub>): δ 19.08, 28.71, 75.47, 128.31, 136.90, 142.33, 158.92, 160.72 ppm. HRMS (ES+) calcd (M) 243.1372, obsd 243.1361

**8-Formyl-2,6-diethyl-1,3,5,7-tetramethyl Pyrromethene Fluoroborate (2.8).**

Dess-Martin periodinane (1.5 equiv) was dissolved in dry dichloromethane. To the suspension was slowly added a solution of *meso*-acetoxymethyl BODIPY dyes PMOH(**2.16**)(1 equiv) in dry dichloromethane at 0 °C under argon. After 10 min, the ice bath was removed and the reaction mixture was left stirring at room temperature for extended periods of time as detailed below. The reaction mixture was extracted with saturated aqueous Na<sub>2</sub>S<sub>2</sub>O<sub>3</sub> followed by saturated aqueous NaHCO<sub>3</sub> and brine. The combined organic solutions were dried over MgSO<sub>4</sub>. The solvent was evaporated, and the residue was purified using flash column chromatography with dichloromethane as the eluent. Spectral data is in accordance with literature values.<sup>[9]</sup>

**5-Benzyloxy-4,6-dimethyl-2-chloropyrimidine (2.15).** To a solution of 5-benzyloxy-2-aminopyrimidine (510mg, 2.23 mmol) in 20 mL of drydibromomethane was added benzyltrimethylammonium chloride (2.31g, 10.22 mmol, 4.5 equiv) followed by dropw ise addition of *tert*-butylnitrite (2.34g ,22.73 mmol, 10 equiv). The solution was stirred at room temperature under nitrogen



atmosphere for overnight and was monitored on TLC. Upon completion, the reaction was quenched by addition of aqueous NaHCO<sub>3</sub> solution, and the product was extracted with dichloromethane. The combined organic extracts were washed with brine, dried over Na<sub>2</sub>SO<sub>4</sub>, and concentrated in vacuum. The residue was subjected to flash chromatography (eluent: ethyl acetate/hexanes). The pure product is a yellow oil (171 mg, 31%). <sup>1</sup>H NMR (400 MHz, CDCl<sub>3</sub>): δ 2.35 (s, 6H), 4.79 (s, 2H) 7.28-7.32 (m, 5H) ppm. <sup>13</sup>C NMR (400 MHz, CDCl<sub>3</sub>): δ 19.15, 28.27, 75.58, 128.261, 128.807, 135.63, 149.31, 153.89, 163.72 ppm. HRMS (ES+) calcd (M) 248.0716, obsd 248.0718

**8-Hydroxymethyl-2,6-diethyl -1,3,5,7-tetramethyl pyrromethene fluoroborate (2.16).** To an air equilibrated solution of PM605 (50 mg, 0.13 mmol, 1 equiv.) in 110 mL of 1:1 (v:v) distilled deionized H<sub>2</sub>O/ THF was added LiOH (112 mg, 2.68 mmol, 20.2 equiv.) under stirring. The solution was stirred at room temperature in the dark for 2.5 hours. The reaction was quenched with 10.0 mL of saturated aqueous solution of NH<sub>4</sub>Cl. The resulting mixture was extracted with DCM (100 mL x 3) and dried with anhydrous MgSO<sub>4</sub>. It was then gravity filtrated and concentrated under reduced pressure to give a desired alcohol as a pink solid (the yield of the crude mixture is 98%). The compound was used in the next step without further purification. Spectral data is in accordance with literature values.<sup>[15]</sup>

**4-(((5-(benzyloxy)-4,6-dimethylpyrimidin-2-yl)(methyl)amino)methyl)benzaldehy**

**de (2.21).** To a stirred solution of 4-bromomethyl-benzaldehyde (**2.3**, 804mg,4mmol) and 5-benzyloxy-4,6-dimethyl-2-N-methylaminopyrimidinol (**2.7**, 243mg,1mmol) in acetonitrile (5ml) was added potassium carbonate(70mg,0.5mmol), and the resulting solution was heated at reflux for overnight, the resulting brown solution was directly loaded on a column to purify with 5% EtOAc/Hexanes to afford pure product as colorless oil(398mg,69%). <sup>1</sup>H NMR (300 MHz, CDCl<sub>3</sub>): δ 2.31 (s, 6H), 3.11 (s, 3H) 4.73 (s, 2H), 4.94 (s, 2H), 7.34-7.81 (m, 9H), 9.94 (s, 1H) ppm. <sup>13</sup>C NMR (300 MHz,CDCl<sub>3</sub>): δ 19.27, 35.16, 52.54, 75.29, 127.06, 127.54, 129.01, 129.65, 130.99, 135.32, 136.94, 142.20, 146.66, 157.97, 160.30, 191.85 ppm. HRMS (ES+) calcd (M) 361.1790, obsd 361.1798

**4-(((5-(benzyloxy)-4,6-dimethylpyrimidinol)(methylamino)methyl)benzol-1,3,5,7-tetramethylpyrromethene Fluoroborate (2.22).** To a stirred solution of compound **2.21**(290mg,0.5mmol) in dry DCM (20ml) was added 2,4-dimethyl pyrrole(114mg,1.2mmol), and TFA(10μL), the reaction solution was then kept stirring at room temperature under argon for overnight until the TLC shows complete consumption of the starting materials, and then DDQ (115mg,0.5mmol) in dry DCM(1ml)was added while the reaction solution was cooled down to 0°C,the reaction solution was then left stirring for another 40 minutes at room temperature and triethylamine (1ml) and boron trifluoride etherate (1ml) was added, and the reaction was left stirring for another 1 hour, the resulting solution was quenched with water and extracted with DCM, the DCM extraction is then concentrated and subjected to

flash chromatography with 12.5% EtOAc/Hexanes to afford the pure product as a dark brown oil(69.5mg,24%). <sup>1</sup>H NMR (300 MHz, CDCl<sub>3</sub>): δ 1.36 (s, 6H), 2.31 (s, 6H) 2.53 (s, 6H), 3.07 (s, 3H), 4.73 (s, 2H), 4.93 (s, 2H), 5.95(s, 2H), 7.17-7.44(m, 9H) ppm.

**4-((4,6-dimethylpyrimidinol)(methylamino)methyl)benzol-1,3,5,7-tetramethylpyrromethene Fluoroborate (2.23).** To a stirred solution of compound **2.22**(29mg,0.05mmol) and Pd/C(5mg) in methanol was connected to a balloon filled with hydrogen gas, the reaction was then left stirring for 2 hours at room temperature until TLC showed complete consumption of starting material. The Pd/C was filtered and the resulting solution was concentrated and purified through flash chromatography with 25% EtOAc/Hexanes to afford the pure product as a orange solid.(22mg,90%).<sup>1</sup>H NMR (300 MHz, CDCl<sub>3</sub>): δ 1.35 (s, 6H), 2.32 (s, 6H) 2.53 (s, 6H), 3.05 (s, 3H), 3.96 (bs, 1H), 4.91 (s, 2H), 5.95(s, 2H), 7.15-7.36(m, 4H) ppm. <sup>13</sup>C NMR (300 MHz,CDCl<sub>3</sub>): δ 14.34, 14.55, 18.81, 33.82, 52.53, 121.15, 127.91, 128.38, 131.49, 133.23, 133.34, 133.44, 138.57, 141.89, 143.20, 154.13, 155.30, 156.89 ppm. HRMS (ES+) calcd (M) 489.2511, obsd 489.2564

**3-((4,6-dimethylpyrimidinol)(methylamino)methyl)benzol-1,3,5,7-tetramethylpyrromethene Fluoroborate (2.36).** Same procedures as making compound **2.23**, as starting material and producing the pure product as an orange solid.(23mg,94%)<sup>1</sup>H NMR (400 MHz, CDCl<sub>3</sub>): δ 1.34 (s, 6H), 2.27 (s, 6H) 2.52 (s, 6H), 3.06 (s, 3H), 3.94 (s, 1H), 4.85 (s, 2H), 5.93 (s,2H), 7.06-7.49(m,4H) ppm. <sup>13</sup>C

NMR (300 MHz, CDCl<sub>3</sub>):  $\delta$  14.21, 14.40, 14.58, 18.84, 18.88, 35.20, 52.59, 108.465, 114.897, 121.15, 126.08, 126.23, 128.23, 128.68, 131.41, 134.87, 138.77, 142.00, 143.21, 154.62, 155.31, 156.76 ppm. HRMS (ES+) calcd (M) 489.2511, obsd 469.2490 [M-HF]<sup>+</sup>

**3-bromomethyl-benzaldehyde (2.38)**. Same procedures as making compound **2.3**, yield a white solid (1.835g, 90%), spectral data is in accordance with literature values.<sup>[26]</sup>

**3-(((5-(benzyloxy)-4,6-dimethylpyrimidin-2-yl)(methyl)amino)methyl)benzaldehyde (2.39)**. Same procedures as making compound **2.21**, yielding a colorless oil (317mg, 55%). <sup>1</sup>H NMR (300 MHz, CDCl<sub>3</sub>):  $\delta$  2.32 (s, 6H), 3.11 (s, 3H), 4.74 (s, 2H), 4.94 (s, 2H), 7.34-7.78 (m, 9H), 9.98 (s, 1H) ppm. <sup>13</sup>C NMR (300 MHz, CDCl<sub>3</sub>):  $\delta$  19.31, 35.07, 52.29, 75.41, 128.10, 128.30, 128.51, 128.65, 128.76, 129.10, 133.82, 136.62, 137.01, 140.39, 142.15, 157.99, 160.38, 192.50 ppm. HRMS (ES+) calcd (M) 361.1790, obsd 361.1791

**2-bromomethyl-benzaldehyde (2.41)**. A solution of 2-(bromomethyl)benzotrile (5.0 g, 25.5 mmol) in anhydrous CH<sub>2</sub>Cl<sub>2</sub> (75 mL) was cooled in an ice-water bath and maintained under an inert atmosphere. A 1.0 M solution of diisobutyl aluminum hydride (26.0 mL, 26.0 mmol) in heptane was added in a drop-wise manner over a period of 30 min. The resulting solution was then allowed to warm slowly to rt with

stirring for a period of 3 h by removing the ice-water bath. The reaction mixture was cooled again with an ice-bath, and directly poured into a 1000-mL beaker containing ice (100 g) and a pre-cooled HBr aqueous solution (6.0 N, 100 mL). The resulting mixture was vigorously stirred for 1 h and then extracted with CH<sub>2</sub>Cl<sub>2</sub>. The combined extracts were washed with 1 N NaHCO<sub>3</sub>, H<sub>2</sub>O, and dried (MgSO<sub>4</sub>). Evaporation of solvent gave product **2.41** (4.9 g, 97% yield) as a clear brown liquid with sufficient purity to proceed with next step. Spectral data is in accordance with literature values.<sup>[22]</sup>

**8-[[Bis(pyridin-2-ylmethyl)amino]methyl]-4,4-difluoro-1,3,5,7-tetramethyl-2,6-diethyl-4-bora-3a,4a-diaza-s-indacene (2.49).** To a 500 mL round-bottomed flask containing 250 mL argon-degassed CH<sub>2</sub>Cl<sub>2</sub> were added 2,4-dimethyl-3-ethyl pyrrole (11.4 mmol, 1.5 g) and chloroacetyl chloride (5.7 mmol, 0.64 g) and the resulting mixture was stirred for 2 hours at room temperature. 8 mL of Et<sub>3</sub>N and 10 mL of BF<sub>3</sub>.OEt<sub>2</sub> were successively added and after 30 min, the reaction mixture was washed three times with water and carefully dried over anhydrous Na<sub>2</sub>SO<sub>4</sub>. The solvent was concentrated and the residue was purified by silica gel column chromatography using 3:1 Toluene: Hexanes as the eluent. To a solution of the purified residue (0.57 mmol, 0.2 g) in 200 mL acetonitrile was added KI (0.60 mmol, 0.10 g) and the resulting mixture was refluxed until NMR indicate that all the starting material had been consumed. Solvent was evaporated and the reaction mixture was washed three times with water and chloroform. Organic phase was dried over anhydrous Na<sub>2</sub>SO<sub>4</sub>. Red

solid obtained from the evaporation of the solvent. Spectral data is in accordance with literature values.<sup>[25]</sup>

**4-((5-(benzyloxy)-4,6-dimethylpyrimidin-2-yl)(methylamino)butanenitrile (2.55).**

To a stirred solution of 5-benzyloxy-4,6-dimethyl-2-N-methylaminopyrimidinol (**2.7**, 243mg, 1mmol) and 4-bromobutanenitrile (444mg, 3mmol) in acetonitrile (1ml) was added potassium carbonate (69mg, 0.5mmol), the reaction was heated to reflux and running for overnight. The resulting solution is purified through flash chromatography and yield compound **2.55** as a colorless oil (158mg, 51%). <sup>1</sup>H NMR (400 MHz, CDCl<sub>3</sub>): δ 1.94 (t, 2H), 2.29 (s, 6H), 2.32 (t, 2H), 3.11 (s, 3H), 4.69 (s, 2H), 7.29-7.44 (m, 5H) ppm. <sup>13</sup>C NMR (400 MHz, CDCl<sub>3</sub>): δ 14.83, 19.26, 23.99, 35.68, 48.04, 75.37, 119.89, 128.12, 128.28, 128.63, 137.03, 141.9, 157.89, 160.22 ppm. HRMS (ES+) calcd (M) 310.1794, obsd 310.1784

**N<sup>1</sup>-(5-(benzyloxy)-4,6-dimethylpyrimidin-2-yl)-N<sup>1</sup>-methylbutane-1,4-diamine**

**(2.56)** To a stirred solution of LiAlH<sub>4</sub> (76mg, 2mmol) in dry Et<sub>2</sub>O (5ml) was added compound **2.55** (155mg, 0.5mmol), the reaction was heated to reflux for 3 hours, and the resulting solution was quenched using sat. NH<sub>4</sub>Cl and the resulting solution was evaporate to dryness and the residue was washed with methanol, and the methanol solution is concentrated to yield compound **2.56** as a colorless oil (149mg, 95%).

**2-((4-aminobutyl)(methylamino)-4,6-dimethylpyrimidin-5-ol (2.58).** To a stirred

solution of compound **2.56** (314mg,1mmol) and Pd/C (5mg) in methanol was connected to a balloon filled with hydrogen gas, the reaction was then left stirring for 2 hours at room temperature until TLC showed complete consumption of starting material. The Pd/C was filtered and the resulting solution was concentrated to afford the pure product as a colorless oil.(212mg,95%) <sup>1</sup>H NMR (400 MHz, CDCl<sub>3</sub>): δ 1.63-1.71 (m, 4H), 2.27 (s, 6H), 2.98 (t, 2H), 3.04 (s, 3H), 3.62 (t, 2H) ppm. <sup>13</sup>C NMR (400 MHz,CDCl<sub>3</sub>): δ 17.65, 24.04, 24.53, 34.39, 39.28, 49.78, 138.44, 155.72, 156.15 ppm. HRMS (ES+) calcd (M) 224.1637, obsd 224.1610

**5-[5-benzyloxy-4,6-dimethyl-2-N-methylaminopyrimidinol]-1-pentanol (2.60).**

NaCNBH<sub>3</sub> (0.16 g, 2.4 mmol) was added to a solution of compound **2.61** (157mg, 0.5 mmol) in MeOH (2 mL) and aqueous formaldehyde (37%, 1.2 mL). After 2 h, the reaction was quenched with HOAc (0.16 mL, 2.8 mmol) and stirred until gas evolution ceased. The reaction mixture was poured into H<sub>2</sub>O (5 mL) and extracted with EtOAc (3 x 10 mL). The organics were washed with brine and dried over MgSO<sub>4</sub>. The product was isolated as a colorless oil (110mg, 67%) after column chromatography (2:1, hexanes:EtOAc).

**5-[5-benzyloxy-4,6-dimethyl-2-aminopyrimidinol]-1-pentanol (2.61).** To a stirred solution of 5-Benzyloxy-4,6-dimethyl-2-chloropyrimidine (**2.15**, 248 mg,1 mmol) in acetonitrile(2 ml) was added 5-aminopentanol(412 mg,4 mmol) and potassium carbonate (69 mg,0.5 mmol), the reaction was heated to reflux and running overnight,

the resulting solution was purified using flash chromatography with EtOAc, yields a colorless oil (255 mg, 81%). <sup>1</sup>H NMR (400 MHz, CDCl<sub>3</sub>): δ 1.41 (dd, 2H), 1.55 (dd, 4H) 2.24 (s, 6H) ppm, 3.32(dt 2H), 3.54(bs, 1H), 3.56(t, 2H), 4.66(s, 2H), 5.10(s, 1H), 7.28-7.36(m, 5H) <sup>13</sup>C NMR (400 MHz,CDCl<sub>3</sub>): δ 18.99, 23.23, 29.53, 32.45, 41.64, 62.13, 75.45, 128.10, 128.30, 128.62, 136.83, 142.26, 158.29, 160.78 ppm. HRMS (ES+) calcd (M) 315.1994, obsd 315.1944

**5-[5-benzyloxy-4,6-dimethyl-2-N-methylaminopyrimidinol]-1-pentanoic acid**

**(2.62)**. To MeCN (4 mL) was added H<sub>5</sub>IO<sub>6</sub> (250 Mg, 1.1 mmol) and the mixture was stirred vigorously at r.t. for 15 min. Alcohol **2.60** (165 mg, 0.5 mmol) was then added (in ice-water bath) followed by addition of PCC (2.2 mg, 2 mol%) in MeCN (2 × 0.5 mL) and the reaction mixture was stirred for 3 h. The reaction mixture was then diluted with EtOAc (10 mL) and washed with brine–water (1:1), sat. aq NaHSO<sub>3</sub> solution, and brine, respectively, dried over anhyd Na<sub>2</sub>SO<sub>4</sub> and concentrated to give the clean carboxylic acid **2.62** (164 mg, 96% yield). HRMS (ES+) calcd (M) 343.1896, obsd 343.1897

**5-[4,6-dimethyl-2-N-methylaminopyrimidinol]-1-pentanoic acid (2.63)**. Same procedures as making compound **2.59**,using **2.60** as starting material and producing the pure product as an colorless oil.(11 mg, 90%) calcd (M) 253.1423, obsd 253.1437

**5-[5-benzyloxy- 4,6-dimethyl-2-N-methylaminopyrimidinol]-1-pentanoic acid,**



**4-(4,4-Difluoro-4-bora-3a,4a-diaza-s-indacene-8-yl)-methanoly Ester (2.64).** To a stirred solution of acid compound **2.60** (0.5mmol) and BODIPY-OH(**2.45**)(0.75 mmol) in dry THF (5 ml) was added EDC.HCl (0.5 mmol) and DMAP (0.5 mmol) and DIPEA (0.5 mmol), the reaction was kept stirring under argon at 50°C for 6h, the resulting solution was washed with water and extracted using DCM for several times, concentrated and purified using flash chromatography, giving the product as a purple oil.(80%) <sup>1</sup>H NMR (300 MHz, CDCl<sub>3</sub>): δ 1.02 (t, 3H), 1.63-1.64 (m, 4H), 2.21 (s, 6H), 2.27(s, 6H), 2.36 (q, 4H), 3.07 (s, 3H), 3.60 (t, 2H), 4.68 (s, 2H), 5.28(s, 2H), 7.32-7.43(m, 5H) ppm.

**5-[4,6-dimethyl-2-N-methylaminopyrimidinol]-1-pentanoic acid,4-(4,4-Difluoro-4-bora-3a,4a-diaza-s-indacene-8-yl)-methanoly Ester (2.65).** To a stirred solution of acid compound **2.61**(0.1 mmol) in dry THF(2 ml) was added CDI (0.1mmol) and the reaction was kept stirring under argon at rt until TLC shows the starting material consumed completely, then BODIPY-OH(0.1mmol) in dry THF (1 ml) was added, and the reaction was kept stirring under argon at 40°C for O/N. The resulting solution was washed with water and extracted with DCM, concentrated and purified using flash chromatography, giving the product as a purple oil (18%). <sup>1</sup>H NMR (400 MHz, CDCl<sub>3</sub>): δ 1.02 (t, 6H), 1.58-1.67 (m, 4H), 2.15 (s, 6H), 2.18 (s, 6H), 2.36 (q, 4H), 2.49 (s, 6H), 3.01 (s, 3H), 3.58 (t, 2H), 5.24 (s, 2H) ppm HRMS (ES<sup>+</sup>) calcd (M) 569.3349, obsd 549.3206[M-HF]<sup>+</sup>

**4-(4,4-Difluoro-4-bora-3a,4a-diaza-s-indacene-8-yl)-butyric Acid, 5-[5-benzyloxy-4,6-dimethyl-2-N-methylaminopyrimidinol]-1-ethanolyl Ester (2.69).** To a stirred solution of BODIPY-butyric acid(0.1 mmol) in dry THF (2 ml) was added DCC(0.1 mmol) and DMAP(0.1 mmol) and compound 2.76 (1 mmol), the solution was kept stirring under argon for 2 hours, and then washed with water and extract with DCM for several times, concentrated and purified using flash chromatography, giving the product as a red solid (22 mg, 45%). <sup>1</sup>H NMR (300 MHz, CDCl<sub>3</sub>): δ 2.14 (s, 6H), 2.24 (s, 6H) 2.50 (s, 6H), 2.84(t, 2H), 3.17 (s, 3H), 3.40 (t, 3H), 3.70 (t, 2H), 3.85(t, 2H), 6.07(s, 2H) ppm. <sup>13</sup>C NMR (400 MHz,CDCl<sub>3</sub>): δ 14.50, 16.34, 16.40, 18.99, 35.01, 36.09, 49.73, 53.33, 63.11, 120.96, 123.33, 127.27, 128.48, 129.98, 131.11, 134.55, 140.25, 142.27, 155.07, 156.98, 158.98, 159.88, 169.69 ppm. HRMS (ES+) calcd (M) 499.2566, obsd 499.2287

**5-[5-benzyloxy-4,6-dimethyl-2-aminopyrimidinol]-1-ethanol (2.70)** Same procedures as making compound **2.58**,using ethanolamine (244 mg, 4 mmol) as starting material, producing the pure product as an white solid. (229mg,84%). <sup>1</sup>H NMR (400 MHz, CDCl<sub>3</sub>): δ 2.25 (s, 6H) ppm, 3.49(dt 2H), 3.76(t, 2H), 4.69(s, 2H), 5.62(bs, 1H), 7.33-7.37(m, 5H) <sup>13</sup>C NMR (400 MHz,CDCl<sub>3</sub>): δ 19.08, 36.87, 53.43, 63.44, 75.48, 128.161, 128.65, 136.81, 141.94, 158.61, 160.31 ppm HRMS (ES+) calcd (M) 273.1477, obsd 273.1484

**5-[5-benzyloxy-4,6-dimethyl-2-N-methylaminopyrimidinol]-1-ethanol (2.71).**

Same procedures as that of making compound **2.60**, using **2.70** as starting material, producing the pure product as a white solid. (101 mg, 71%). <sup>1</sup>H NMR (300 MHz, CDCl<sub>3</sub>): δ 2.29 (s, 6H) ppm, 3.17(s 3H), 3.68(t, 2H), 3.84(t, 2H), 4.70(s, 2H), 5.16(bs, 1H), 7.31-7.44(m, 5H) HRMS (ES+) calcd (M) 287.1634, obsd 287.1591

**5-[5-benzyloxy-4,6-dimethyl-2-N-methylaminopyridinol]-acetic acid methyl ester (2.72)**. To a stirred solution of 5-benzyloxy-4,6-dimethyl-2-N-methylamino Pyridinol (2.44, 242 mg, 1 mmol), in dry DMF (5 ml) was added bromomethylacetate (765 mg, 5 mmol) and DIPEA (258 mg, 2 mmol), reaction was heated at 55 °C for 6 hours and monitored on TLC, upon completion the reaction solution was purified using flash chromatography with 10% EtOAc/Hexanes to yield pure product as a colorless oil (267 mg, 85%). <sup>1</sup>H NMR (400 MHz, CDCl<sub>3</sub>): δ 2.21 (s, 3H), 2.34 (s, 3H) 3.04 (s, 3H), 3.70(s, 3H), 4.32 (s, 2H), 4.71 (s, 2H), 6.22 (s, 1H), 7.24-7.43 (m, 5H), ppm. <sup>13</sup>C NMR (400 MHz, CDCl<sub>3</sub>): δ 16.63, 19.46, 37.76, 51.72, 51.86, 74.81, 105.09, 127.94, 128.03, 128.55, 137.59, 141.60, 144.49, 149.15, 154.18, 172.11 ppm. HRMS (ES+) calcd (M) 314.1630, obsd 314.1647

**5-[5-benzyloxy-4,6-dimethyl-2-N-methylaminopyridinol]-acetic acid (2.73)**. To a stirred solution of 5-[5-benzyloxy-4,6-dimethyl-2-N-methylaminopyridinol]-acetic acid methyl ester (2.76, 62 mg, 0.2 mmol) in DCM/Methanol=9:1 (2 ml) was added sodium hydroxide and the reaction was running at room temperature for overnight. The resulting solution was neutralized using 5% HCl solution, the neutralized solution

was evaporated to dryness under high vacuum and washed with methanol, the methanol solution was concentrated and yield the product as a colorless oil (57mg, 95%). <sup>1</sup>H NMR (400 MHz, MeOD):  $\delta$  2.17 (s, 3H), 2.27 (s, 3H) 3.05 (s, 3H), 4.04(s, 2H), 4.71 (s, 2H), 6.25 (s, 1H), 7.24-7.43 (m, 5H), ppm. <sup>13</sup>C NMR (400 MHz, CDCl<sub>3</sub>):  $\delta$  19.37, 21.53, 40.65, 57.96, 78.67, 109.40, 131.66, 131.87, 132.06, 141.46, 146.03, 147.39, 151.85, 158.99, 180.42 ppm. HRMS (ES+) calcd (M) 300.1474, obsd 300.1482

**5-[4,6-dimethyl-2-N-methylaminopyridinol]-acetic acid (2.74).** To a stirred solution of 5-[5-benzyloxy-4,6-dimethyl-2-N-methylaminopyridinol]-acetic acid (0.5 mmol) and Pd/C (5 mg) in methanol (5 ml) was filled with hydrogen, the reaction was kept stirring for 5 h, the resulting solution was filtered and concentrated, giving the product as a colorless oil (99 mg, 94%). <sup>1</sup>H NMR (300 MHz, MeOD):  $\delta$  2.27 (s, 3H), 2.38 (s, 3H) 3.10 (s, 3H), 4.06(s, 2H), 6.59 (s, 1H) ppm. <sup>13</sup>C NMR (300 MHz, CDCl<sub>3</sub>):  $\delta$  14.80, 15.93, 37.39, 54.90, 107.35, 138.69, 141.25, 142.65, 151.57, 175.43 ppm. HRMS (ES+) calcd (M) 210.1004, obsd 210.0958

**4,6-dimethyl-2-amino-5-iodopyridine (2.75)** A mixture of 4,6-dimethyl-2-amino-pyridine (3.05 g, 25 mmol), periodic acid dihydrate (0.86 g, 3.75 mmol) and iodine (2.7 g, 10.7 mmol) was heated in a mixed solution of acetic acid (60 mL), water (3 mL) and sulfuric acid (0.5 mL) at 80 °C for 4 h. The reaction mixture was then poured into 10% aq. Na<sub>2</sub>S<sub>2</sub>O<sub>3</sub> solution to quench any unreacted iodine and extracted

with ether. The extract was washed with 10% aq. NaOH, dried and concentrated in *vacuo*, and the residue purified by flash chromatography. Yield a yellow solid (4.8g,79%). The spectral data is in accordance with literature values.<sup>[1]</sup>

**1-(5-iodo-4,6-dimethylpyridin-2-yl)-2,5-dimethyl-1H-pyrrole (2.76).** 2-Amino-5-iodo-2,4dimethylpyridine (11.6 mmol), 2,5-hexanedione(1.65 mL, 14.0 mmol), and *p*-TsOH (0.023 g, 0.08 mmol) were dissolved in toluene (10mL) and heated in a Dean-Stark apparatus for 2 h.8 After cooling, the dark brown reaction mixture was washed with satd. aq. NaHCO<sub>3</sub> solution, five times with water, and with brine. After the mixture had been dried with Na<sub>2</sub>SO<sub>4</sub>, the solvent was removed in*vacuo*. The dark residue was subjected to flash chromatography on silica gel (eluent:ethyl acetate/hexanes). The purified product was a yellow solid(80%). The spectral data is in accordance with literature values.<sup>[1]</sup>

**1-(5-benzyloxy-4,6-dimethylpyridin-2-yl)-2,5-dimethyl-1H-pyrrole (2.77).** To a mixture of CuI (0.40 mmol), 1,10-phenanthroline (0.80 mmol), cesium carbonate (6.00 mmol) and 1-(5-iodo-4,6-dimethylpyridin-2-yl)-2,5-dimethyl-1H-pyrrole (**2.76**,4.00 mmol) in a dry Schlenk flask (evacuated and nitrogen purged) were added 5 mL of toluene and benzyl alcohol (40 mmol) and the reaction was heated in an oil bath at 110°C for 24 h.To the reaction mixture another lot of 10 mol% of CuI and 20 mol% of 1,10-phenanthroline was added and heated in an oil bath at 110°C for 24 h to drive it to completion. The reaction was quenched by filtering the reaction mixture

through silica plug and evaporating solvent. The crude residue obtained was subjected to flash chromatography (eluent: ethyl acetate/hexanes) and the purified product was a yellow oil(68%). The spectral data is in accordance with literature values.<sup>[1]</sup>

**5-benzyloxy-4,6-dimethylpyridinol (2.78).** A mixture of 1-(5-benzyloxy-4,6-dimethylpyridin-2-yl)-2,5-dimethyl-1*H*-pyrrole (**2.77**, 17.3 mmol), hydroxylamine hydrochloride(12.02 g, 173 mmol), triethylamine (4.8 mL, 34.6 mmol), ethanol (30 mL),and water (15 mL) was heated at reflux for 20 h. The cooled solution was quenched with cold HCl (50 mL), washed with diethyl ether, and the pH was adjusted to 9-10 with 6 N NaOH. The resulting mixture was extracted several times with dichloromethane. The combined organic phases were dried with Na<sub>2</sub>SO<sub>4</sub> and the solvent was removed in *vacuo*. The oily residue was purified by silica gel column chromatography (75%). The spectral data is in accordance with literature values.<sup>[1]</sup>

**8-(but-3-enyl)-2,6-diethyl -1,3,5,7-tetramethyl pyrromethene fluoroborate (2.81).** A mixture of 3-ethyl-2,4-dimethylpyrrole (1.0 mL, 8.1 mmol) and pentenoyl chloride (0.45mL, 4.05 mmol) in 1,2-dichloroethane (50 mL) was refluxed under argon for 30 min. Triethylamine (2 mL, 15.4 mmol) was then added at room temperature, and the mixture stirred for 30 min. Then, boron trifluoride diethyl etherate (2 mL, 16 mmol) was added, and it was refluxed for 2 h. The subsequent work-up yielded a red residue that was purified by flash column chromatography (silica gel, n-hexanedichloromethane 9:1 as eluent). Red crystals were obtained. Yield: 40%. The

spectral data is in accordance with literature values<sup>[28]</sup>

**4,6-dimethyl-2-N-methyl-N-allyl-aminopyrimidinol (2.83)** To a stirred solution of 5-benzyloxy-4,6-dimethyl-2-N-methylaminopyrimidinol(**2.7**, 243 mg, 1mmol) in dry DMF(5ml) at 0°C was added sodium hydride(24mg,1mmol), the solution was stirred at 0°C under argon for 15 minutes, then allyl iodide (336mg,2mmol) was added and the solution was heated to 60°C for overnight. The resulting solution was quenched with water and extract with EtOAc, the EtOAc extract was then concentrated and purified using flash chromatography with 10% EtOAc/Hexanes to yield a yellow oil (65%,184mg). This yellow oil is then dissolved in 5 ml dry DCM, and 2ml of BCl<sub>3</sub>(1.0 M solution in DCM) was added under argon after cooling the solution to -78°C. The reaction was then run at -78°C for 30min, and run at rt for another 30 min.The resulting solution was quenched with Sat NaHCO<sub>3</sub>,extracted with DCM and yield the product as a yellow oil(110mg, 98%).<sup>1</sup>H NMR (400 MHz, CDCl<sub>3</sub>): δ 2.22 (s, 6H), 3.00 (s, 3H) 4.17 (d, 2H), 5.06-5.12(m, 2H), 5.73-5.83 (m, 1H) ppm. <sup>13</sup>C NMR (400 MHz,CDCl<sub>3</sub>): δ 18.87, 34.80, 51.92, 116.09, 134.52, 138.43, 155.24, 156.83 ppm. HRMS (ES+) calcd (M) 193.1215, obsd 193.1208

**8-(1H-imidazole-1-carboxymethyl)-2,6-diethyl-1,3,5,7-tetramethyl pyrromethene fluoroborate (2.84).**To a stirred solution of 8-Hydroxymethyl- 2,6-diethyl-1,3,5,7-tetramethyl pyrromethene fluoroborate(**2.16**,33mg,0.1mmol) in dry

DCM(1ml) at 0°C was added CDI(24mg,0.15mmol), the solution was then resumed to room temperature and stirred for 15 minutes. The resulting solution was purified using flash chromatography with 20% EtOAc/Hexanes, yielding a red solid(40.6mg,95%). <sup>1</sup>H NMR (300 MHz, CDCl<sub>3</sub>): δ 1.03 (t, 6H), 2.27 (s, 6H) 2.38 (q, 4H), 2.51(s, 6H), 5.65 (s, 2H), 6.25 (s, 1H), 7.05-7.07 (m, 1H), 7.39-7.40 (m, 1H) 8.12 (m, 1H), ppm. <sup>13</sup>C NMR (400 MHz,CDCl<sub>3</sub>): δ 10.20, 11.89, 13.58, 13.80, 15.42, 15.48, 17.10, 17.16, 18.78, 18.84, 61.45, 115.77, 118.46, 128.59, 129.82, 132.22, 132.35, 132.51, 134.14, 135.67, 136.25, 138.55, 148.37, 155.97 ppm. HRMS (ES+) calcd (M) 428.2195, obsd 428.2191

#### **General Procedures for Fluorescent Study of para-Pyrimidyl-BODIPY(2.23)**

2ml 0.8mM AIBN solution in toluene in a cuvette is heated up to 55°C, 50μL of 0.123mM para-Pyrimidyl-BODIPY solution in toluene was added, and the fluorescence intensity was recorded at 520 nm upon exciting at 470 nm.

#### **General Procedures for Clock Calibration (thermal conditions).**

Pyrimidyl-BODIPY (2.23 or 2.36) (0.01-0.04M) and perester (2.28 in Scheme 2.29, 0.01 M, 10 μL of 0.1 M) were mixed and diluted up to 100 μL with benzonitrile in 2.0 mL HPLC vials. The vials were capped and incubated at 37 °C for 4 h. After the incubation reaction mixtures were quenched with PPh<sub>3</sub> (50 μL of 1.0 M in benzene) and diluted up to 1.8 mL with hexanes. Decomposition products were determined by GC. The ratio of non-conjugated to conjugated alcohols was plotted versus the



Pyrimidyl-BODIPY (**2.23** or **2.36**) concentration.

#### 2.4 References:

- [1] Nara, S.J; Jha, M.; Brinkhorst, J.; Zemanek, T. J.; Pratt, D. A. *J. Org. Chem.*, **2008**, 73,9326–9333
- [2] Loudet, A.; Burgess, K. *Chem. Rev.* **2007**, 107, 4891-4932
- [3] Wagner, R. W.; Lindsey, J. S. *Pure Appl. Chem.* **1996**, 68, 1373.
- [4] Antina, E. V.; Berezin, M. B.; Semeikin, A. S.; Dudina, N. A.; Yutanova, S. L. *Russian Journal of General Chemistry* **2010**, 80, 1214
- [5] Li, Z.; Mintzer, E.; Bittman, R. *J. Org. Chem.* **2006**, 71, 1718.
- [6] Minkenberg, C. B.; Florusse, L.; Eelkema, R.; Koper, G. J. M.; Esch, J. H.V. *J. Am. Chem. Soc.*, **2009**, 131, 11274–11275
- [8] Singh, O. M.; Singh, J.; Kim, S.; Lee, S. G. *Bull. Korean Chem. Soc.* **2007**, 28, 115
- [9] Krumova, K.; Cosa, G. *J. Am. Chem. Soc.* **2010**, 132, 17560–17569
- [10] Amat-Guerri, F.; Liras, M.; Carrascoso, M. L.; Sastre, R. *Photochem. Photobiol.* **2003**, 77, 577.
- [11] Amundsen, L. H.; Nelson, L. S. *J. Am. Chem. Soc.*, **1951**, 73,242–244
- [12] Placzek, A. T.; Donelson, J. L.; Trivedi, R.; Gibbs, R. A.; De, S. K. *Tetrahedron Letters* **2005**, 46, 9029–9034

- [13] Nara, S. J.; Valgimigli, L.; Pedulli, G. F.; Pratt, D. A. *J. Am. Chem. Soc.*, **2010**, *132*, 863–872
- [14] Roschek, B. Jr.; Tallman, K. A.; Rector, C. L.; Gillmore, J. G.; Pratt, D. A.; Punta, C.; Porter, N. A. *J. Org. Chem.*, **2006**, *71*, 3527–3532
- [15] Oleynik, P.; Ishihara, Y.; Cosa, G. *J. Am. Chem. Soc.*, **2007**, *129*, 1842–1843
- [16] Ferná'ndez-Rodríguez, M. A.; Andina, F.; Garcí'a-Garcí'a, P.; Rocaboy, C.; Aguilar, E. *Organometallics* **2009**, *28*, 361–369
- [17] M. Hunsen, *Synthesis*, **2005**, 2487-2490.
- [18] Corey, E. J.; Schmidt, G. *Tetrahedron Lett.* 1979, **20**, 399.
- [19] Hattori, G.; Sakata, K.; Matsuzawa, H.; Tanabe, Y.; Miyake, Y.; Nishibayashi, Y. *J. Am. Chem. Soc.*, **2010**, *132*, 10592–10608
- [20] Wang, D.; Fan, J.; Gao, X.; Wang, B.; Sun, S.; Peng, X. *J. Org. Chem.* **2009**, *74*, 7675–7683
- [21] Ehrenschwender, T.; Wagenknecht, Hans-Achim. *J. Org. Chem.*, **2011**, *76*, 2301–2304
- [22] West, R.; Panagabko, C.; Atkinson, J. *J. Org. Chem.* **2010**, *75*, 2883.
- [23] Ehrenschwender, T.; Wagenknecht, H. *J. Org. Chem.* **2011**, *76*, 2301–2304
- [24] Shaha, J. R.; Mosiera, P. D.; Peddia, S.; Rothb, B. R.; Westkaemper, R. B. *Bioorganic & Medicinal Chemistry Letters*. **2010**, *20*, 935–938
- [25] Guliyeva, R.; Buyukcakira, O.; Sozmenb, F.; Bozdemira, O. A. *Tetrahedron Letters*. **2009**, *50*, 5139-5141.
- [26] Simpson, M. G.; Pittelkow, M.; Watson, S. P.; Sanders, J. K. M. *Org. Biomol.*

*Chem.*, **2010**, *8*, 1181-1187

[27] Wijtmans, M.; Pratt, D. A.; Valgimigli, L.; DiLabio, G. A.; Pedulli, G. F.; Porter,

N. A. *Angew. Chem. Int. Ed.* **2003**, *42*, 4370–4373

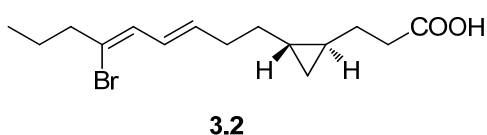
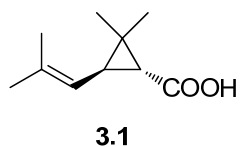
[28] Liras, M.; García, O.; Quijada-Garrido, I.; París, R. *Macromolecules* **2011**, *44*,

1335–1339

**Chapter 3**  
**Cyclopropane Lipids: Autoxidizability and Potential as**  
**Inhibitors of Lipoxygenases**

### 3.1 Introduction

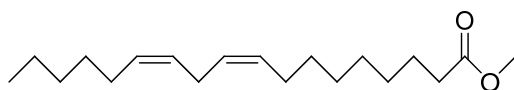
Cyclopropane fatty acids (CFAs) occur naturally in plants and microorganisms, but rarely in animals. They are often highly reactive due to their unusual bonding and inherent ring strain (27.5 kcal/mol), which leads to their cleavage upon hydrogenation, or via reaction with strong Lewis or protic acids. For example, mycolic acids, a kind of cyclopropanated fatty acids found in the cell walls of mycolata taxon, lend the bacteria increased resistance to chemical damage and dehydration, and prevent the effective activity of hydrophobic antibiotics; chrysanthemic acid(**3.1**) and its derivatives, produced in plants via the isoprenoid pathway are precursors to potent insecticides; majusculoic acid(**3.2**), which is isolated from a cyanobacterial mat assemblage, exhibits antifungal activity against *Candida albicans* ATCC 14503 (a type of fungus that causes opportunistic oral and genital infections in humans) with a MIC of 8  $\mu\text{M}$ <sup>[1]</sup>.



The cyclopropanation of membrane lipids in bacteria is proposed to play a key role in cell survival and the tolerance of extreme conditions (e.g. acids), and the virulence of bacteria when confronted by a host organism's immune response (e.g. mycolic acid in *Mycobacterium tuberculosis*). It seems reasonable to suggest that the cyclopropanation of unsaturated membrane lipids should confer resistance to

autoxidation induced by the inflammatory response of the host organism, but this has yet to be demonstrated quantitatively.

Linoleic acid and its esters (methyl ester, **3.3**) are the archetype polyunsaturated fatty acid, featuring the characteristic cis,cis-1,4- pentadiene structure that leads to their facile autoxidation (see Chapter 1) and their enzyme-catalyzed oxidation by lipoxygenases, cyclooxygenases and heme-dependent mono-oxygenases (see Chapter 1). It seems reasonable to suggest that the cyclopropanation of polyunsaturated membrane lipids, such as linoleic acid, may afford competitive inhibitors of enzymes which utilize polyunsaturated lipids as substrates, and this could prove useful in their further characterization and/or the development of drugs that target these enzymes.



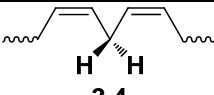
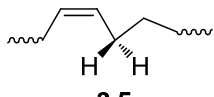
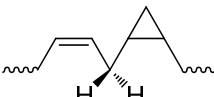
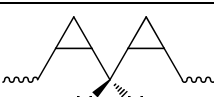
**3.3**

Despite the potential relevance of the oxidative stability of cyclopropane lipids to bacteriology and its potential to aid in structure/function studies of enzymes which utilize polyunsaturated lipids as substrates, this has not been quantitatively assessed. Likewise, to the best of our knowledge, cyclopropanated lipids have not been examined as inhibitors of enzymes which utilize the corresponding polyunsaturated lipids as substrates.

### **3.1.1 Potential Selective Lipoxygenase Inhibitors Design Based on Linoleic Acid**

The cyclopropanation of one or both the double bonds of the cis,cis-1,4-pentadiene moiety of linoleic acid might be expected to yield compounds that still bind and are oxygenated by the enzymes that utilize linoleic acid or other polyunsaturated fatty acids. The introduction of one or two extra methylene groups are relatively minor structural perturbations, especially since they will retain the cis (syn) stereochemistry that is presumably important for binding. While they are likely to retain binding activity, the substitution of an alkene for a cyclopropane moiety should also result in an increase in the C-H BDE, which should make it a more difficult substrate for oxidation. How difficult is not clear. Cyclopropyl groups can still interact with adjacent radical or carbocationic centres through the  $\pi$ -character of their C-C single bonds.

Preliminary calculations of the C-H BDEs of models of cyclopropanated lipids has been carried out at the CBS-QB3 level of theory<sup>[2]</sup> and compared to those of models of mono- and polyunsaturated lipids. As shown in Table 3.1 below, the calculated BDE of the mono-cyclopropanated model is 82.4 kcal/mol; slightly lower than the monoene model (84.5 kcal/mol), but quite a bit higher than the non-conjugated diene model (74.2 kcal/mol; in good agreement with the experimental value of 76.4 kcal/mol). This implies that the  $k_p$  will be larger than the  $1 \text{ M}^{-1}\text{s}^{-1}$  known for monounsaturated lipids (e.g. methyl oleate), but much smaller than the  $60 \text{ M}^{-1}\text{s}^{-1}$  known for polyunsaturated lipids (e.g. methyl linoleate). In contrast, the predicted C-H BDE for the di-cyclopropanated model is 95.3 kcal/mol, which should result in a very low  $k_p$  similar to a cycloalkane.

	BDE <sup>a</sup> (kcal/mol)	$k_p$ <sup>b</sup> (M <sup>-1</sup> s <sup>-1</sup> )
 <p style="text-align: center;"><b>3.4</b></p>	74.2	62
 <p style="text-align: center;"><b>3.5</b></p>	84.5	1
 <p style="text-align: center;"><b>3.6</b></p>	82.4	nd
 <p style="text-align: center;"><b>3.7</b></p>	95.3	nd

**Table 3.1** Calculated BDE and experimental  $k_p$  for 3.4-3.7.<sup>a</sup>Calculated at the CBS-QB3 level of theory. <sup>b</sup>Data from reference 3

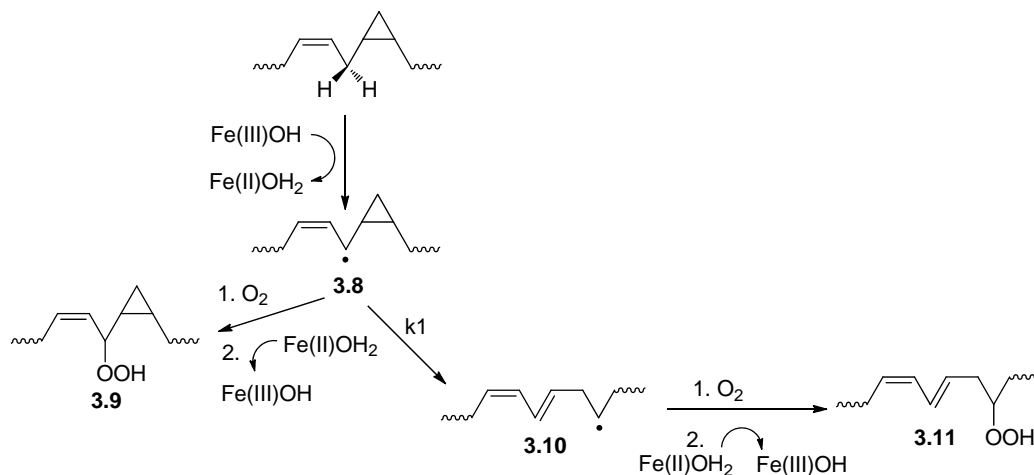
The lack of three-dimensional structural information available for the six known human LOX isoforms has significantly hampered the development of isoform-specific inhibitors as potential therapeutic agents. Only one of the human enzymes has been crystallographically characterized to date, and this was accomplished but a few months ago after decades of effort. More importantly, no structural information is available for the enzymes in their productive conformation. We hypothesize that cyclopropanated lipids may be ideal non-oxidizable substrate analogs for use co-crystallization studies with the enzyme; first with linoleic acid and sLOX-1 and sLOX-3, and later with arachidonic acid and the human LOX isoforms.

While LOX catalysis is reasonably well understood, how the regioselectivity of



the reaction is controlled is still unclear. It has been known for some time that LOX enzymes do not actively bind molecular oxygen to control substrate oxygenation, as there is no experimental evidence of Fe-O<sub>2</sub> or Fe-OOH species formation, and it can be concluded from kinetic isotope effects that molecular oxygen is not bound to the iron, at least up to and including the initial hydrogen abstraction from the substrate. [4] So, is oxygen held in a particular spot next to the putative reaction center? Is it channeled to one specific site for reaction?

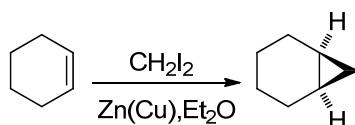
When using mono-cyclopropanated linoleic acid as substrate (Scheme 3.1), upon initial hydrogen abstraction, the formed radical (**3.8**) can react with oxygen or go through ring opening to form a conjugated radical (**3.10**) which will then react with oxygen to form hydroperoxide products. As the rate constant for ring opening and oxygen insertion is known, by using the ratio of [**3.9**] to [**3.11**] we can calculate the oxygen concentration, which will give us some insight regarding the issue of molecular oxygen binding to LOX during the oxygenation. Of course, this depends on whether the cyclopropanated lipid is a substrate of the lipoxygenase.



### Scheme 3.1 Mechanism of formation of possible peroxide products

#### 3.1.2 Synthetic Approaches to Cyclopropanated Lipids

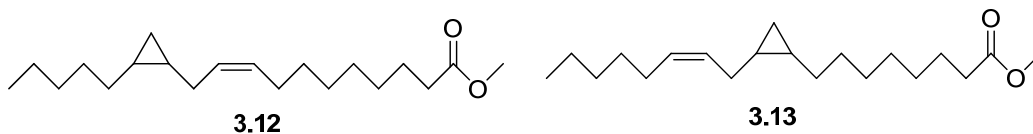
The most common way to make cyclopropanes from alkenes is the Simmons-Smith reaction, in which a carbenoid reacts with an alkene to form a cyclopropane in a chelotropic reaction.<sup>[5]-[7]</sup> Such a reaction is shown for cyclohexene in Scheme 3.2.<sup>[8]</sup>



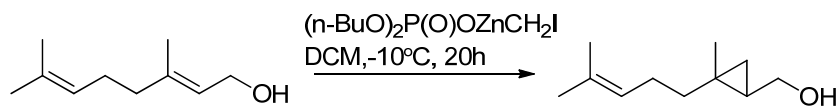
Scheme 3.2 Cyclopropanation of cyclohexene.<sup>[8]</sup>

The only reported cyclopropanated linoleate is the di-cyclopropanated linoleate, which is obtained by treating methyl linoleate with excess (10 eq) of Simmons-Smith reagent.<sup>[9]</sup> However, the synthesis of mono-cyclopropanated linoleate has not yet been reported.

The simplest way to make mono-CP linoleic acid is to treat methyl linoleate with one equivalent of cyclopropanating reagent, separate the resulting Mono-CP and Di-CP lipids using flash column chromatography on  $\text{SiO}_2$  impregnated with  $\text{AgNO}_3$ , and then hydrolyze the methyl ester. This separation technique utilizes the high affinity of  $\text{Ag}^+$  to alkenes, and has been routinely and successfully used to separate compounds with different numbers or stereochemistry of alkenes.<sup>[10]</sup>



The way to make compound **3.12** and **3.13** separately is by selectively reacting one of the double bonds with the cyclopropanating reagent to form the cyclopropane. Such reaction is possible if the two double bonds are in quite different chemical environments, as shown in Scheme 3.3.



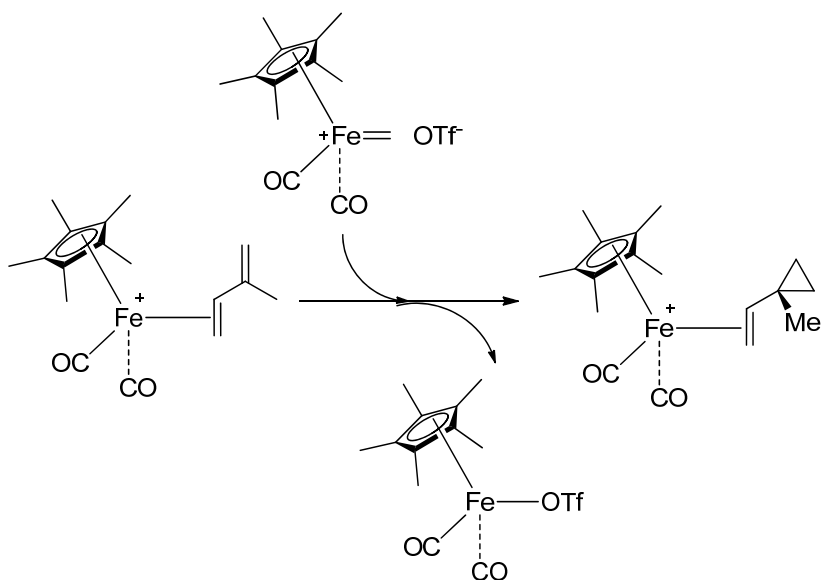
**Scheme 3.3** Selective cyclopropanation reaction through complexation

In this reaction, the electron rich hydroxyl group complexes to zinc and thus gets the adjacent double bond react with the carbenoid first.

The steric effects can also be applied into selective cyclopropanation of diene compound. Such reactions have been done by temporary  $\eta^2$ -coordination of the diene to a transition metal<sup>[11][12]</sup>, and the subsequent cyclopropanation can thus be directed by the resulting  $\eta^2$ -complexes. In fact, the regiospecific methylenation of dienes mediated by  $[(\eta^5\text{-C}_5\text{Me}_5)\text{Fe}(\text{CO})_2]^+ = \text{Fp}^{\bullet+}$ <sup>[13]</sup> has been reported, wherein the organometallic unit acts as a protecting group toward both the methylene fragment and the less substituted alkene function.

Complexation of the dienes is easily achieved from the aquo complex  $[\text{FP}'(\text{H}_2\text{O})][\text{BF}_4]$ <sup>[14]</sup> in refluxing DCM in the presence of the appropriate substrates.

$[\text{Fp}'(=\text{CH}_2)]^+$  is used as a methylene transfer reagent (Scheme 3.4) to achieve the intermolecular cyclopropanations. Reactions are performed at  $-80^\circ\text{C}$  by treating a solution of the diene complex methylene chloride with an equimolar quantity of  $[\text{Fp}'(\text{CH}_2)][\text{OTf}]$  which can be generated in situ from  $[\text{Fp}'-(\text{CH}_2\text{OMe})]$  with 1 equivalent of  $\text{Me}_3\text{SiOTf}$ .



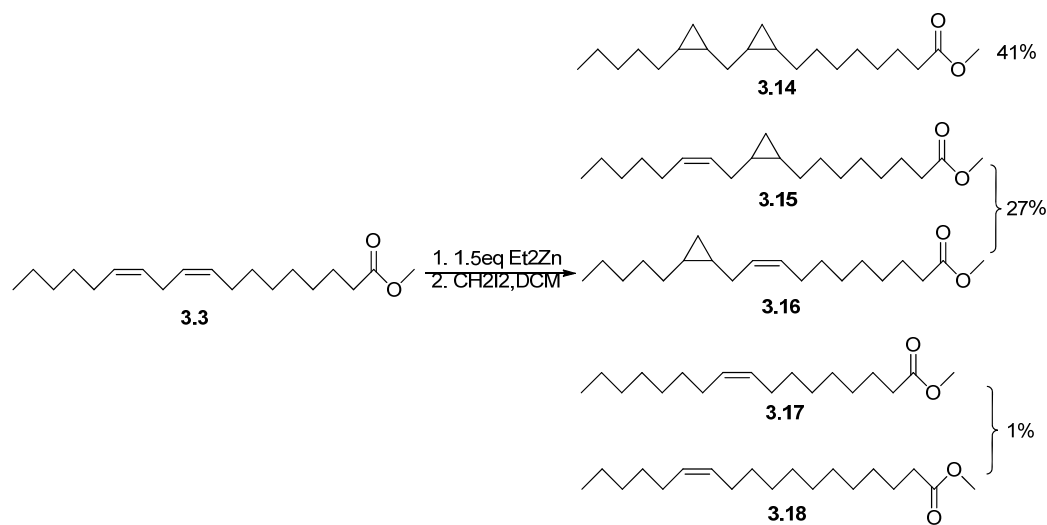
**Scheme 3.4** Selective cyclopropanation using steric effects.<sup>[13]</sup>

However, in the case of methyl linoleate(**3.3**), the chemical environment and steric effects on the two double bond are very much the same, so unless the two mono-cyclopropyl methyl linoleate are synthesized separately, it is very hard to get them by selective cyclopropanation of methyl linoleate. This means to get the regioisomeric mono-CP products, one need to do a de novo synthesis, which has not been reported to date.

## 3.2 Results and Discussion

### 3.2.1 Synthesis of Cyclopropanated Linoleate Derivatives

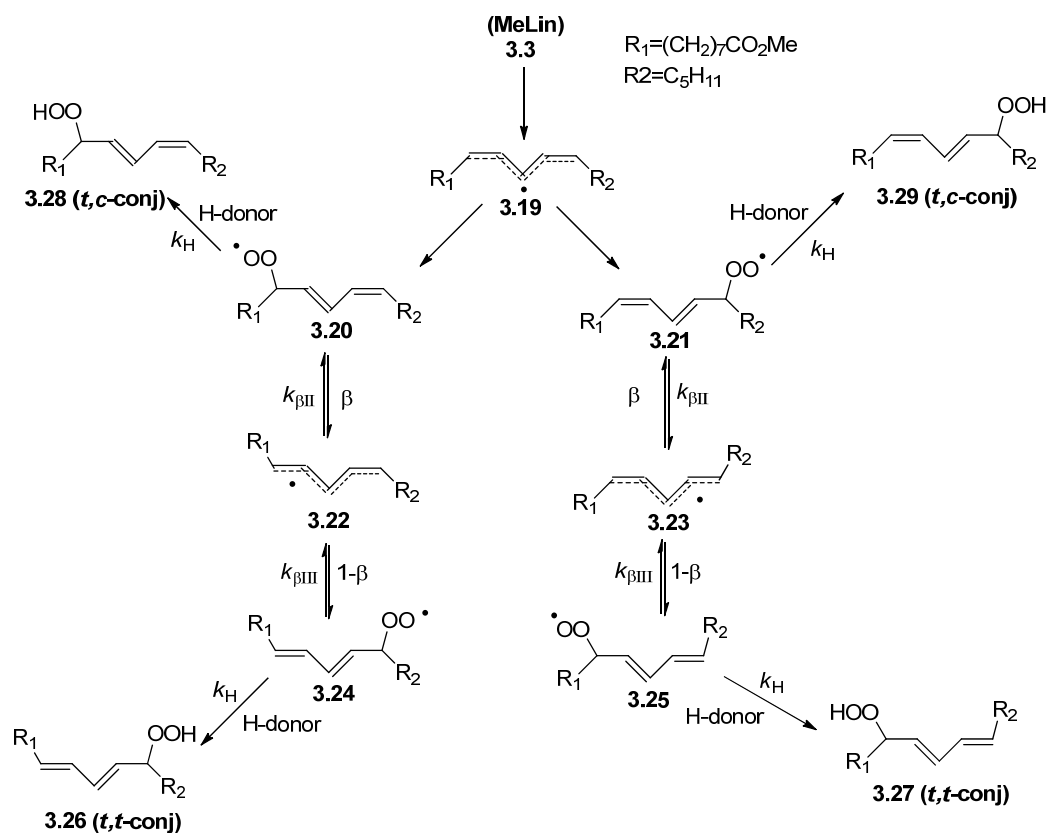
The synthesis of mono- and di-cyclopropanated (methyl) linoleate derivatives was carried out according to standard Simmons-Smith reaction conditions, using 1.5 equivalents of iodomethylzinc iodide ( $\text{ICH}_2\text{ZnI}$ ), generated from addition of  $\text{CH}_2\text{I}_2$  to diethyl zinc solution in hexanes (Scheme 3.5). Subsequent purification using either flash column or thin layer chromatography on silver nitrate impregnated silica gel was then carried out to obtain the methyl mono-CP linoleate as a 50/50 mixture of isomers **3.15** and **3.16** and methyl di-CP linoleate **3.14** in 27% and 41% yield, respectively. The partially reduced compounds **3.17** and **3.18** were also observed by GC, and accounted for roughly 1% of the mass balance. The use of either more or less Simmons-Smith reagent lead to lower yields of the methyl mono-CP linoleates. The reported synthesis<sup>[9]</sup> of di-cyclopropanated (methyl) linoleate derivatives uses 10 eq of Simmons-Smith reagent and the conversion is complete.



**Scheme 3.5** Synthesis of methyl monocyclopropanated and dicyclopropanated linoleate.

**3.2.2 Autoxidizability of Methyl Mono-CP Linoleate**

The propagation rate constant of methyl mono-CP methyl linoleate was determined by the ‘slow’ peroxy radical clock approach reported by the Porter group. [15]



**Scheme 3.6** Mechanism of slow peroxy radical clock approach, where  $k_{\beta\text{II}} = 27 \text{ s}^{-1}$ ,  $k_{\beta\text{III}} = 430 \text{ s}^{-1}$ . [15]

In the initial step of the autoxidation of methyl linoleate, oxygen partitions itself across the three positions of the pentadienyl radical (3.19) to form conjugated (3.20

and **3.21**) peroxy radicals. Bond rotation and subsequent  $\beta$ -fragmentation will form the new pentadienyl radical (**3.22** and **3.23**) with the trans,cis-conformation. Oxygen partitions itself at the transoid or cisoid ends of **3.22** and **3.23** to form either the trans,-cis- (**3.20** and **3.21**) or trans,trans-conjugated peroxy radicals (**3.24** and **3.25**) with partitioning coefficients of  $\beta$  and  $1-\beta$ , respectively. The conjugated peroxy radicals can undergo  $\beta$ -fragmentation to reform the original pentadienyl radical, denoted by  $k_{\beta\text{II}}$  and  $k_{\beta\text{III}}$ . Competing with this fragmentation is hydrogen atom transfer to the peroxy radical to form either the trans,cis- (**3.28** and **3.29**) or the trans,trans-conjugated hydroperoxides (**3.26** and **3.27**). This competition between hydrogen atom transfer and  $\beta$ -fragmentation establishes the slow peroxy radical clock.

Steady-state analysis of the mechanism presented in Scheme 3.6 leads to **equation 3.1** which describe the product distribution as a function of oxygen partitioning,  $\beta$ -fragmentation, and [H-donor].  $k_{\text{H}}$

$$\frac{[11+12]}{[9+10]} = \frac{k_{\text{H}}[\text{H-donor}]}{k_{\beta\text{II}}(1-\beta)} + \frac{k_{\beta\text{III}}}{k_{\beta\text{II}}} \left( \frac{\beta}{1-\beta} \right) \quad \mathbf{3.1}$$

**Figure 3.1a** shows the linear relationship between the ratio of  $[11+12]/[9+10]$  and  $[\text{MCP-ML}]$ , from which the propagation rate constant of MCP-ML can be calculated using Eq. 3.1. The resultant value of  $k_{\text{p}}$  was determined to be  $3.60 \pm 0.67 \text{ s}^{-1}$ ; slightly larger than that of monounsaturated fatty acids (e.g. oleate,  $\sim 1 \text{ M}^{-1}\text{s}^{-1}$ ) as we expected on the basis of our calculations and the known  $\pi$  character in the C-C

single bonds of cyclopropane rings. It is also similar to that of allylbenzene ( $5.5 \text{ M}^{-1}\text{s}^{-1}$ ), which was determined using the same methodology.<sup>[15]</sup>

Attempts to determine the propagation rate constant for methyl dicyclopropanated linoleate failed, presumably since it is too poor a H-atom donor to compete with methyl linoleate itself for the chain-carrying peroxy radicals (see zero-order dependence in Figure 3.1b

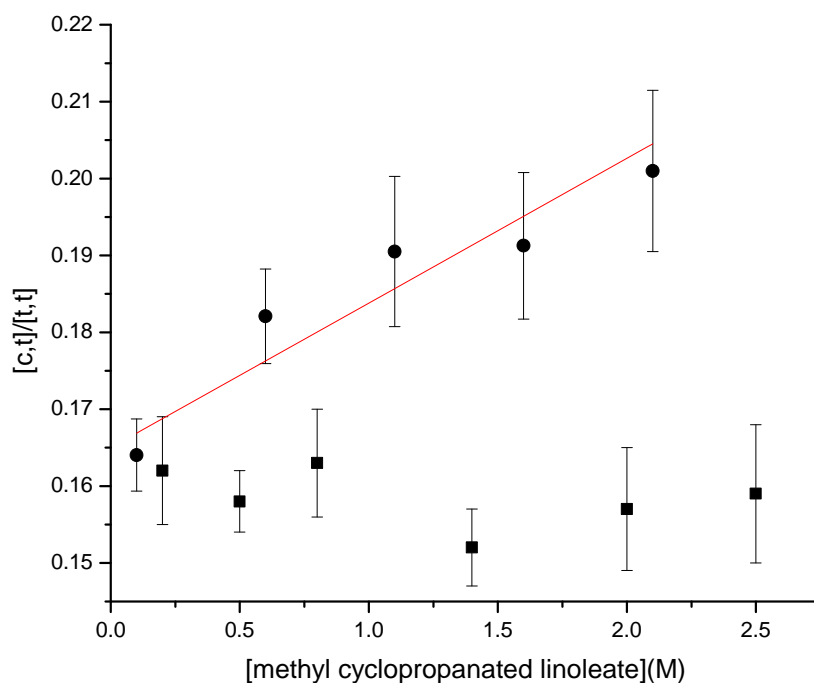


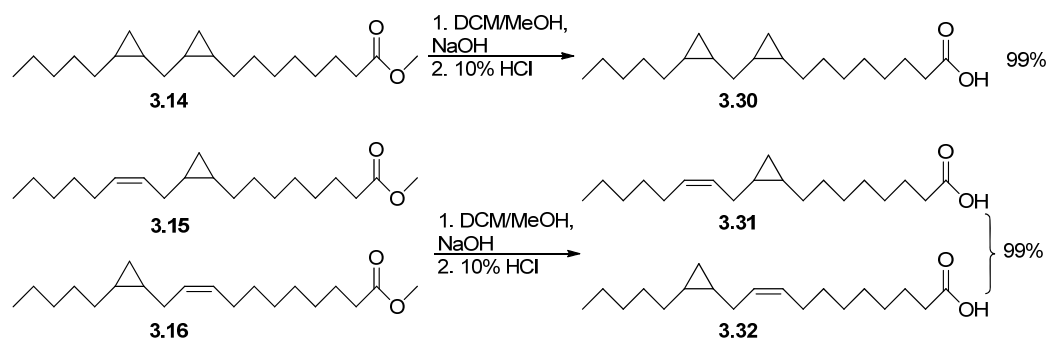
**Figure 3.1** Ratio of *cis,trans* to *trans,trans* methyl hydroperoxyoctadecadienoate oxidation products as a function of mono-(●) and di-(■) cyclopropanated methyl linoleate concentration in MeOAMVN-initiated autoxidations of methyl linoleate at 37°C in chlorobenzene.



### 3.2.3 Inhibition of Soybean Lipoxygenase by Cyclopropanated Linoleic Acids.

#### 3.2.3.1 Synthesis of Cyclopropanated Linoleic Acids

Hydrolysis of compounds **3.14**, **3.15** and **3.16** in DCM/MeOH (9:1) in the presence of NaOH and subsequent neutralization with 10% HCl gave the di- and mono-cyclopropanated linoleic acids **3.30**, **3.31** and **3.32** in quantitative yields.



**Scheme 3.7** Synthesis of cyclopropanated linoleic acids

#### 3.2.3.2 Soybean Lipoxygenase Assays

The mono CP linoleic acid was assayed for its ability to act as a substrate for sLOX-1. The di CP was not assayed since its *kp* was much too small to expect that it would be a reasonable substrate. The ability of sLOX-1 to convert its natural substrate, linoleic acid, to 13-hydroperoxyoctadecadienoic acid (13-HPODE) itself was assayed in parallel under the exact same conditions for comparison. The results are presented in Figure 3.2.

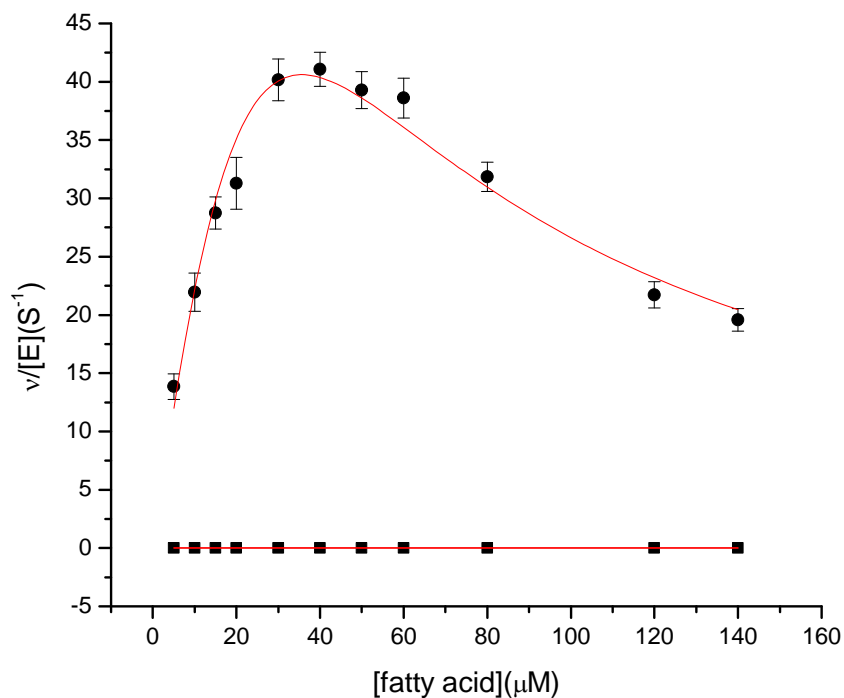


**Figure 3.2.** Michealis-Menten plots for the utilization of mono-Cp linoleic acid(■) and linoleic acid(●) by sLOX-1 in borate buffer pH 9.2.

Since the mono CP linoleate was clearly not a substrate for the enzyme, we wondered whether it might be a competitive inhibitor. We assayed both the mono and di-CP lipids for their ability to competitively inhibit sLOX-1. Thus, soybean lipoxygenase and linoleic acid was treated with different concentration of Mono- and Di- cyclopropanated linoleic acids separately, incubated at rt and monitored their UV absorbance at 234nm. Fig 3.3 shows the initial rates plotted as a function of added inhibitor concentration relative to the initial rates measured under identical

experimental conditions, but without added inhibitor.

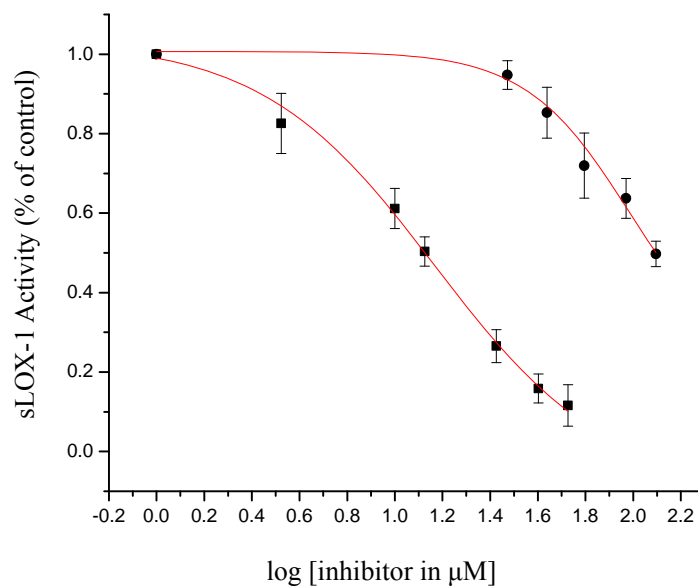
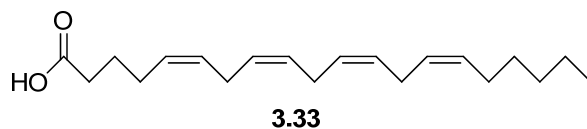


**Figure 3.3** Soybean lipoxygenase activity plotted as a function of added inhibitor concentration determined relative to the initial rates measured under identical experimental conditions, but without added inhibitor. Inhibitors: dicyclopropanated linoleic acid **3.30** (●) and monocyclopropanated linoleic acid **3.31** and **3.32** (■).

Figure 3.3 clearly shows that the monocyclopropanated linoleic acid is a much better inhibitor against sLOX-1 than dicyclopropanated linoleic acid. The derived  $\text{IC}_{50}$  value is  $16.8 \mu\text{M}$  for monocyclopropanated linoleic acid and  $221 \mu\text{M}$  for dicyclopropanated linoleic acid. The  $\text{IC}_{50}$  value of monocyclopropanated linoleic acid is roughly the same with the reported  $K_m$  value ( $39 \mu\text{M}$ )<sup>[16]</sup> for linoleic acid, which suggests that methylenation of one double bond of the substrate linoleic acid does not affect the binding with enzyme at all. The  $\text{IC}_{50}$  value of the latter should be interpreted

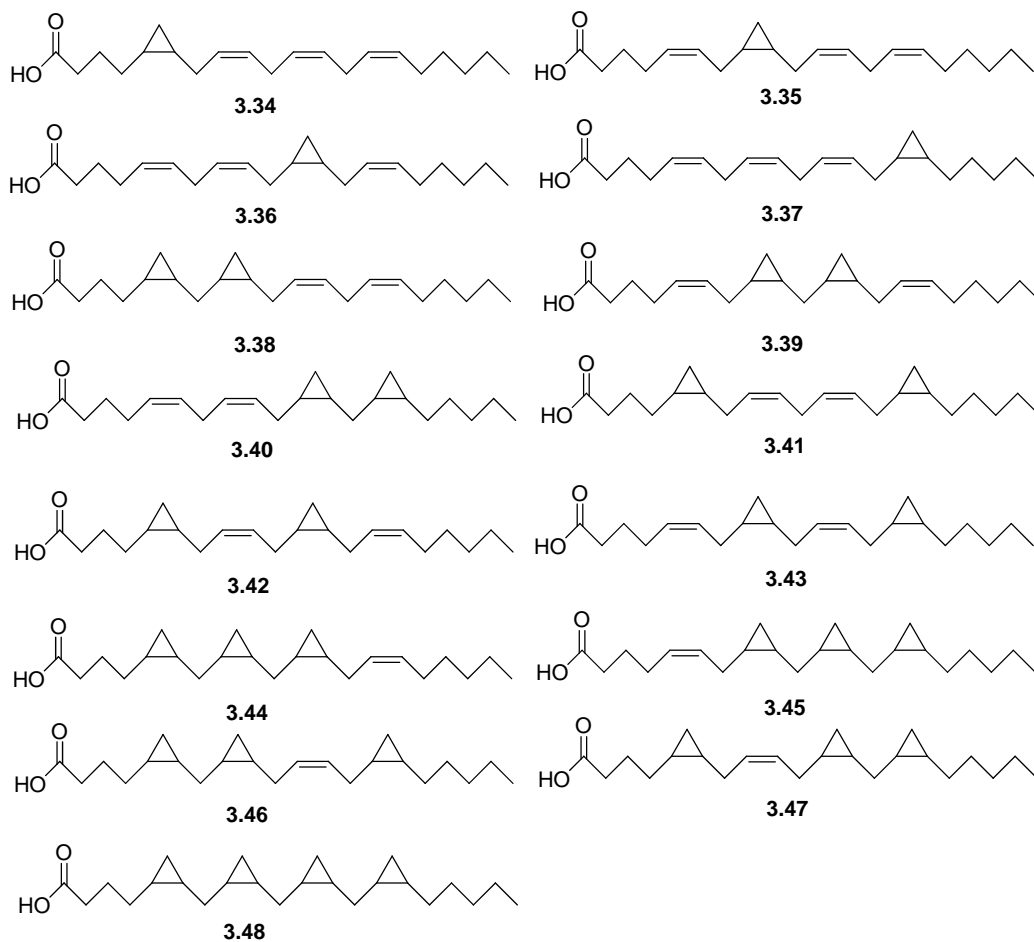
with caution. Since the critical micelle concentration of linoleic acid is ca.150  $\mu\text{M}$  in 0.1 M borate buffer (pH=9.2), it is possible that the apparent diminution of sLOX-1 activity at higher concentrations of **3.30** is simply the result of incorporation of the substrate in micelles of **3.30**. This requires further investigation.

With the Mono-CP linoleate being such a good inhibitor, it is possible that co-crystallization of sLOX-1 and/or sLOX-3 with these substrates should be attempted. To approach the more physiologically-relevant targets of the human LOX isoforms would require cyclopropanation of arachidonic acid (**3.33**);



The expected 15 cyclopropanated arachidonic acids are shown below, by adopting the similar synthesis and separation method used in preparing cyclopropanated linoleate, it is possible to get mono-, di-, tri- and tetra-cyclopropanated arachidonic acids as mixtures. If so, it will give us an easy way to get to these cyclopropanated arachidonic acids and allow us to test their inhibition ability towards human LOX enzymes so we can have some insights into which type of these CP arachidonic acids can bind to the enzyme better, which will save us a lot efforts of synthesizing these compounds individually. And to increase the yields of each of these four types of cp arachidonic acids, we can use the Fe complexes shown in Chapter 3.1.3 to coordinate with certain amount of double bonds and

cyclopropanate the rest double bonds.



### 3.3 Experimental Procedures

#### General Procedures of Simmons Smith Reaction

Diethylzinc (1.5 ml, 1.5 mmol, 1M solution in hexanes) was added to dry  $\text{CH}_2\text{Cl}_2$  (5 ml) under argon, the solution was cooled to  $0^\circ\text{C}$ , and  $\text{CH}_2\text{I}_2$  (536 mg, 2 mmol) was added slowly (this process releases ethane, and should be handled carefully). During addition of the  $\text{CH}_2\text{I}_2$  a white solid appeared which represents formation of the

iodomethylzinc iodide species. Following addition of  $\text{CH}_2\text{I}_2$  the reaction was kept stirring at  $0^\circ\text{C}$  for 15 minutes. Methyl linoleate (294 mg, 1 mmol) was then added in one portion and the reaction was allowed to come to room temperature and stirred overnight. The resulting solution was quenched using sat.  $\text{NH}_4\text{Cl}$ , extracted several times with ether and then dried over anhydrous  $\text{MgSO}_4$  and concentrated under reduced pressure.

TLC plates was dipped into 10% silver nitrate solution in acetonitrile for 15 seconds, and then heated to evaporate the solvents with a heat gun.(the silver nitrate impregnated plates should be used right after prepared, storage cause oxidation to silver nitrate and damage the separation of the plate). Usually one standard plate can be cut in half, and the concentrated ether solution was added on the baseline, the plates were running in a 6.25% EtOAc/Hexanes solution, the Mono-CP ML and Di-CP ML can then be separated by scratching different parts of the plates, the collected silica is then washed with ether, which is then washed with 10% HCl solution, and dried over  $\text{MgSO}_4$ .

**Methyl cis,cis-9,10,12,13-methylene- octadecanoate (3.14).** 41% yield as colorless oil. Spectral data is in accordance with literature value.<sup>[9]</sup>

**Methyl cis,cis-9,10-methylene-12-octadecenoate (3.15) and Methyl cis,cis-12,13-methylene-9-octadecenoate (3.16).** 27% yield as colorless oil.  $^1\text{H}$  NMR (400 MHz,  $\text{CDCl}_3$ ):  $\delta$  -0.29 (m, 1H), 0.57 (m, 1H) 0.68 (s, 6H), 0.87 (m, 3H), 1.28-1.37(m, 16H),

1.51 (s, 2H), 1.60(m, 2H), 2.06(m, 4H), 2.28(t, 2H), 3.64(s, 3H), 5.32-5.47(m, 2H) ppm. <sup>13</sup>C NMR (400 MHz, CDCl<sub>3</sub>): δ 10.77, 14.10, 14.14, 15.86, 15.90, 22.61, 22.75, 24.98, 26.46, 27.30, 28.78, 29.15, 29.19, 29.33, 29.48, 29.71, 29.90, 30.13, 31.56, 31.93, 34.13, 51.44, 129.61, 129.71, 174.31 ppm. HRMS (ES<sup>+</sup>) calcd (M) 308.2749, obsd 308.2707

**General Procedures for Hydrolysis of Methyl Cyclopropanated Linoleate.** To a stirred solution of cyclopropanated methyl linoleate (1mmol) in DCM/MeOH (9:1) 10 ml was added NaOH(4mmol), the reaction was kept stirring at rt for overnight. The resulting solution was neutralized by 10% HCl and then extracted with EtOAc for several times, concentrated and purified using flash chromatography.

**Cis,cis-9,10,12,13-methylene-octadecanoic acid (3.30).** Colorless oil, 97%. <sup>1</sup>H NMR (400 MHz, CDCl<sub>3</sub>): δ -0.31 (m, 2H), 0.56-1.65(m, 31H), 2.33(t, 2H) ppm. <sup>13</sup>C NMR (400 MHz, CDCl<sub>3</sub>): δ 10.87, 11.05, 14.13, 15.67, 15.96, 16.08, 22.75, 24.71, 27.91, 28.05, 28.75, 28.91, 29.10, 29.32, 29.45, 29.92, 30.16, 31.93, 34.13, 180.35 ppm. HRMS (ES<sup>+</sup>) calcd (M) 308.2715, obsd 237.1808[M-C<sub>5</sub>H<sub>11</sub>]<sup>+</sup>

**Cis,cis-9,10-methylene-12-octadecenoic acid (3.31) and cis,cis-12,13-methylene-9-octadecenoic acid (3.32).** Colorless oil, 97%. <sup>1</sup>H NMR (400 MHz, CDCl<sub>3</sub>): δ -0.28 (m, 2H), 0.54-2.06(m, 28H), 2.35(t, 2H), 5.26-5.51(m, 2H) ppm. <sup>13</sup>C NMR (400 MHz, CDCl<sub>3</sub>): δ 10.78, 14.15, 15.90, 22.62, 22.75, 24.711, 26.46, 27.31, 28.79, 29.11,

29.31, 29.48, 29.71, 29.89, 30.14, 31.57, 31.93, 34.04, 129.66, 179.95 ppm. HRMS (ES+) calcd (M) 294.2559, obsd 294.2542

### **General Procedures for Radical Clock Experiment**

Stock solution of MeOAMVN (0.1M), MeLin (1.0M) were prepared in chlorobenzene. Samples were assembled in 1 mL HPLC autosampler vials with a total reaction volume of 100 $\mu$ L. Solutions were prepared in the following order to avoid premature oxidation: compound **3.15** and **3.16** (0.10-2.5M), MeLin(0.1M) and then MeOAMVN (0.01M), and diluted to 100 $\mu$ L with chlorobenzene. The sealed samples were then heated to 37°C for 1 hour. After 1 hour, the oxidation was stopped by the addition of BHT (50 of 1.0M solution in hexanes), followed by reduction of the hydroperoxides to alcohols by triphenylphosphine(50 $\mu$ L of 1 M solution in chlorobenzene). The samples were then diluted to 1ml with HPLC grade hexanes and analyzed by HPLC (1.5% *i*-PrOH in hexanes, 1 mL min<sup>-1</sup>, 30 min, Sun-Fire Silica, 5 mm 4.6 x 250 mm column, UV detection at 234 nm). The ratio of products (*Z,E* :*E,E*) was plotted *versus* thiosulfinate concentration to derive  $k_h$ .

### **General Procedures for Enzyme Inhibition Experiment**

The effects of added inhibitors on the initial rates of conversion (less than 10%) of linoleic acid (LA) to cyclopropanated linoleic acids(**3.30-3.32**) by soybean LOX-1, were determined by monitoring the conversion of LA to 13-HPODE on a spectrophotometer at 234 nm. Briefly, to a solution of 20  $\mu$ M LA in 100 mM borate



buffer (pH 9.2) was added the inhibitor as a concentrated solution in ethanol (to final concentrations of 3.0 to 125  $\mu$ M depending on the inhibitor and less than 5% ethanol, by volume), and then sLOX-1 to a final concentration of 3 nM. The initial rates were then plotted as a function of added inhibitor concentration relative to the initial rates measured under identical experimental conditions, but without added inhibitor.

### 3.4 References

- [1] Carballeira, N. M.; Montano, N.; Vicente, J.; Rodriguez, A. D.; *Lipids* **2007**, *42*, 519–524.
- [2] Lynett, P. T.; Butts, K.; Vaidya, V.; Garretta, G. E.; Pratt, D. A. *Org. Biomol. Chem.* **2011**, *9*, 3320–3330
- [3] Howard, J. A. *Adv. Free Radical Chem.* **1972**, *4*, 85-109.
- [4] Knapp, M. J.; Klinman, J. P. *Biochemistry* **2003**, *42*, 11466–11475.
- [5] Simmons, H. E.; Smith, R. D. *J. Am. Chem. Soc.* **1958**, *80*, 532.
- [6] Simmons, H. E.; Smith, R. D. *J. Am. Chem. Soc.* **1959**, *81*, 4256.
- [7] Denis, J. M.; Girard, J. M.; Conia, J. M. *Synthesis* **1972**, 549.
- [8] Ito, Y.; Fujii, S.; Nakatuska, M.; Kawamoto, F.; Saegusa, T. *Org. Synth.* **1988**, *6*, 327.
- [9] Tanaka, A.; Nishizaki, T. *Bioorg. Med. Chem. Lett.* **2003**, 1037-1040.
- [10] Li, T.S.; et al., *Journal of Chromatography A*, **1995**, *715*, 372-375.
- [11] Nicholas, K. M. *J. Am. Chem. Soc.* **1976**, *97*, 3254.

- [12] Reger, D. L.; Gabrielli, A. *J. Am. Chem. Soc.* **1976**, *97*, 4421
- [13] Guerchais, V.; Leveque, S.; Hornfeck, A.; Lapinte, C. *Organometallics* **1992**, *11*,  
3926-3920
- [14] Tahiri, A.; Guerchais, V.; Toupet, L.; Lapinte, C. *J. Organomet.Chem.* **1990**,*381*,  
C47.
- [15] Roschek, B.; Tallman, K. A.; Rector, C. L.; Gillmore, J. G.; Pratt, D.A.; Punta,  
C.; Porter, N. A. *J. Org. Chem.* **2006**, *71*, 3527-3532
- [16] Sheng, P.; Wilfred, A. van der Donk. *J. Am. Chem. Soc.* **2003**, *125*, 8988.